BIOPHYSICAL STUDIES OF BLOOD PROTEINS AND VIRAL PROTEINS

INAKI AZPIAZU B.Sci.

Department of Protein and
Molecular Biology
Royal Free Hospital School
of Medicine
LONDON

Submitted in fulfilment of the requirements for the degree of Doctor of Philosophy for the University of London, 1993.

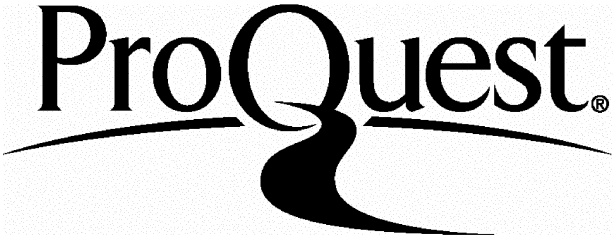

ABSTRACT.

The structure of various proteins have been examined using Fourier Transform Infrared (FT-IR) spectroscopy.

These studies show that the structure of human fibrinogen contains 35% α-helix, 29% ß-sheet and 15% turns. Examination of its plasmin-derived fragments indicates that Fragment E (Mw 45 KDa), with part of the central and of the coiled-coil domains, adopts a solvent-exposed structure with 50% α-helix. Fragment D (Mw 100 KDa), with the main globular domain and part of the coiled-coil, shows that the globular domain is twice richer in ß-sheet than in α-helix, and that its coiled-coil adopts 70% α-helix.

The FT-IR spectra of the Pf1 and fd coat proteins indicates a similar percentage of 90-100% α-helix when present in the filamentous phages, in detergent micelles or reconstituted in phospholipid membranes. Internal reflectance (ATR) FT-IR studies of the fd coat protein in the membrane shows evidence of a structure with segments adopting orientations parallel and perpendicular to the plane of the lipid bilayer. Fluorescence depolarization and calorimetric studies of Pf1 protein/lipid systems are consistent with the existence of a single helix spanning the lipid bilayer. ATR FT-IR of the ^{13}C-shifted amide band of serine residues of the Pf1 protein suggests that its amino-terminus adopts an orientation predominantly perpendicular with respect to the plane of the lipid bilayer.

The FT-IR spectra of human C-reactive protein indicates a structure rich in ß-sheet and turns, and poor in α-helix. $H/^{2}H$ exchange of the human C-reactive protein indicates a solvent-accessible conformation. The FT-IR spectra of human C-reactive protein and those of Limulus C-reactive and serum amyloid proteins indicate structural differences between their α-helical structures. Some similarities of the spectrum of human C-reactive protein with the spectra of amyloid proteins are indicated.

ACKNOWLEDGEMENTS.

I would like to thank to all people for their much needed support and encouragement without whom this thesis would not be a reality.

Special thanks to Dorian K. for his help and continuous encouragement. Thanks to all the members of my Department, of those, my regards to Christine H. and Lacks S. for their company and help, Parvez I.H. and Bala R. for discussions, and to Brenda H., Michael J., Yandao G., Chonkee, Kiriakos, Helen, Cristina, Kaila, Johnnatan, Michael, Frederick Kurzor, Marian, Helen and to many others. To Dr. Bambos Charalambous for his advice in the preparation of the filamentous phages. To Dr. S. Gillespie for his assistance in the preparation of the PC-affinity resins. To Professor Juan Carmelo Gomez-Fernandez (Murcia, Spain) for his assistance in the DSC studies and for the long conversations on current spanish affairs in the summer 1992. To Dr. S. Opella and cooworkers (Philadelphia U.S.A.) for the supply of fd phages and the sample of Pf1 protein in DPC solution.

To my dear parents, sister and brothers that have been away from all this. To the forgotten friends that I hope to see again.

I wish to express my admiration to Professor Dennis Chapman for the supervision of my work, my writing and his support in those crucial moments.

ABBREVIATIONS.

Arg= arginine

Asn= asparagine

Asp= aspartic acid

ATR= attenuated total reflectance

BSA= bovine serum albumin

Ca^{2+}-ATPase= Ca^{2+}·Mg^{2+}-dependent ATPase from sarcoplasmic reticulum of rabbit muscle

$CaCl_2$= calcium chloride

CaF_2= calcium fluoride

CD= circular dichroism spectroscopy

CMC= critical micellar concentration

CRP= C-reactive protein

CsCl= cesium chloride

dp= penetration depth

DR= dichroic ratio

DMPC= L-α-dimiristoyl-phosphoryl-choline

DNA= deoxyribunocleic acid

DPC= dodecyl phosphocholine

DPH= diphenyl-hexatriene

DPPC= L-α-dipalmitoyl-phosphoryl-choline

DSC= differential scanning calorimetry

EDTA= ethylenaminotetraacetatic acid

EGTA= ethyleneglycol diaminetetracetate

ELISA= enzyme-linked immunosorbent assay

EM= electron microscopy

FT= fourier transform

FT-IR= fourier transform infrared

Gln= glutamine

Glu= glutamic acid

He-Ne= Helium/Neon

HWHH= half width half height

IR= infrared

K= ratio of the narrowed bandwidth to the original bandwidth

KRS-5= thallium bromoiodide

Lys= lysine

m.o.i= multiplicity of infection

Mw= molecular weight

NIH= National Institute of Health, U.S.A.

NMR= nuclear magnetic resonance

PC= phoshoryl-choline

PEG= polyethylene glycol

pH= - log $[H^+]$

p^2H= pH - 0.7

PMSF= phenyl methyl sulphonyl fluoride

SAP= serum amyloid P component

SDS= sodium dodecyl-sulphate

SDS-PAGE= sodium-dodecyl-sulphate polyacrylamide gel electrophoresis

SNR= signal-to-noise ratio

TGS= triglycine sulfate

T_t= temperature of phase transition

TABLE OF CONTENTS.

INDEX TO FIGURES.

INDEX TO TABLES.

CHAPTER 1.

PROTEINS AND LIPID MEMBRANES: STRUCTURE

1.1. INTRODUCTION.

In this introductory chapter the various levels of organization in the structure of proteins are presented. The types of secondary structure and their prediction are examined. The formation and stability of the tertiary structure in proteins are examined in relationship with the primary sequence.

In the second part of the chapter the different types of lipids found in biological membranes are presented. The influence of factors such as temperature, composition of lipids, presence of proteins, upon the fluidity of the membranes is examined.

1.2.1. THE STRUCTURE OF PROTEINS.

Proteins are linear polymers of aminoacids bonded by formation of amide groups. According to the chemical nature of the side-chains, the aminoacids can be classified, in general, as hydrophobic or hydrophilic. The sequence of the aminoacids along the polypeptide chain is defined as the primary structure of the protein. The diversity of sequences of aminoacids in proteins confer them with the structural versatility needed for the vast variety of functions and enzymatic reactions that they fulfil in living organisms.

It was not until 1958 that the first detailed atomic structure of a protein, myoglobin, was described using X-ray diffraction (Kendrew et al., 1958). One of the first observations made on the atomic structure of myoglobin was that the hydrophobic aminoacids have their side-chains buried inside the protein core and protected from contact with the solvent, whereas the hydrophilic sidechains are exposed to it (Kendrew et al., 1960; Kendrew et al., 1961). In order to neutralise the hydrophilic peptide groups in the protein core, the polypeptidic backbone adopts mainly α-helical structures and other structures, that allow distant amide groups to come together forming hydrogen-bonds. Subsequent atomic models of various proteins have revealed that the α-helix and other regular structures are common. These are

termed secondary structures, and refer to the local nature of the folding of the polypeptide chain.

The tertiary structure describes the three-dimensional organisation of the protein where the secondary structure elements and aminoacid side-chains pack to give a stable structure to the folded protein.

1.2.2. Secondary structure.

Part of the backbone of a polypeptide chain is presented in figure 1.1. By convention, the polypeptide backbone is defined from the free amino end to the carboxy end. Due to its chemical structure, the amide group is planar and behaves as a rigid unit, with the trans conformation (torsion angle W= 180°$\pm$ 15) being sterically favoured. The angle for the $C_{\alpha(i)}$-C bond is denoted δ, and for the N-$C_{\alpha(i)}$ bond is ϕ. The value of these two bond angles is +180° for a fully stretched chain counted clockwise from the N-C_{α} bond. Of all the possible torsion angles only some are sterically allowed due to constraints imposed by the positions of polypeptide atoms and the size of aminoacid sidechains. A study of the permitted torsion angles δ and ϕ is given by the Ramachandran plot (Ramachandran et al., 1968).

Figure 1.1.

Peptidic backbone, showing C_α, C, O and N atoms and angles of torsion δ and ϕ.

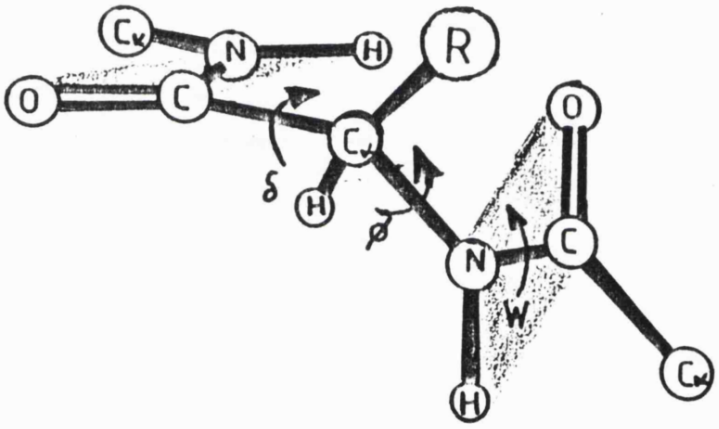
Cα
N
H
R
O
C
Cα
O
δ
H
ψ
φ
N
C
W
H
Cα

Figure 1.2.

The atomic arrangement and hydrogen-bonding (....) in the α-helix (Right) and the 3_{10}-helix (Left).

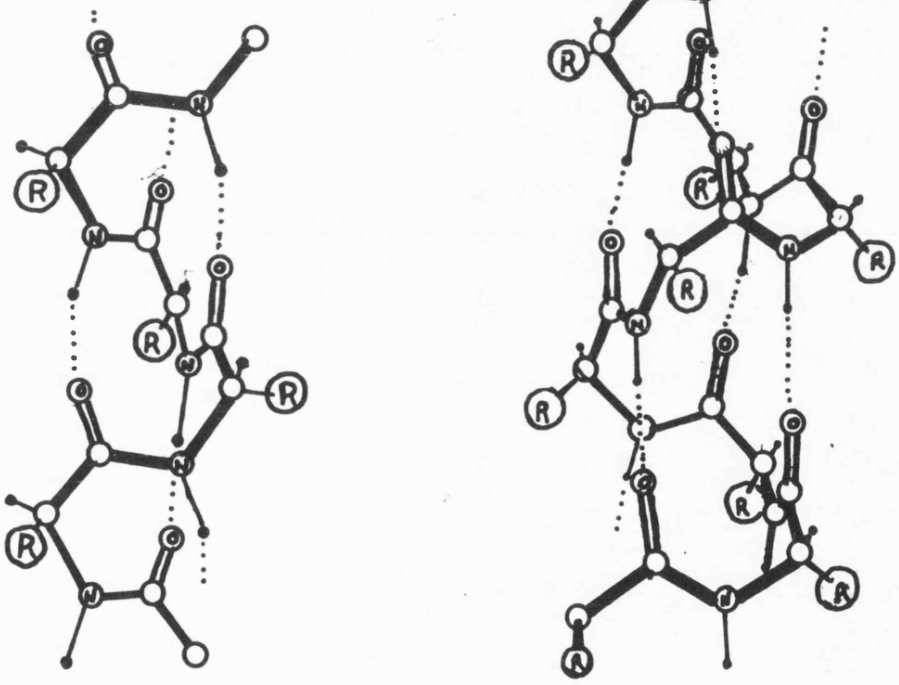

1.2.2.1. The α-helix.

The existence of the α-helix in proteins was predicted by Pauling and co-workers (1951a,b) in their studies of the molecular structure of keratin proteins. The polypeptidic backbone of the α-helix twists in a right-handed coil to allow hydrogen-bond formation between the amino group of residue i with the carboxy of residues i+4, with 3.4 aminoacid units per turn (figure 1.2 right). The torsion angles δ and ϕ have values of -55 and -40°, respectively, are favourable for most residues, except for those of proline and hydroxylproline. The planes of the peptidic groups and the hydrogen-bond pattern are aligned parallel to the axis of the α-helix and the side-chains project outwards from this axis.

The α-helix is commonly observed in proteins and may contain from 6 to 18 aminoacid units in soluble proteins. It permits by an alternation of hydrophilic and hydrophobic sidechains the formation of amphiphilic faces such as those observed in myoglobin (Richarson, 1981).

1.2.2.2. The ß-sheet.

This structure was proposed as the main conformation of the silk protein (Pauling et al., 1951c). In this structure alternating peptidic groups of adjacent chains (also called strands) form hydrogen-bonds, and the orientation of the

Figure 1.3.

The planar arrangement and hydrogen-bonding in the antiparallel ß-sheet (Top). The antiparallel (bottom-left) and parallel ß-sheet (bottom-right).

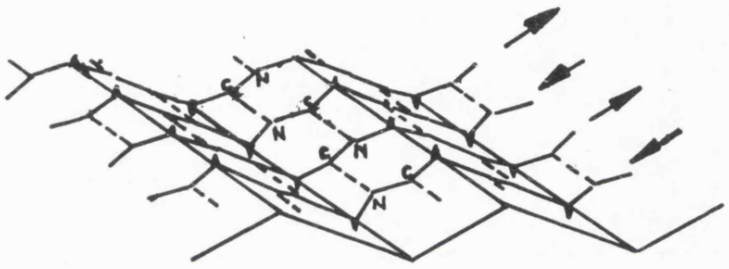

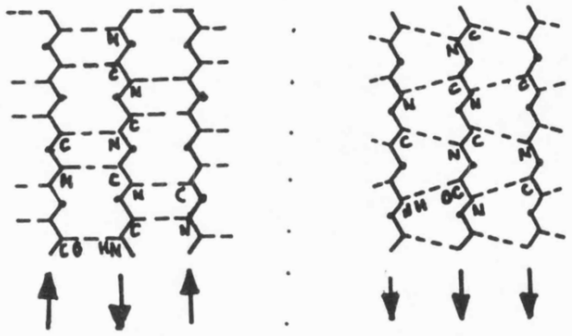

chains may be parallel or antiparallel to each other (figure 1.3 top). The antiparallel sheet shows a regular pattern of adjacent hydrogen-bonded pairs alternating with wide spaces, in the parallel chain this spacing is more even (figure 1.3 bottom). The peptide groups lay in planes perpendicular to the direction of the polypeptide backbone and the side-chains project above and below the plane of the sheet (figure 1.3 top).

The ß-sheet in a great number of proteins shows a right-handed orientation, and the number of residues per strand ranges usually from 5 to 10. Both parallel and/or antiparallel sheets have been observed in proteins such as immunoglobulin (Richardson, 1981; Epp et al., 1974), concanavalin A (Reeke et al., 1975) and prealbumin (Blake et al., 1978). One particular type, the cross ß-sheet, has been detected by X-ray diffraction as the main motif in amyloid-containing deposits in tissues of patients suffering diseases such as Alzheimer's (Kirschner et al., 1986). The cross ß-sheet has been studied in a variety of fibrillar aggregates of denatured proteins, where the polypeptide backbone forms a continuous arrangement of layers of antiparallel strands transversely aligned with respect to the fibrillar axis (Burke & Rougvie, 1972).

Figure 1.4.

The ß-turns type I (left) and II structures (right).

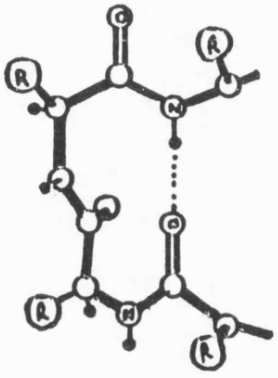

I

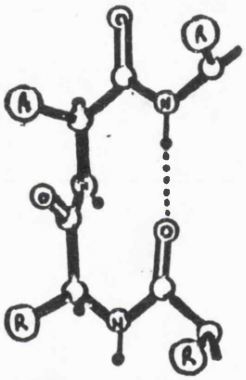

II

1.2.2.3. 3_{10}- and π-helices.

These are conformations rarely observed in proteins. The 3_{10}-helix consists of a helix with 3 aminoacids per turn and the planes of the peptidic groups are relatively out of alignment with the helical axis (figure 1.2 left). The side-chain packing in the 3_{10} helix is not favoured.

It has only been observed at the end of α-helices in proteins as part of turns (Pauling et al., 1959ab) but it has been found in polypeptides containing a high percentage of α-aminoisobutyric aminoacids e.g. alamethicin (Fox & Richards, 1982) and pentaibol antibiotics (Bruckner & Cirat, 1983; Marshall et al., 1990) where the dominant α-aminoisobutyric sidechains impose steric constraints to the α-helix.

The π-helix has 4 aminoacids per turn, with the planes well aligned. This helix reduces van-der-Waals attraction between atoms participating in the helix and it is unfavoured sterically.

1.2.2.4. ß-turn structures.

They consist of four aminoacids with only the C_i and N_{i+3} forming a hydrogen-bond (Venkatachalam, 1968; Lewis et al., 1973). The types of ß-turn are denoted as I, II and III: a type III ß-turn is identical to one turn of a 3_{10}-helix; a type I ß-turn is a deformed 3_{10}-helix with different torsion angles of residues $C_{\alpha\ i+1}$ and $C_{\alpha\ i+2}$ (figure

1.4 left). In type II turns there is a reversal of the amide bond shared by residues i+1 and i+2 (figure 1.4 right). Some positions in turns are sterically demanding and are usually occupied by aminoacids with small sidechains, for example glycine and serine. Some 25% of turn structures, including those containing proline residues, do not establish hydrogen-bonds and are usually referred as non-standard turns .

The turn structures are abundant in proteins (Crawford et al., 1973) and found at sites of reversal or reorientation of the polypeptide chain, and are usually solvent-exposed.

1.2.2.5. Random structures.

Random structures refer to a heterogeneous group of structures. Random structures may or not form intramolecular peptidic hydrogen bond and they are characterised commonly by a structure accessible to the aqueous solvent. Of these, loops are regarded as loose segments, whose aminoacid sequence is usually not conserved (Birktoff & Blow, 1972). Loops may be found at important places such as the antigen-sites in immunoglobulins (Richardson, 1981).

1.2.3. Prediction of secondary structure.

The aminoacid sequence of a protein specifies its three-dimensional structure, and its secondary structure.

Studies of the position of aminoacid in globular proteins indicated that residues such as glycine, proline and asparagine tend to be present in turns. Residues more likely to be present in α-helices are glutamic acid, alanine and leucine; whereas others like methionine, valine and isoleucine prefer ß-sheet (Chou & Fasman, 1973).

Subsequently, attempts have been made in search of methods able to predict the secondary structure from the aminoacid sequence. Two methods have received wide acceptance for their user-friendly approach and relative versatility to allow levels of constraints: the first created by Chou and Fasman (1974) uses the probability of finding a particular aminoacid in the secondary structure (α-helix, ß-sheet and turns) of a number of known globular proteins in order to sample regions in the aminoacid sequence of the protein with a secondary structure potential. Briefly, the method locates small clusters in the aminoacid sequence with a critical number of residues prone to be found in a type of structure, then these clusters are extended to other residues solving possible overlaps in terms of highest probability of secondary structure. The Garnier & Robson method (1978) is different and involves the use of decision constants based on percentages of secondary structure obtained from CD spectra or other data of the protein. The individual decision constants are used to determine segments of the

primary sequence of the protein with a particular secondary structure potential. Both methods have accuracies of 50-60% when compared with the real data, but predictions are improved when both methods are combined (Nikishikawa, 1983).

Another approach for the prediction of secondary structures is to look for regular patterns in the aminoacid sequence of proteins having a hydrophobic or hydrophilic character. A remarkable case is that of coiled-coil structures of proteins such as tropomyosin (Parry, 1975), myosin (Quinlan & Stewart, 1987), kynesins (Scholey et al., 1989; Endow, 1991), fibrinogen (Doolittle et al., 1978), where the sequence contains consecutive groups of seven aminoacids with hydrophobic residues every third and/or fourth position and charged hydrophilic on the first and second positions.

The aminoacid sequences of membrane proteins contain a pattern of segments rich in aminoacids with hydrophobic residues which are thought to span the lipid bilayer as α-helical domains (Engelman et al., 1986).

1.2.4. Tertiary structure.

The tertiary structure of a protein is a higher level of structural organisation where the secondary structure elements fold packing hydrophobic residues into the protein interior and bringing together aminoacid residues distant in the primary sequence.

A property of proteins is that they adopt a unique tertiary structure, its native structure. Under physiological conditions of pH and temperature, the stability of the native structure of a protein is founded to a large extent in the balance of two different thermodynamic forces, first, the need to pack the hydrophobic residues in the interior of the protein, avoiding solvent-contact and maximising van-der-Waals interactions, and second, the entropy-driven tendency of the polypeptide to undergo random motion. The net energetic balance in proteins in aqueous media favours stability and therefore formation of folded structures. In some cases these latter structures serve as intermediates for the formation of proenzymes, i.e. trypsinogen (Kassel & Kay, 1973), or precursors of prohormones, i.e. proinsulin (Kemmler et al., 1971), or latent inhibitors of proteases such as serpins (Löberman et al., 1984).

The denaturation of proteins is an unfolding proccess, usually irreversible, occurring under many conditions such as the presence of urea, high temperatures, pH, where proteins unfold or/and aggregate to form insoluble complexes. Unfolding of proteins exposed to acid pH occurs as a result of repulsion of charged sidechains on the surface of proteins and therefore instability of the folded structures (Pace, 1990).

All the information necessary for the formation of the tertiary structure of a protein is contained in the aminoacid sequence. In comparison with the large diversity of aminoacid sequences known in proteins, the number of three-dimensional structures is far smaller. Often proteins serving similar functions in different tissues or species have similar three-dimensional structures. Their aminoacid sequence differ to some degree, but some positions are occupied by the same aminoacid or by another aminoacid with similar chemical properties (Chothia & Lesk, 1986). It appears that conservation at these positions of the aminoacid sequence is critical both for the preservation of the structure, and thus for protein function. In general it seems that for evolutionary related proteins the aminoacid sequences tend to be conserved in the core of the protein, but not in solvent-exposed segments such as loop structures. The homology between primary sequences serves as a basis for the prediction of secondary and tertiary structures from the aminoacid sequences of novel proteins (Benner & Gerloff, 1990).

Comparative studies of the aminoacid sequence of many proteins have revealed the existence of basic entities, called modules in many proteins, which show a mosaic of several moieties in their primary sequence. i.e proteins of the clotting cascade and fibrinolytic enzymes (Katayama et

al., 1979; Ny et al., 1984). It seems that in the course of evolution and experimentation, numerous proteins have been created by mixing, duplication such as haemoglobin and integration of small genes to give rise to proteins with advantageous properties for the host.

1.2.5. Quaternary structure.

Many proteins are constituted by subunits of polypeptides held together by electrostatic and hydrophobic interactions. Examples are multi-enzymatic complexes of the mitochondria, ribosomes and viral particles such as the tobacco mosaic virus (Namba et al., 1985). Specific assembly of proteins in response to signals such as a change of pH or the concentration of divalent ions or nucleotides, is also a common occurrence in cellular events and depends on specific protein/protein interactions.

1.3. THE STRUCTURE OF BIOLOGICAL MEMBRANES.

1.3.1. Introduction to biological membranes.

Membranes in living cells constitute physical barriers between the outer and the inner cell media, e.g. the plasmatic membrane, and serve to establish intracellular compartments for specialised purposes such as those occurring in the mitochondria and lysosomes. Membranes also have active involvement in the transport of substances and cross-communication between cells via signal transmission.

The basic structure of membranes is widely recognised as a bilayer matrix of lipid molecules (figure 1.5) in which other components such as proteins are embedded (Singer & Nicholson, 1972). The percentage of lipids can range from 75% in the myelin sheath to 25% in the inner mitochondrial membrane.

All membrane lipids have an amphiphilic character due to one part of molecule being hydrophilic and the other being hydrophobic. Owing to this dual property, the lipid molecules aggregate in water to give ordered arrangements that allow the hydrophilic groups to interact with the aqueous solvent and permit the hydrophobic regions to be shielded in the solvent-free interior.

Lipids give rise to various types of arrangement and these are determined to a large extent by the size of the

Figure 1.5.

Representation of a biological membrane, showing lipid and protein molecules, in accordance to the model of Singer & Nicholson (1972).

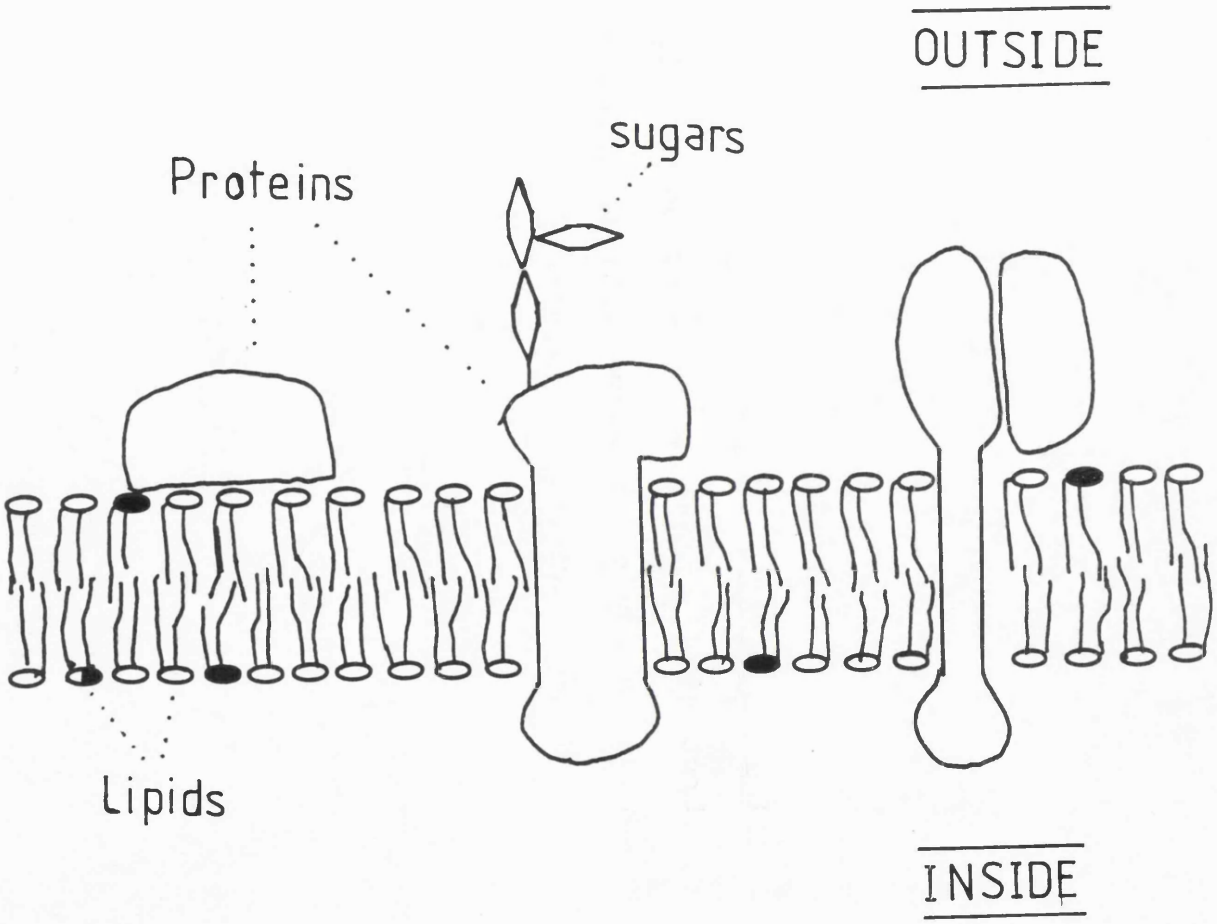
OUTSIDE
sugars
Proteins
Lipids
INSIDE

Figure 1.6.

Structural arrangements adopted by lipid molecules in aqueous systems: (A) Inverted micelles, (B) Vesicles and (C) Micelles.

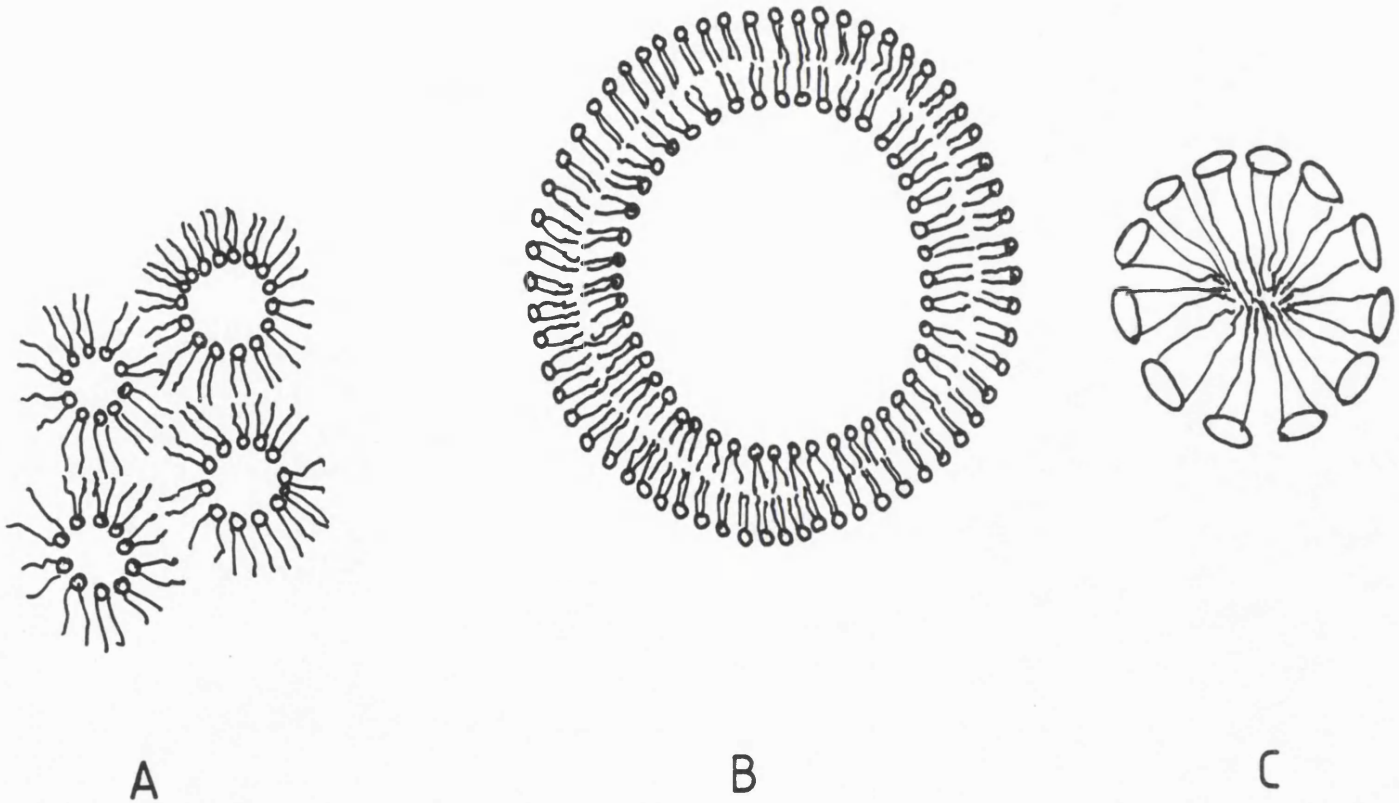
A
B
C

hydrophilic part relative to the hydrophobic part of the molecule. Other important factors are the degree of hydration of the lipid headgroup, as determined by the pH, ionic strength and the presence of divalent ions. Among these arrangements (figure 1.6), micelles are formed by lysophospholipids and some sphingolipids, vesicles are formed by phosphatidylcholines and charged phospholipids and inverted micelles constituted under certain conditions by phospholipids such as phosphatidyl-ethanolamine.

1.3.2. Composition of lipids.

According to their chemical structure lipids are classified into phospholipids and glycolipids, sphingolipids and cholesterol (figures 1.7 and 1.8). The phosphatidic acid is a derivative of a glycerol molecule esterified by fatty acids at positions 1 and 2 and by phosphoric acid at position 3. In phospholipids, the phosphoryl group of the phosphatidic acid is itself bound to an alcohol, giving phosphatidyl derivatives of choline, ethanolamine, serine and more infrequently of inositol (figure 1.7 centre).

The long saturated aliphatic chains of the fatty acids may contain between 12 and 24 methylene groups (figure 1.7 top). In cell lipids at least one of the aliphatic chains may be unsaturated with double bonds at one or more positions.

Figure 1.7.

Types of lipids:

Phospholipids.

PHOSPHOLIPIDS.

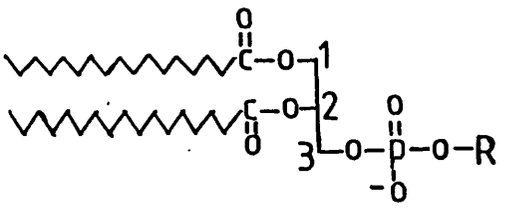

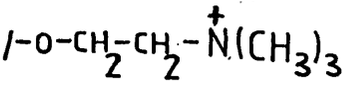

CHOLINE

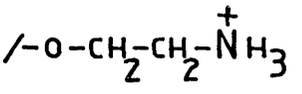

ETHANOLAMINE

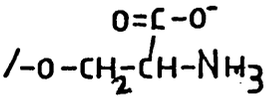

SERINE

Figure 1.8.

Types of lipids:

Sphingolipids and cholesterol.

SPHINGOLIPIDS.

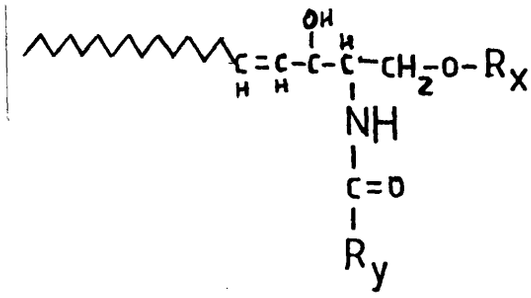

R_y = Aliphatic chain

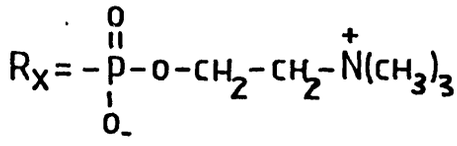

R_x = Oligosacharide

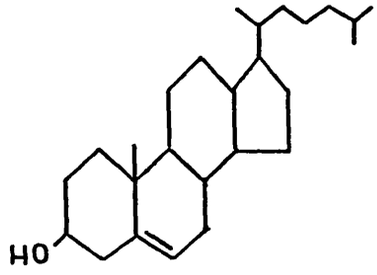

CHOLESTEROL

The most common sphingolipid is sphingomyelin, which is similar to phosphatidyl-choline in its polar headgroup, phosphoryl-choline, but with its glyceryl-fatty acid ester backbone substituted with the alcohol sphingosine. The amino group of the latter forms an amide bond with a fatty acid (figure 1.8). Other sphingolipids, such as the glycosphingolipids are relatively rare. Their polar headgroup is a linear or branched oligosachariде, sometimes modified with other groups such as in galactocerebrosides and in gangliosides.

Cholesterol is found almost entirely in the plasma membranes of mammalian cells and is absent in bacterial membranes. Its chemical structure is different to that of the above related lipids because it contains a large planar steroid apolar region with a short aliphatic chain at one end and at the other one hydroxyl group. The two parts render cholesterol with a amphiphilic character (figure 1.8 bottom).

1.3.3. Lipid phase transitions.

Phospholipids, the most abundant lipids in cell membranes, spontaneously form lipid lamellar arrangements in aqueous environments. Studies of pure phospholipid aqueous systems (Chapman, 1975) indicate that within a range of temperatures the phospholipid molecules adopt two distinct lamellar physical states: (1) the L_β state, observed at a

lower temperature, is a solid crystalline state where the phospholipid molecules are packed in a quasihexagonal array. The acyl chains are fully extended parallel to the normal of the lipid bilayer with the C-C bonds adopting an all-trans configuration. (2) In the L_α, also called the liquid-crystalline state, the phospholipid molecules can diffuse laterally at a rate of several orders of magnitude faster than in the solid crystalline state. The C-C bonds of the acyl chains form gauche isomers, causing disorder in the packing of the lipid molecules in the bilayer.

The transition between the L_β to the L_α state is a cooperative process , involving an increase in hydration of the polar headgroup and a change in the arrangement of the acyl chains to accommodate gauche isomers of the C-C bonds. The transition from the L_β to the L_α state is accompanied by lateral expansion and a decrease in the thickness of the bilayer, both due to kinks resulting from trans<-->gauche isomerization of C-C bonds of the acyl chains. In general the net effect of the phase transition is an increase in the mobility of lipid molecules and in the fluidity of the membrane. Phase transitions of aqueous suspensions formed by phosphatidylcholines are preceded by a small pretransition where the molecules rearrange to allow increased hydration of the polar headgroup, whilst keeping the acyl chains in all-trans order.

1.3.4. Modulation of the fluidity in the membrane.

Biological membranes contain many types of phospholipids. For each particular type, the enthalpy and temperature at which the phase transition occurs are influenced by the nature of the polar headgroup and the length and type of the acyl chain present. The enthalpy and temperature of the phase transition increases with the length of the acyl chain, however phospholipids with unsaturated acyl chains show a lower transition temperature due to disruption of the crystalline state by kinks created by the double bonds. Naturally occurring lipids usually contain one saturated and one unsaturated acyl chain per molecule.

Bilayers formed by phospholipids of different acyl chain length can undergo separate phase transitions, with solid and liquid phases patches coexisting in the same membrane. Phase separation is also induced by complexation of divalent cations like Ca^{2+} and Mg^{2+} to the charged headgroups of phosphatidyl-serine and -glycerol.

Inclusion of cholesterol in phospholipid aqueous systems effects important changes in the fluidity of the bilayer. The cholesterol molecule intercalates between the lipid molecules with its apolar core deeply buried between the acyl chains and the hydroxyl group forming a hydrogen-bond with the ester groups of the lipid headgroup. Above T_t, the

planar shape of cholesterol has a condensing effect upon the acyl chains of the lipid which leads to a more ordered lipid bilayer. Below T_t, the hydrogen-bonding with the lipid headgroups obstructs the close association of the headgroups of the phospholipid molecules which is necessary for the packing in the crystalline-solid state. Thus cholesterol exerts a modulating role in the fluidity of the bilayer.

1.3.5. Structure of membrane proteins.

Most of the structural analysis of membrane proteins has been based on the secondary structure prediction of bilayer-spanning α-helical domains and the alternation between the cytoplasmic and exoplasmic sides in membranes (Engelman et al., 1986). The determination of the atomic structure of membrane proteins has been extremely difficult owing to the specific properties and requirements for crystallisation in amphiphilic environments. The first model structure of a membrane protein, bacteriorhodopsin, based on cryo-electron microscopy studies of purple membrane, defined the seven α-helical domains that span the lipid membrane (Henderson & Unwin, 1975; Baldwin et al., 1988). The three-dimensional structures of other proteins such as porin (Jap et al., 1991), photosynthetic reaction-centre (Deisenhofer et al., 1985) and recently for Ca^{2+}-ATPase (Toyoshima et al., 1990) have been described at 0.25-1.5 nm resolution using cryo-electron microscopy techniques. These studies indicate that,

except for porin which shows ß-sheet strands spanning the lipid bilayer, the α-helical structure is the main motif for transmembrane domains.

1.3.6. Reconstitution of proteins in aqueous lipid systems.

1.3.6.1. Detergents.

These are compounds with amphiphilic properties, containing a hydrophobic and hydrophilic portions. Detergents are soluble in aqueous solvent, but above a certain concentration aggregate to form micelles (figure 1.6) (Tanford, 1980). The number of detergent molecules per micelle and the minimal concentration for micellization (CMC) depends on each type of detergent, the pH and ionic strength of the solvent. The hydrophobic part of the detergent can be a steroid moiety such as in cholic acid, or an aliphatic chain such as in docecyl-sulphate. The hydrophilic group can be a charged group, e.g. dodecyl-sulphate, zwitterionic, e.g. sulpho-betaines, or may have a more hydrophilic nature, e.g. glycosides.

In an excess of detergent, biological membranes are solubilised into separate micellar complexes with lipids and proteins. The functional activity of the protein in these micelles has been shown to decrease, but it usually recovers to the original levels after reconstitution in lipid mem-

branes (Jones et al., 1986).

1.3.6.2. Reconstitution of membrane proteins in lipid systems.

Detergents are used to solubilise biological membranes so that proteins are purified from the other components. The inverse process , called reconstitution, can be carried out in the presence of solubilised lipids in order to incorporate purified membrane proteins in simple phospholipid systems. Usually solutions of the lipid and protein solubilised in detergent micelles are mixed and the detergent is removed by dialysis or sucrose centrifugation. After reconstitution, many membrane proteins have been shown to recover functional activity and native structure (Jones et al., 1986).

1.3.7. Lipid-protein interaction.

Biological membranes are basically lattices of two components, lipid and protein molecules, that extend in two-dimensions continuously to enclose whole cells or separate compartments. In this lattice the lipid molecules in the bilayer act as a solvent and structural support for the proteins which would flow freely in the lipid bilayer. The study of the mutual interaction of protein and lipid in the membrane has been addressed thoroughly in simple protein-

lipid systems such as reconstituted Ca^{2+}-ATPase/lipid systems (Kleeman & McConnell, 1976).

These studies have shown that the activity of Ca^{2+}-ATPase is strongly affected by the physical state of the lipid. They indicate that in protein/lipid systems a minimum number of lipids are necessary for the protein to become fully functional (Hesketh et al., 1976). It was proposed that the protein requires these lipid molecules as solvating elements and for structural stability in order to adopt the native conformation in the membrane.

1.3.7.1. Calorimetric studies.

Studies of protein-lipid aqueous systems show that the dynamics of the lipid molecules in the phase transition is perturbed by the presence of the protein. For most cases of integral membrane proteins, the cooperativity of the phase transition and the value of its enthalpy diminish with an increase of the concentration of protein relative to the lipid. This perturbation seems to be relatively neutral, when compared to that of glycophorin and cytochrome c which interact with the lipid bilayer via electrostatic interactions with the lipid headgroups (Van Hoden et al, 1978; Chapman & Urbina, 1971). In protein-lipid systems such as cytochrome oxidase, Ca^{2+}-ATPase and lipophilin; the enthalpy of the phase transition decreases linearly with the increase

in the protein/lipid ratio (Semin et al., 1984; Gomez-Fernandez et al., 1980; Bogg & Moscarello, 1978). Below a certain value of lipid/protein ratio, the phase transition of the lipid is abolished. It has been noted that the latter value of the lipid/protein ratio in Ca^{2+}-ATPase approximates to the number of lipids shown to be necessary for function in Ca^{2+}-ATPase (Hesketh et al., 1976). The ratio lipid/protein at *H=0* would therefore be informative on the perimeter of the protein.

Freeze-fracture electron microscopy studies of some protein/lipid systems prepared below T_t, a condition necessary for the DSC measurement of the enthalpy of the phase transition, indicate that the lipid molecules tend to segregate separately in order to form pure lipid areas and protein-rich patches, where protein-protein contact is possible (Gomez-Fernandez et al., 1980; Cherry, 1979). The lipid/protein ratio for H=0 measured in DSC studies may not therefore correspond to a situation of protein molecules surrounded by a population of randomly distributed lipid molecules.

1.3.7.2. Spectroscopic studies.

Vibrational spectroscopic studies indicate that, in some protein/lipid systems above the T_t, the protein reduces the formation of C-C gauche isomers and thus increases the order of the lipid bilayer (Cortijo et al., 1982). In all cases

studied below T_t, the presence of the protein increases the proportion of gauche isomers which block the formation of all-trans isomers of the acyl chains necessary to render the crystal-solid state L_β (Cortijo et al., 1982).

Evidence of the existence of a population of lipid molecules restricted in motion by the presence of the protein has been obtained from electron spin resonance spectroscopic studies of the rotational constant of probe-labelled lipids in aqueous protein/lipid systems (Knowles et al., 1979; Ryba & Marsh, 1992). These studies indicate that above T_t, two kinds of lipid molecules occur according to their rate of motion, one corresponding to the bulk lipid and the other with restricted motion which appears only upon incorporation of the protein in the aqueous lipid system. The values of the motionally restricted lipid per rhodopsin monomer were in agreement with the number of lipids expected to surround the perimeter of a single monomer of rhodopsin (Ryba & Marsh, 1992).

Fluorescence studies of the hydrophobic probe DPH in various lipid/protein systems indicates that the increase in DPH polarization approaches a exponential curve with respect to the protein concentration. This change of DPH polarization has been evaluated with a mathematical model that proposes that the probe, free to move in the lipid bilayer,

changes its motion upon contact with a protein molecule (see section 2.6.3). The model fits the probability of occurrence of an encounter with a protein molecule of M contact sites to the change in the polarization of the fluorescence of the DPH probe in the fluid lipid bilayer (Hoffman et al., 1981; Pink et al., 1984). This mathematical model can be approached to an exponential curve $P=1-e^{-Mx}$ which enables a deduction of the number of contact sites of the protein with the probe and therefore of the approximate perimeter of the section of the protein embedded in the lipid bilayer.

CHAPTER 2.

BIOPHYSICAL TECHNIQUES.

2.1.INTRODUCTION.

In this chapter the principles of infrared spectroscopy for the study of the structure of biomolecules such as proteins and lipids are presented. The methods of DSC and fluorescence depolarization for the study of the dynamics of lipids and proteins in membranes are introduced.

2.2. INFRARED SPECTROSCOPY.

2.2.1. Introduction to the infrared spectra.

Infrared radiation corresponds to a broad region of the electromagnetic spectra ranging from frequencies of 10^{12} to 10^{14} Hertz, or in wavenumber units 100 to 10,000 cm^{-1}. The energy of these photons covers the range of energies required to effect changes in the energy levels of the molecular vibrations.

According to quantum law, molecules can attain only a discrete number of vibrational energy levels. Transitions between energy levels can only occur via the absorption of electromagnetic radiation of energy equal to the difference between the energy levels of the vibrational states.

In order for a vibration to be infrared active, it must effect a net change in the dipole moment of the molecule. Only heteroatomic molecules have a dipole moment. Figure 2.1.1. shows a diagram of the stretching vibration of the methylene molecule. This consists of a periodic motion of the atoms along the chemical bond that approximately obeys the motion of a simple harmonic oscillator of a defined frequency (10^{12} to 10^{14} Hz in molecules). The stretching vibration of the atoms causes a periodic change in the dipole moment of the molecule and hence creates an electromagnetic fluctuation of equal frequency to that of the vibration.

Figure 2.1.

Stretching vibration of the methylene group.

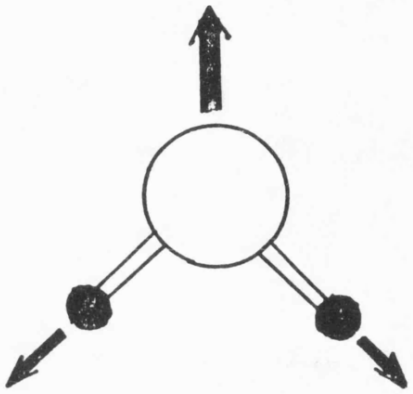

Figure 2.2.

Fundamental vibrations of the methylene group.

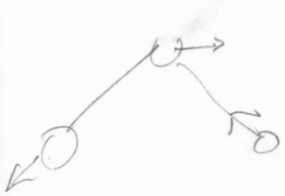

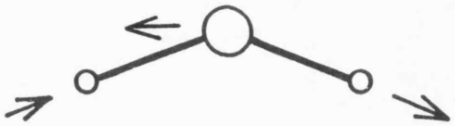

Anty-
-symmetric
stretching

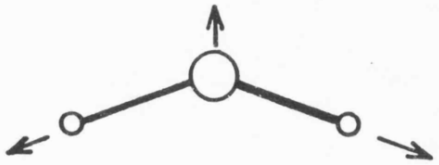

Symmetric
stretching

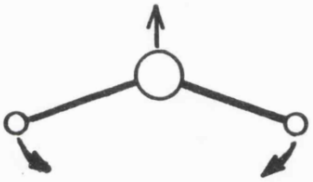

Deformation

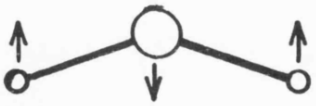

Wagging

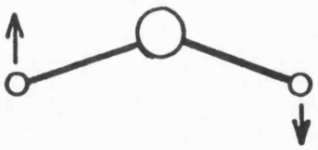

Twisting

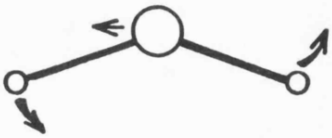

Rocking

The vibrational motion in a molecule of *N* atoms can be described by the three coordinates in the space. The number of possible vibrations in such a molecule is *(3N - 6)* and *(3N - 5)* for a linear molecule, where *6* accounts for the rotation and translation motions of the entire molecule. The infrared absorption band of the methylene groups of a biomolecule of *N* atoms such as a polypeptide cannot be assigned to the vibration of a single methylene group. Rather it is the contribution from all the methylene groups of the molecule, vibrating independently of each other. These are called the fundamental vibrations. As shown for the methylene group in figure 2.2, these fundamental vibrations are named as stretching, bending, twisting and deformation, whose bands appear in order of decreasing frequency in the infrared spectra.

Other types of vibration rarely important in studies of biomolecules are those that arise from overtones of fundamental vibrations and others such as combinations of two vibrations. When two vibrations of the same group have close frequencies, a mutual interaction takes place which changes the frequency and intensity of both bands. This coupling is called 'Fermi resonance.'

TABLE 2.1.

Infrared bands characteristics of phospholipids[a]

Group	Frequency (cm^{-1})	Vibration
R-C=O \ O-R	1,735-40	-C=O stretching \
	1,180-1,100	-C-O-C stretching (Antisy.&Symm.)
O / R-O-P=O \ O-R'	1,250-30	Antisym. PO_2 stretching
	1,150-30	Symm. PO_2 stretching
$R-CH_3$	2,965-55	Antisym. stretching
	2,870-80	Symmet. stretching
$R-CH_2-R'$	2,925-35	Antisym. stretching
	2,850-60	Symmet. stretching
	1,440-60	Antysym. bending
	1,370-5	Symmet. bending
$R-CH_3$	1,200	Wagging
$R-CH_2-R'$	1,180-1350	Wagging

[a]Data obtained from Fringeli & Gunthard (1981).

2.2.2.Infrared bands of biomolecules.

2.2.2.1. Phospholipids.

Infrared bands that originate from the polar headgroup and the acyl chains of phospholipids provide information about the extent of hydration and dynamics of phospholipids, specially phosphatidylcholine, in membranes (Fringeli & Gunthard, 1981). The bands and their origin are listed in table 2.1. From the polar headgroup, the band at approximately 1735-40 cm^{-1} arising from the stretching vibration of C=O ester group undergoes a change in frequency during the phase transition, usually explained as an increase in hydration. Similar changes are observed in the bands of the ester C-O-C stretching vibration at 1180 and 1,100 cm^{-1} and the P=O stretching vibrations observed at 1250 and 1150 cm^{-1}. Other bands such as those specific of the choline group, appear below 1000 cm^{-1} and are difficult to study in aqueous solutions due to the low transmission properties of optical materials e.g. CaF_2 in certain frequency ranges.

For the hydrophobic acyl chains the bands of the CH_2 stretching vibrations at 2935-2850 cm^{-1} show a decrease in frequency along the phase transition, indicating the appearance of gauche isomers along the chains. Bands at 1450-1370 cm^{-1} originate from bending vibrations and those at 1180-1350 cm^{-1} from wagging vibrations of methylene groups. The bands corresponding to a symmetric CH_3 stretching and wag-

ging modes that appear at 2870-80 and 1200 cm^{-1}, respectively, and show a marked dichroism in oriented lipid films (Fringeli & Gunthard, 1981).

Most of these bands from the polar headgroup and the apolar acyl chains show some dichroism in their intensity in oriented films of phospholipid when studied with polarized infrared radiation. This is the case for the bands that correspond to vibrations of the CH_3 group, the C-O-C and the P=O group.

2.2.2.2. Proteins.

In proteins, the infrared spectra is dominated by bands that originate from vibrations of the amide groups of the polypeptide chain (Susi, 1969). There are a total of nine amide bands: the amide A and B, and amides I-VII, which are observed in order of decreasing frequency along the infrared spectra of proteins (see table 2.2).

The amide A band corresponds to the N-H stretching and overlaps with the amide B band at a frequency of 3400-3300 cm^{-1}; the amide B corresponds to the first overtone of the amide II vibration (table 2.2 and figure 2.3). Fermi resonance between both vibrations affects the intensities and frequencies of both amides A and B. The amide I band appears at 1700-1600 cm^{-1} and corresponds primarily to the stretching mode of the C=O of the amide group with weak contribu-

TABLE 2.2.

Infrared bands characteristic of proteins[a]

Name	Frequency(cm^{-1})	Vibration
A	3300	N-H str.
B	3100	amide II overtone
I	1700-1600	C=O str. (80%), N-H b. (10%) C-N str. (10%)
II	1575-1480	N-H b. (60%), C-N str. (40%)
III	1300-1230	C-N s., N-H b., C=O s., CO-N b.
IV-VII	800-200	CO-N b., N-H b., C=O b., others

str.: stretching

b.: bending

[a]Data obtained from Susi (1969).

Figure 2.3.

The vibrational modes of the peptidic bond.

AMIDE A

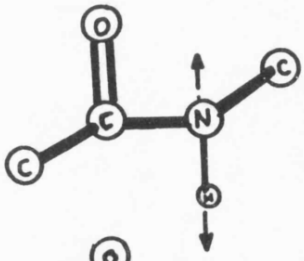

AMIDE B

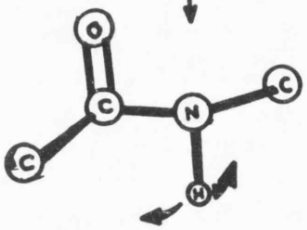

AMIDE I

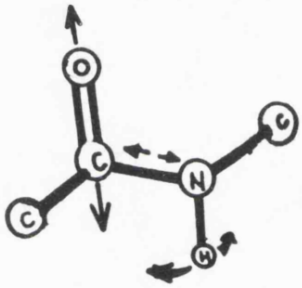

AMIDE II

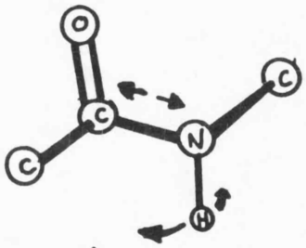

AMIDE III

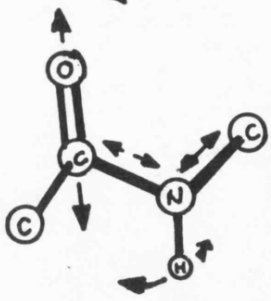

tions from C-N stretching and N-H bending modes (table 2.2 and figure 2.3). The amide I band and the amide A band are in-plane modes and the direction of their transitional vibrational moments coincide approximately with that of the amide plane. The frequency of the amide I band is very sensitive to the secondary structure present in proteins (Susi, 1969).

The amide II band appears at 1590-1500 cm^{-1} and is a mixture of two modes: the N-H bending and the C-N stretching vibrations. It has therefore an in-plane and an out-of-plane modes. The amide III band is observed at 1300 cm^{-1} and arises from a number of vibrational modes, it is therefore of limited use in the analysis of the structure of proteins. The amide IV-VII are seen in a region of the spectra between 800-200 cm^{-1} which is difficult to study or is outside of the range of the normal infrared spectrometer.

2.2.3. Assignment of secondary structures.

The basis of the assignment of protein secondary structure to the amide I band is based on experimental evidence and mathematical analysis of the molecular vibrations (Jackson et al., 1989a; Krimm & Bandekar, 1986). Each protein secondary structure has its own unique hydrogen-bonding pattern between the oxygen of the amide C=O groups and the hydrogen of the N-H groups of the polypeptide backbone. The

hydrogen-bonding and the molecular geometry in each secondary structure affects the electron density of the C=O group, and hence the frequency of the infrared absorption for each secondary structure (Susi, 1969).

Approaches to the prediction of amide I band frequencies are based on force-field analysis of the molecular geometry of the vibration of the atoms intervening in each secondary structure (Susi, 1969). Most recent approaches have included another term, the transition dipole coupling, and accounts for the band split observed in spectra of proteins rich in ß-sheet structures (Krimm & Bandekar, 1986; Torii & Tasumi, 1992). In general the application of this approach is very useful for the prediction of the band frequencies of secondary structures and is currently the only guide for the prediction of the frequencies of turn structures (Bandekar & Krimm, 1979).

Early experimental work on the structure of polypeptides such as poly-L-glutamic methyl ester indicated that the frequency of the amide I band was closely associated with the secondary structure present (Elliot and Ambrosse, 1950). These studies indicated that ß-sheet rich polypeptides tend to absorb at lower frequencies than those rich in α-helical structures. Studies in aqueous media of polymers of single aminoacids such as polyalanine and polylysine, under conditions that promote α-helix or ß-sheet confirmed previous

predictions (Susi et al., 1967).

With the application of computers and the interactive treatment of spectra, it has been possible to obtain the spectra of the amide I and II bands of proteins in aqueous solution. These studies indicate that the amide I and II bands are formed by components overlapping underneath the complex band envelope (Byler & Susi, 1986). Over the years a series of experimental observations have been made in order to analyse the amide I and II bands and assign the components to each type of secondary structure present (table 2.3).

2.2.3.1. Assignments to the α-helix.

Vibrational analysis for α-helical models predicts a strong band between 1650-8 cm^{-1} (Krimm & Bandekar, 1986). Typically the intensity of bands at those frequencies has been shown to correlate well with the content in α-helix as studied by CD spectroscopy and X-ray diffraction (Byler & Susi, 1986). To ensure the correct assignment to α-helical structures, spectra are also recorded in ^2H_2O where bands of random structures show a 10 cm^{-1} shift and do not overlap with α-helical bands (Susi, 1969; Jackson et al., 1989a; Surewitz & Mantsch, 1988).

TABLE 2.3.

Main assignments for protein secondary structures in H_2O solution

Band frequency (cm^{-1})	Assignments
1630-40	ß-sheet
1650-55	α-helix/random coil
1670-60	ß-turns
1690-70	ß-sheet/ß-turns

Main assignments for protein secondary structures in ^2H_2O solution

Band frequency (cm^{-1})	Assignments
1630-40	ß-sheet
1650-45	Random coil
1650-55	α-helix
1670-60	ß-turns
1690-70	ß-sheet/ß-turns

Byler & Susi (1986) have observed an amide I band component at 1640 cm^{-1} in α-helical proteins such as cytochrome C and hemoglobin. It was suggested that this component arises from distorted α-helical residues or part of other structures such as a turn or a 3_{10}-helical structure.

In some soluble proteins with solvent-exposed α-helical segments, e.g. calmodulin, the frequency of the amide I band in ^2H_2O is observed to undergo a shift of 10 cm^{-1} to approximately 1645 cm^{-1}. This has been attributed to solvation of the exposed α-helical segments by ^2H_2O molecules that possibly reduces the frequency of the amide I band (Jackson et al., 1991).

2.2.3.2. Assignments to the ß-sheet.

Components of antiparallel ß-sheet usually give rise to at least two elements in the amide I band, one of them strong at 1630-40 cm^{-1}, the other weak between 1675-85 cm^{-1} (Susi & Byler, 1987). Both frequencies are in agreement with vibrational analysis (Bandekar & Krimm, 1986).

Vibrational analysis predicts a band frequency at 1646 cm^{-1} for parallel ß-sheet structures and therefore it is theoretically distinguishable from the frequency of antiparallel ß-sheet structures (Bandekar & Krimm, 1986). FT-IR studies of proteins containing the two types of ß-sheet do not show this, first, because the frequencies of bands of ß-

sheet structures seem to spread over a range of frequencies between 1645-25 cm^{-1} and second, bands at 1675-85 cm^{-1} are also observed, however with lower intensity, in proteins containing only parallel ß-sheet (Susi & Byler, 1987).

The frequency of the bands associated to ß-sheet structures may undergo a shift in ^2H_2O solution (Olinger et al., 1986). This has been interpreted as a structural difference in terms of backbone hydrogen-bonding and has been shown to occur from a difference in the degree of $H/^2H$ exchange (Byler & Susi, 1986; Haris et al., 1986).

2.2.3.3. Assignments to the ß-turns and the 3_{10}-helix.

Vibrational analysis for several types of ß-turn (I, II and III) indicates that their frequencies spread over a wide range between 1690-1655 cm^{-1} but have been suggested to be more intense at 1695-1670 cm^{-1} (Bandekar & Krimm, 1979; Susi & Byler, 1983). The fact that bands of ß-turns and those of ß-sheet overlap, makes individual assignment difficult and in practice only possible for those bands at 1660-5 cm^{-1}.

Synthetic peptides containing stable 3_{10}-helical structures absorb at 1660-7 cm^{-1} (Kennedy et al., 1991). As this structure is not usually observed alone in protein structures but as part of ß-turns (see section 1.2.2.4.), the 3_{10}-helical bands tend to be assigned to ß-turn structures.

2.2.3.4. Assignment to random structures.

These structures give rise to bands around 1650-5 cm^{-1} in H_2O and shift down to 1640-50 cm^{-1} upon $H/^2H$ exchange due to peptide-to-solvent bonding (Susi, 1967). As the amide groups of random structures have been shown to undergo rapid $H/^2H$ exchange, it is usual to evaluate the percentage of these structures when the $H/^2H$ exchange of the protein is near completion as indicated by the absence of intensity in the amide II band.

The presence of an amide I band component at 1650-9 cm^{-1} in ^2H_2O solution has been noted for some proteins with none or low α-helical content as deduced from CD or X-ray data of homologous proteins (Wilder et al., 1992; Prestrelski et al., 1991). Those components were provisionally assigned to the loops or single-stranded chains of non-amide hydrogen-bonded C=O groups.

2.2.3.5. The amide II band.

The amide II band appears at 1570-1525 cm^{-1} overlapping with components of aminoacid sidechains. Studies of the infrared spectra of synthetic polypeptides with a ß-sheet conformation, e.g. ß-polyalanine or polyglycine, show an amide II band at 1525 cm^{-1} (Krimm & Bandekar, 1986), whereas the α-helical band appears at 1545 cm^{-1}. In proteins in aqueous solution, however, the amide II band frequency is

not sensitive to the type of secondary structure present, usually arising at 1555-45 cm^{-1}. It usually shows a 10 cm^{-1} shift down in frequency upon drying in films, probably as a result of dehydration (Koenigg & Tabb, 1980).

The amide II band originates from bending vibrations of the N-H group of the amide groups. In ^2H_2O solution the N-H groups form N-^{2}H upon H/^{2}H exchange whose frequency appears at 1450 cm^{-1}. By observing the rate of decrease in intensity of the amide II band, it is possible to obtain an indication of the degree of accessibility of the structure to the solvent and of changes in protein stability occurring in response to ligand-binding, temperature. The degree of H/^{2}H exchange can be estimated by measuring the amide I band to amide II band intensity ratio with respect to the band ratio in the spectra in H_2O (Rath et al., 1991; Lee et al., 1987).

2.2.3.6. Contributions of aminoacid side-chains.

Early observations indicated that some aminoacid side-chains absorb in the infrared region corresponding to the infrared amide I and II bands of proteins in H_2O (Chirgatze et al., 1975). Recent detailed studies (Venyanimov & Kalnin, 1990) have shown that glutamine, asparagine and arginine sidechains absorb along the amide I band spectra but with more intensity at 1670-80 cm^{-1}. Contributions of sidechains of other aminoacids are negligible in the amide I band.

Glutamic and aspartic acid sidechains (ionised at neutral pH) show bands at 1560 and 1580 cm^{-1}, but appear above 1700 cm^{-1} as a result of disionization. The in-plane ring vibration of the phenolic group of ionised tyrosines appears at 1515 cm^{-1}, usually as a narrow band. The contribution of each aminoacid sidechain to the amide I and II band will depend on the content of each aminoacid in the protein.

2.2.4.Quantitative analysis of secondary structure.

2.2.4.1. Curve-fitting analysis.

This procedure was proposed by Byler & Susi (1986) for the estimation of α-helical and ß-sheet structures. This method relies on the fact that the amide I absorption (1700-1620 cm^{-1}) of a protein is comprised of several component bands, each with different widths and heights, and whose values can be determined to enable the reconstruction of the original amide I band envelope. Initially, a choice of the number of components and their frequencies is made from the second derivative spectra. With those components recognised, the curve-fitting method will match the original amide I band envelope or the band-narrowed amide I band (usually the deconvolved spectra) with the sum of the components already identified. The curve-fitted band is iteratively adjusted in frequency, height and width, until a satisfactory match to the band-narrowed amide I band is reached. The areas of the

components are quantified and then assigned to different types of secondary structure.

Susi & Byler (1986) showed that the calculated estimates of secondary structures are in agreement with X-ray data of a number of reference proteins containing both α-helical and ß-sheet structures with standard errors of 2.5 and 2.7%, respectively. However for proteins of high α-helical content, such as hemoglobin and myoglobin, the estimations for α-helix are lower than those deduced by X-ray analysis. The differences of the prediction for α-helical structures with respect to those obtained from X-ray analysis have been attributed to some amide residues situated in the α-helix termini, showing bands at lower frequencies than those typical of α-helices.

The most important criticisms to this method are that, firstly, the choice of the band elements is made eventually subjective as more components have to be added for a satisfactory fit; secondly the components have a type of band-shape (Lorentzian, Gaussian or a combination of both); thirdly it assumes that the molar absorptivities for each secondary structure are the same and finally that several solutions to the curve-fitting 'problem' can be obtained.

2.2.4.2. Factor analysis.

This technique has been proposed by Lee et al. (1990) to carry out the calculation of percentages of α-helical, ß-sheet and turn secondary structure of proteins using multifactorial regression analysis. Lee and cooworkers (1990) applied the programme CIRCOM (computerised infrared characterization of materials), released by Perkin-Elmer Ltd, to construct a calibration set of secondary structure values via regression analysis with the infrared amide I and II bands of a pool of proteins of known secondary structure (as determined from X-ray diffraction data). The amide I band (1700-1600 cm^{-1}) in the difference spectra of proteins in H_2O was shown to have maximum correlation between the percentages of secondary structure obtained from X-ray diffraction data and those predicted by multifactorial regression. The standard errors of prediction are: 3.9% for α-helix, 8.3% for ß-sheet and 6.6% for turns. The contributions of aminoacid sidechains are included in the standard error for the prediction of each secondary structure.

The advantages of this method is that (1) no spectral manipulation are required, (2) no identification and assignment of components is involved, therefore no subjective judgments are introduced and finally (3), unlike in previous methods, the quantification of secondary structures values is made automatically. The predictions of secondary struc-

ture for proteins of structure or spectral properties different to those of the reference proteins may not be accurate. It is expected that this situation will be solved with the inclusion of spectra of novel proteins in the data bank of reference spectra.

2.3.DATA ACQUISITION IN INFRARED SPECTROSCOPY.

2.3.1. Introduction.

The generation of the infrared spectra of a biological material can be performed in two different ways with the current instrumentation. In the dispersive spectrometer, a beam of continuous infrared radiation is dispersed via a prism or grating into an array of its component waves. A slit allows a small range of frequencies to be transmitted to the sample. This operation is repeated for all components of the frequency range to cover the infrared spectra of interest. The resolution can be increased by narrowing the range of frequencies studied, but this reduces the energy arriving to the detector, thus decreasing the SNR. With some instruments the spectra can also be submitted to limited mathematical manipulation, such as interactive subtraction and second derivative.

In the interferometry-based instrument, the continuous infrared beam is encoded in an interferogram which, after Fourier Transformation, is reconstructed into the spectra of

the infrared beam. This second approach offers advantages over the dispersive methods in terms of SNR, frequency accuracy and reduction of the time to collect spectra. Further spectra treatment enables the use of interactive subtraction and band-narrowing methods such as deconvolution.

2.3.2. Interferometry and Fourier transformation.

The interferometry in a FT-IR instrument, such as the one used in these studies, the Perkin-Elmer series 7450 equipped with a TGS detector, follows the basic instrumental design of the Michelson interferometer (see diagram in figure 2.4 centre). In the setup of the interferometer, a continuous infrared radiation illuminates the sample and the transmitted beam reaches the beam-splitter. There the beam is divided, half being reflected to the moving mirror and the other half transmitted to the fixed mirror. The bounced beams recombine back at the splitter and again are half-reflected and half-transmitted to the source and to the detector.

Consider now that one mirror is fixed and the other moves away from the splitter. When the distances from the splitter to each of the mirrors are equal, all wave components will be in-phase at the beam splitter and recombine constructively, and maximum intensity is read at the detec-

Figure 2.4.

The Michelson interferometer (centre).

Interference of cosine waves at the beam splitter (bottom).

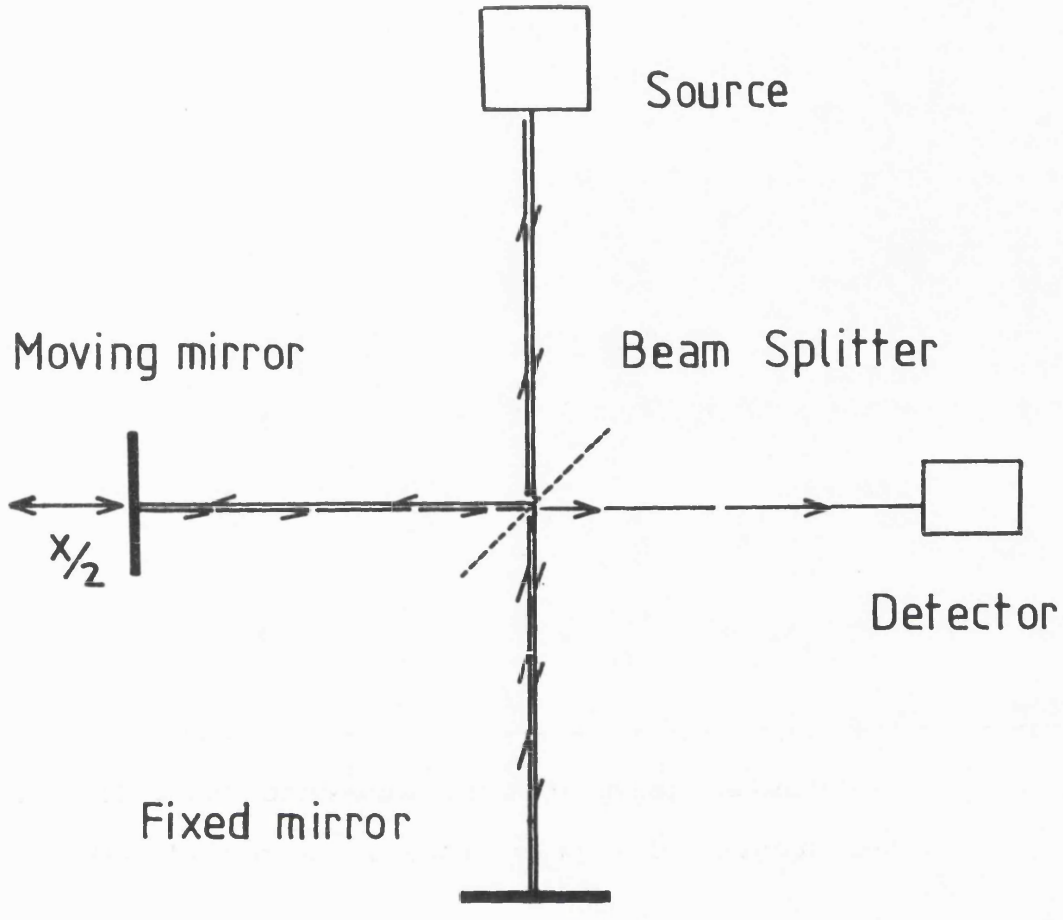
Source
Moving mirror
Beam Splitter
x/2
Detector
Fixed mirror

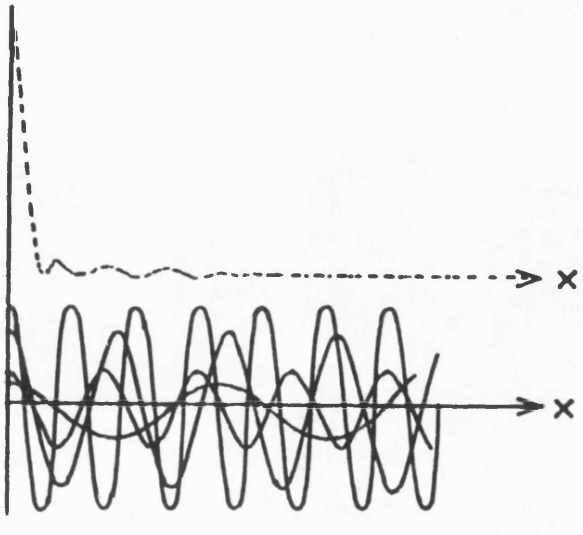
x
x

Figure 2.5.

Interferogram of monochromatic beam (top). Interferogram of a polychromatic beam (bottom).

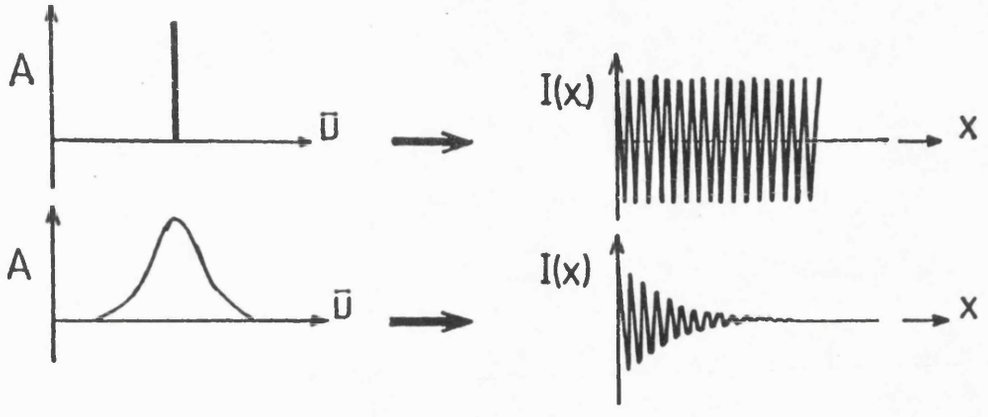
A
Ū
I(x)
x
A
Ū
I(x)
x

tor. A displacement of the moving mirror introduces a path difference between the beams, as one travels further than the other before recombining at the splitter. As a result the waves recombine out-of-phase and therefore they interfere destructively to varying degrees that will depend on the frequency of each cosine wave and the magnitude of the path difference (see diagram in figure 2.4 bottom).

For a monochromatic beam, the intensity of the recombined beam I(x) measured at the detector varies sinusoidally as the mirror moves with constant velocity (figure 2.5 top), whereas for a polychromatic beam the intensity I(x) is seen to diminish gradually with the sweep of the moving mirror (figure 2.5 bottom). An interferogram of a polychromatic beam is proportional to the sum of the cosine waves of its components, each cosine wave expressed in terms of amplitude A_i, frequency V_i. The superimposed waves give the intensity reading, I_x, of the interferogram for a path difference x, where $I_x = \Sigma_i A_i cos(2\pi V_i x)$ (figure 2.4 bottom and 2.5 bottom). The information about the radiation frequencies and amplitudes is therefore gathered in the interferogram.

By extrapolating the equation $I_x = f(V_i, x)$ to a single beam spectra consisting of a continuum of frequencies V_i, an integral expression is obtained which can be described by a pair of Fourier transforms:

$$I(x) = \int_{-\infty}^{\infty} B(V)\ cos2\pi Vx.\delta V$$

$$B(V) = 2\int_{0}^{\infty} I(x)\ cos2\pi Vx.\delta x$$

The latter expression corresponds to the 'frequency-domain' mode of presentation of the intensity $B(V)$ and, in principle, it is possible to obtain the spectrum by FT of the interferogram (Griffiths and De Haseth, 1986). However, a finite limit $2L$ has to be taken for the displacement of the moving mirror, which results in a truncation in the interferogram. After Fourier transformation this results in a spectra with a defined resolution V_r, where $V_r = 1/2L$ This operation creates sidelobes about the bands, therefore distorting their shape (figure 2.6 top). To circumvent this, the interferogram $I(x)$ is multiplied by an apodization function, e.g. triangular function, (figure 2.6 centre and bottom). This minimises the distortion of the side lobes, while maintaining the real absorption band.

The analysis of the infrared spectra using FT of Interferograms offers several advantages over the conventional Dispersive Spectroscopy:

(a) Jacquinot's Advantage. The energy throughput of the FT-IR spectrometer is determined only by the area of the interferometer mirror that is being illuminated, therefore

Figure 2.6.

(A). FT of truncated interferogram of a polychromatic beam.

(B). FT of apodized interferogram of a polychromatic beam. (Centre) Triangle function used for apodization.

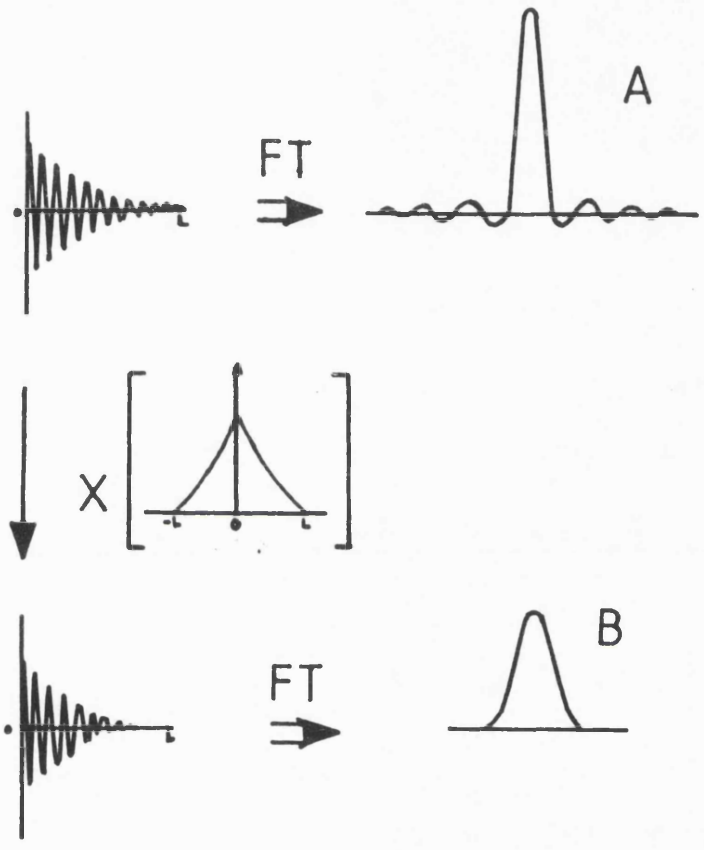
A
FT
X
B
FT

most of the beam is used and therefore the SNR is high. This is different in the dispersive spectrometer, only a fraction of the infrared radiation traverses through in the direction of the exit-slit in order to ensure a certain resolution. If the resolution is doubled, the energy throughput and SNR are reduced by two orders of magnitude.

(b) Fellgett's Advantage. As compared with the dispersive spectrometer, the time required to obtain a spectra for identical SNR and resolution, is considerably reduced.

(c) Conne's Advantage. For the calibration of the frequency, the dispersive instrument relies on external standards and the steady reproducibility of the gearing mechanisms of the grating and prisms. The FT-IR instrument uses an internal standard, the interference fringes of a He-Ne laser, which signal regularly the path-difference spacing. These are used to control the correct motion of the mirror.

2.4. BAND-NARROWING TECHNIQUES.

2.4.1. Introduction.

In studies of biomolecules, some infrared bands (e.g. the ester carbonyl in phospholipids and the amide I in proteins) are comprised of several overlapping components which arise from the various conformers or species present. The natural bandwidth of those components underneath the band envelope is broad relative to their separation in frequency. An increase in resolution of the spectra does not

Figure 2.7.

Fourier self-deconvolution (see section 2.4.2. for explanations).

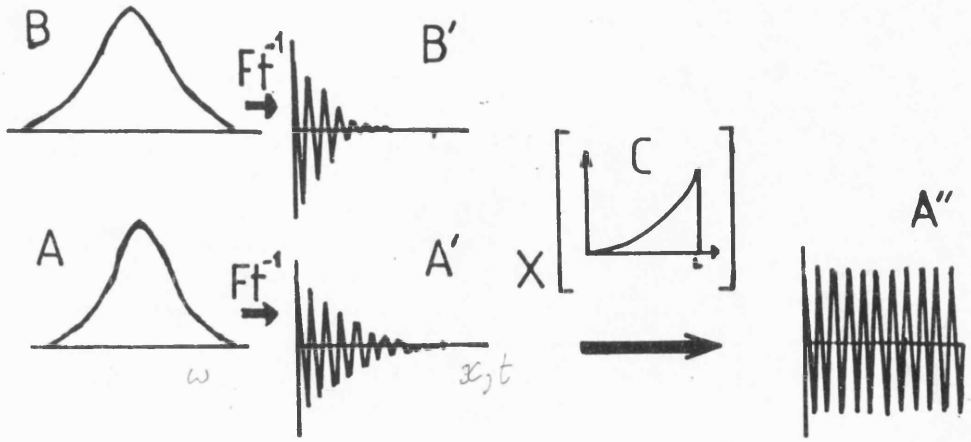
B
Ft⁻¹
B'
A
Ft⁻¹
A'
ω
x, t
X
C
t
A''

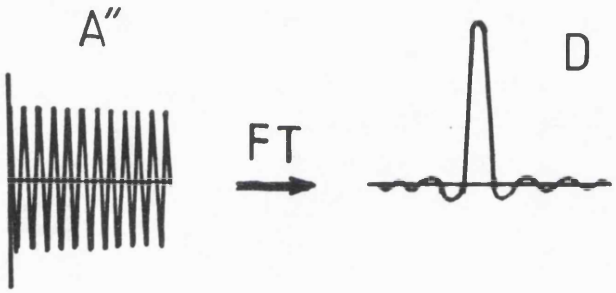
A''
FT
D

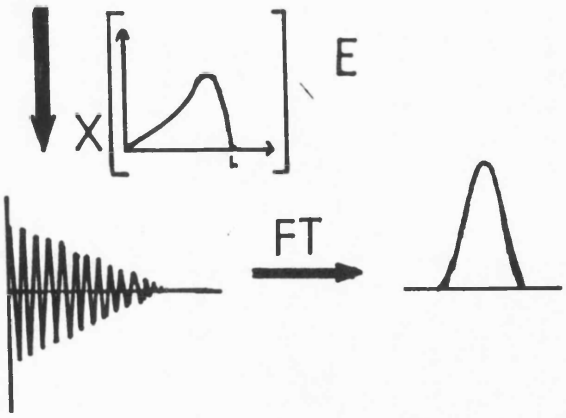
X
t
E
FT

reduce the widths of the component bands and therefore the band envelope is maintained. With the aid of mathematical methods it is possible, however, to "artificially" narrow the widths of those component bands to make them partially or fully resolved.

2.4.2. Fourier self-deconvolution.

Consider that single absorption line corresponding to a polychromatic beam can be approximated to the shape of a Lorentzian function with a bandwidth, σ, (figure 2.7A). Its inverse FT gives a cosine function that decreases exponentially at a rate which is dependent on the bandwidth σ (figure 2.7A'). If σ is increased (figure 2.7B), the rate of the decay of the cosine wave is increased (figure 2.7B'). Multiplying the cosine wave by a exponential function whose increase depends on σ (figure 2.7C), the decay of the cosine wave is eliminated (figure 2.7A''). Upon FT, the observed bandwidth is narrowed compared to that of the original Lorentzian function band (figure 2.7D) (Kauppinen et al., 1981). The side lobes generated by this process can be reduced in the deconvolved spectra by multiplication with an apodization function (figure 2.7E).

Deconvolution of the infrared spectrum of a protein can be achieved without marked distortions to the spectra. Beyond a certain limit the baseline shows spurious bands as a

result of overdeconvolution and enhancement of water vapour bands. It is therefore necessary to use spectra of high SNR and recorded in dried atmosphere.

The degree of deconvolution in a spectrum is given by a resolution enhancement factor K, where $K = \sigma/\sigma'$ and σ and σ' correspond, respectively, to the selected halfwidth half-height (HWHH) and the finally narrowed HWHH (Susi & Byler, 1986). There are several assumptions to be made prior to the deconvolution of spectra: (a) as the natural bandwidth is unknown, it has to be estimated from a preconceived estimation of the actual widths. (b) All component bands are assumed to have equal bandwidths. (c) Absorption bands are assumed to have Lorentzian shape and to be symmetrical, this is not the case for some infrared bands which are not necessarily symmetrical. For bands of Lorentzian shape, the areas of the deconvolved bands are proportional to those originally present in the original band envelope. This is not necessarily the case for non-Lorentzian bands. (d) The degree of noise enhancement in the band-narrowed band can be estimated only by observing the noise and sidelobes created in 'absorption-free' parts of the deconvolved spectra.

2.4.3. Second derivative.

This method is used to calculate the rate of change of slope along the spectra over a range of datapoints.

For a band of Lorentzian shape, the application of second derivative results in a narrowing of the band, where the height of the 'narrowed' band is $A' = -2A_o/\sigma^2$, where A_o is the original height and σ, the HWHH. The HWHH of the 'narrowed' band is $\sigma' = \sigma/2.7$ (Kauppinen et al., 1981). In general the second derivative enhances sharp bands relative to the broad absorption bands observed in biomolecules. The second derivative spectra are usually smoothed, otherwise the signal-to-noise ratio is degraded to significantly distort the spectra.

2.5. SAMPLING MODES.

2.5.1. Measurements in the transmission mode.

Infrared studies of organic materials in aqueous samples are severely hindered by the strong absorptivity of H_2O in regions of the infrared spectra such as 3500-3000 and 1700-1550 cm^{-1}, as is indicated in figure 2.8. As these infrared bands overlap with those of the protein, i.e. amide A, I and II bands; infrared studies had been limited until recently to qualitative studies of biological material, and in particular, to studies of the amide I band in ^2H_2O solution (figure 2.8) (Susi et al., 1967). The use of interactive routines, such as IDIFF of Perkin-Elmer, enables the subtraction of components of the spectra that originate from the aqueous solvent. However the acquisition of protein

Figure 2.8.

Transmittance spectra of H_2O (solid trace) and ^2H_2O (dashed trace).

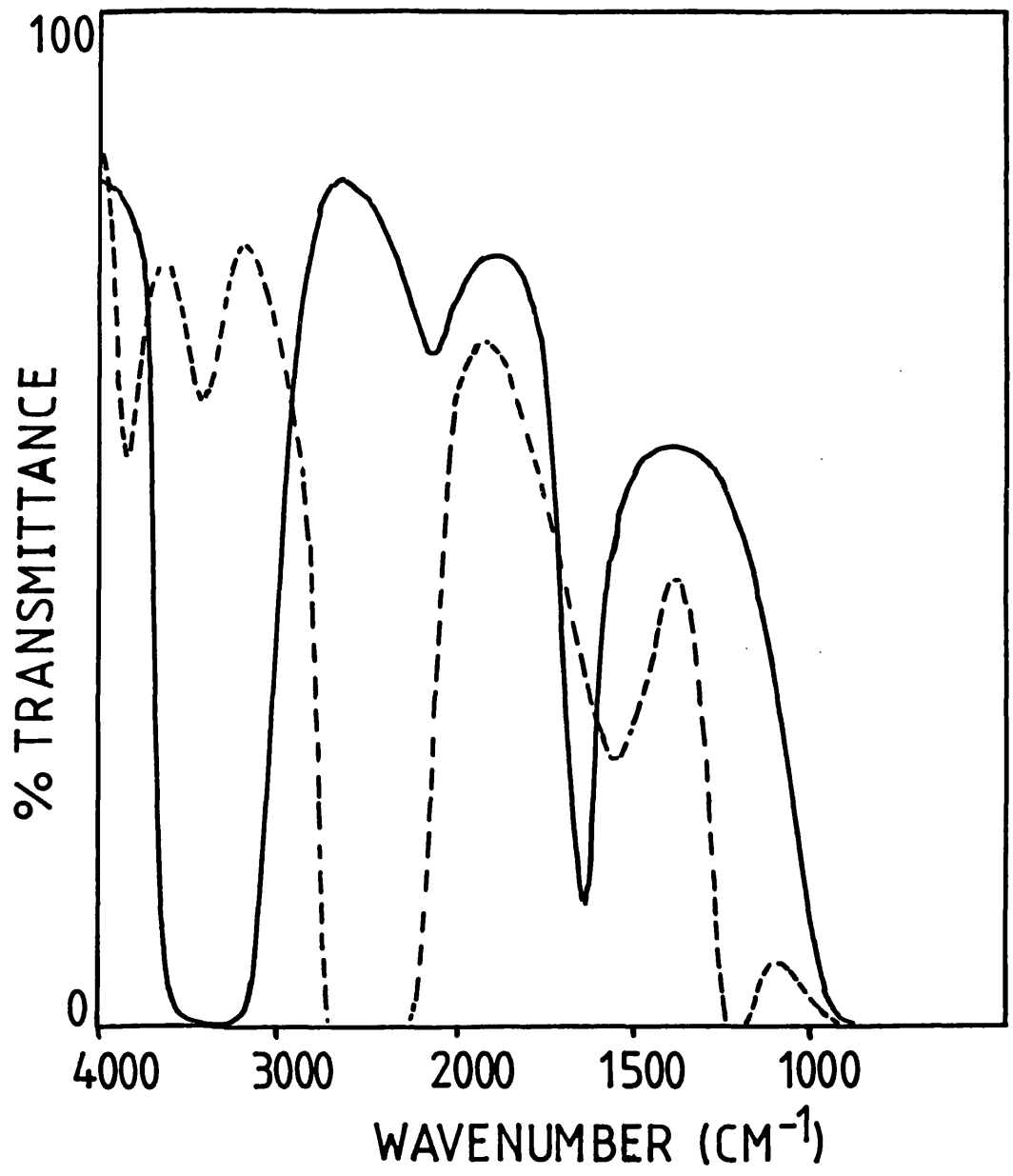
100
0
% TRANSMITTANCE
4000
3000
2000
1500
1000
WAVENUMBER (CM^{-1})

Figure 2.9.

Absorbance spectrum of water vapour in atmospheric air.

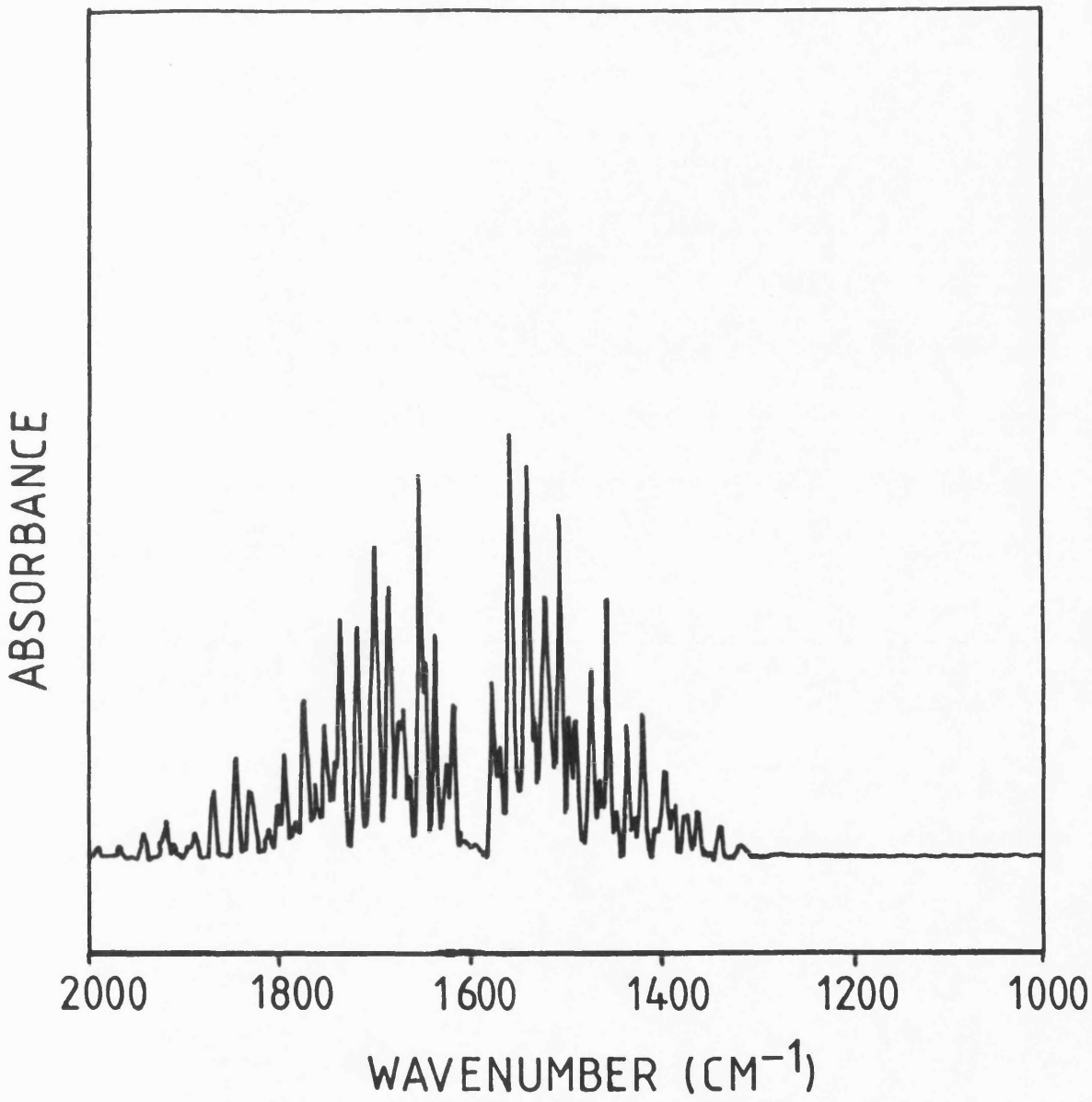
ABSORBANCE
2000
1800
1600
1400
1200
1000
WAVENUMBER (CM^{-1})

spectra is still complicated by the strong absorption of the solvent in those regions of interest. This problem is overcome with the use of short sample pathlengths, 6-12μm for H_2O and 25-75μm for ^2H_2O solutions, and working with high concentrations of protein of 2.5-5% w/w. Typically buffer and sample spectra are recorded separately and subtracted, to obtain the difference spectra of the protein.

The appearance of sharp bands due to the presence of water vapour (figure 2.9) is commonly observed in studies of the amide I and II region of the spectra of proteins. The infrared measurements are therefore carried out in a closed chamber, purged constantly with dried air under positive pressure to ensure non-penetration of outside air to the instrument parts. Otherwise traces of water vapour in the protein spectra are subtracted using a prerecorded water vapour spectrum, as judged by a flat baseline in the infrared region of 1800-1700 cm^{-1}.

Liquid or film samples are typically placed between two CaF_2 windows, enclosed in a cell and mounted in a thermostated cell holder. Along the work to be described, approximately 50 μl of sample were placed between two CaF_2 windows separated by a 6 μm tin spacer for samples in H_2O or 50 μm teflon spacer for samples in ^2H_2O. Solid samples, such as particulates and silk, can be studied in KBr discs or as films preserved inside the mountable cells.

2.5.2. Measurements using Attenuated Total Reflectance.

A beam propagating inside a prism of a infrared transmitting material of high refraction index (n_2) will undergo internal reflection at the air-prism interface (figure 2.10 left) if the beam falls with an incidence angle smaller than a critical angle ϕ_c, where $sin\ \phi_c = n_{air}/n_2$. At those points of reflection the beam transverses the interface into the external medium as a evanescent beam, whose intensity R decreases exponentially with the distance from the interface (figure 2.10 right).

The distance at which the intensity of the beam is $1/e$ (37%) of that in the interface is termed penetration depth (dp). The value of dp is dependent on many variables, such as the wavelength and the angle of incidence of the beam on the prism face, i.e. for our germanium prism of incidence angle 45°. The dp corresponds to approximately one tenth of one wavelength (dp is approximately 0.650 μm for an infrared frequency of 1600 cm^{-1}).

The fact that the evanescent beam penetrates a small distance into the outer medium allows the selective study of thin films or coatings on the surface of the prism. In theory, varying the angle of incidence would permit measurements to be made to different penetration depths in the material in contact with the prism. A useful application of

Figure 2.10.

Internal reflectance in a prism and electric vectors of polarized infrared radiation (left).

Decay of intensity R with distance from the interface (right).

y axis

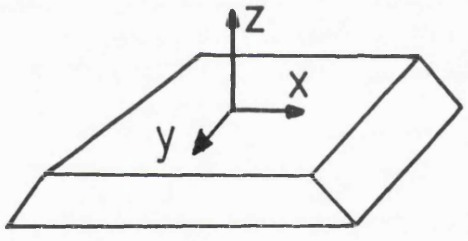

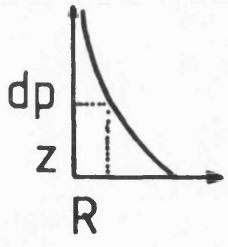

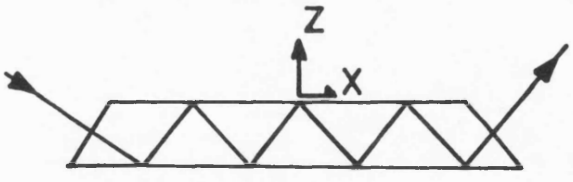

the ATR mode is the study of variations of absorption intensities that result from non-random orientation of molecules in membranes. In general these samples require a careful preparation and evaluation of the correct alignment of lipid molecules in a lamellar arrangement. This is usually confirmed by examination with polarized beams of the changes in intensity of bands of the lipid at 2875 and 1200 cm^{-1}. These bands correspond respectively to the stretching and wagging bands of the CH_3 of the acyl chains (Fringeli & Gunthard, 1981).

This technique uses polarized infrared radiation with their electric vector oriented parallel (=) or perpendicular ($^{\perp}$) to the plane of the ATR element, i.e. germanium prism (figure 2.10 left). With the band absorbances measured with both beams, the dichroic ratio DR= ($A^{\perp}$ / A=) is calculated and related to an average direction of the biomolecule in the sample with respect to the plane of the prism. Several optical constants must be previously known or at least estimated within limits, these are (1) α_{μ}, the direction of the angle of the transition dipole moment of the vibration mode to that of the postulated structure, e.g. the α_{μ} for the α-helix is 22° (Nabedryck et al., 1982) and (2) the value of DR for a randomly oriented structure. In ATR studies the latter value is taken to be larger, DR=1-2, than that obtained by transmission where DR=1. This is so because the

penetration depth of beams of parallel polarization is larger than that of the perpendicular beam (Mirabella, 1985). For frequencies associated to absorbance modes in the sample, the perpendicular spectra would therefore show more intensity relative to that of the parallel one (Mirabella, 1985).

Some groups usually examine the polarized spectra assuming a certain dichroic ratio for a randomly oriented molecules and then report their estimated average orientation (Brauner et al., 1987; Fringeli & Fringeli, 1979; Goormaghtigh & Ruysschaert, 1990). To obtain qualitative information, a comparative study is useful in studies of membrane proteins. Bacteriorhodopsin, the major protein component of the purple membrane, is an α-helical protein with its membrane-spanning domains oriented perpendicular to the plane of the membrane according to cryoelectron microscopy studies (Henderson & Unwin, 1975). The protein in purple membranes shows a DR for the amide A and I bands of approximately 2.5-2.7. These values can serve as reference for comparisons with data from other membrane proteins (Yang et al., 1987).

Samples suitable for ATR spectroscopy are phospholipids in aqueous systems or in organic solution which are dried under a nitrogen current on the surface of a germanium or KRS-5 prisms (Fringeli & Gunthard, 1981). ATR studies are carried out in a dried atmosphere, or hydrated in H_2O or

^2H_2O. In the latter conditions it is usually difficult to minimize absorption from the aqueous solvent. This may be avoided with the use of thick samples, where solvent penetration is minimal.

In the ATR experiment, spectra of the germanium prism with and without film are recorded separately as single beam spectra and ratioed to give transmission spectra. These are shown as *Absorbance = 2-log (Ri/Ro)*, where *Ri* and *Ro* correspond to final and initial reflectance intensities, respectively. When necessary, a KRS-5 grid polarizer is typically used to polarize the infrared radiation in the directions perpendicular or parallel to the plane of the prism.

2.6. FLUORESCENCE DEPOLARIZATION.

2.6.1. Introduction.

Fluorescence spectroscopy is a technique widely used for the study of the dynamics of phospholipids and proteins in membrane systems. In photoactive compounds, absorption of photons of ultraviolet or visible wavelength effect transitions of electrons from the ground state to electronically excited states. For most photoactive substances, the return to the ground state occurs by dissipation of the absorbed energy through a number of non-radiative processes such as solvent-dipole relaxation, energy transfer and quenching. In some substances, the excited electron descends through non-radiative steps to a lower-excited state. The return to the ground state occurs via the emission of a photon. Depending to the nature of the lower-excited state, this emission is called fluorescence or phosphorescence.

2.6.2. Fluorescence polarization.

The emission of photons will tend to be maximum at directions that coincide with the angles of absorption transition moment vectors of the molecule. In the DPH molecule (figure 2.11), the emission and absorption transition moments are almost parallel to each other. The intensity of the emission is maximum for the component parallel to the direction of the exciting beam (Lakowicz, 1983).

Figure 2.11.

The structure of the DPH molecule.

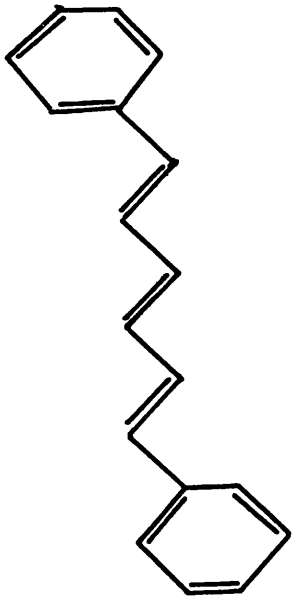

The Structure of DPH
1,6-diphenyl 1,3,5-hexatriene

The degree of polarization P or anisotropy r is usually expressed as

$$P = [I\parallel - I^{\perp}] / [I\parallel + G.I^{\perp}]$$

$$r = [I\parallel - I^{\perp}] / [I\parallel + 2.G.I^{\perp}]$$

where $I\parallel$ and $I^{\perp}$ are the intensities of the emission parallel and perpendicular, respectively, to the direction of the exciting beam and G is a correction factor for the instrumental sensitivities of the detector to the polarized emission.

In highly viscous media and low temperature, where the movement of molecules is restricted, the values of the recorded anisotropy r give an estimate of $[3\cos^2\alpha-1]/2$, where α is the angle of the emission dipole with respect to the absorption dipoles of the excited molecules. For DPH the maximum anisotropy $r=0.39$ (P=0.49) corresponds to an angle $\alpha=7°$. This indicates that the absorption and emission dipoles are almost parallel in the DPH molecule.

The degree of fluorescence polarization, in general, is affected by changes in the rotational diffusion of the molecule induced mainly by the temperature and viscosity in the sample. The extent of the polarization of the fluorescence of DPH has been used in aqueous lipid systems to study the dynamics of the phospholipids molecules (Gomez-Fernandez et al., 1980; Devaut & Seigneuret, 1985; Shinitzky et al., 1971). DPH is a rigid molecule due to the steric

hindrance of its double bonding (figure 2.11).

In our case, changes in the polarization *P* of the probe DPH in the membrane are related to the dynamics of intrinsic molecules such as proteins in the membrane. The polarization *P* of the DPH probe in pure lipid aqueous membranes decreases with the increase in temperature and changes considerably about the T_t of the lipid (Devaut & Seigneuret, 1985; Gomez-Fernandez et al., 1980). Inclusion of intrinsic molecules, such as cholesterol or proteins, in the aqueous lipid system above the T_t of the lipid, generally produces a gradual increase of the probe polarization that reaches a limit at a high concentration of proteins (Gomez-Fernandez et al., 1980; Hoffman et al., 1981). Time-resolved fluorescence studies of the increase in concentration of cholesterol in lipid systems indicate that the observed elevation in the polarization of DPH responds to a restricted motion of the probe and not due to increased microviscosity (Kawato et al., 1977; Devaut & Seigneuret, 1985). It was deduced that one of the rotational modes of the probe about its axis in the membrane was being restricted in some way and the probe could not reorientate at the same rate as in the lipid-pure systems.

2.6.3. Dependence of the fluorescence polarization of DPH on the concentration of protein.

Hoffman and coworkers (1981) investigated the basis of the relationship between the change of polarization and the concentration of the proteins in a number of reconstituted lipid systems. They reasoned that in the lipid membrane the motion of the probe DPH, which is related to the polarization, would be restricted by contacts with the nearby protein molecules. It was envisaged that as the concentration of protein is increased, protein-protein contacts would start to become more likely than probe-protein contacts. The increase in the number of possible probe-protein contacts would gradually become less dependent on the total number of protein molecules present and thus an exponential relationship between polarization and concentration of protein would be obtained.

Hoffman et al. (1981) defined $P(M,x)$ as the probability of the occurrence of no contacts between the probe and the protein (or other molecules such as cholesterol), M represents the number of contact sites per protein molecule and x represents the concentration of protein present if it spans the lipid bilayer or if it does not span it, $x = c/[2 - c]$, where c is the concentration of the protein.

$P(M,x)$ was derived as $P(M,x) = (1 - x)^M$ or for more practical purposes $P(M,x) = exp(-M.x)$. This equation indi-

cates that an increase in x results in a reduction in $P(M,x)$.

Hoffman et al. (1981) explained the dependency of the anisotropy $r(x)$ on the probabilities of occurrence for the contacts probe-molecule $[(1- P(M,x)]$ as :

$$r_{(x)} = r_{(x=0)}.A.\ P(M,x) + B[\ 1 - P(M,x)\ ]$$

where $r_{(x)}$ is the anisotropy at a concentration x of protein. A is an order parameter that depends on the temperature and type of lipid, whereas $r=0$ is the anisotropy at $x=0$. B is a collisional constant dependant on each type of lipid system.

The value of M in the latter equation represents the number of probes that can simultaneously contact one protein molecule and therefore gives a direct estimate of the perimeter of the protein molecule. This will be the case if the distribution of membrane proteins in the lipid bilayer is expected to be random as occur for proteins in the fluid state membrane, above T_t.

For membrane proteins reconstituted in lipid systems such as cytochrome oxidase (Mw 190 KDa) and Ca^{2+}-ATPase (Mw 100 KDa) M was estimated to be 60 and 24, respectively (Hoffman et al., 1981; Pink et al., 1984). For small molecules that do not span the bilayer e.g. cholesterol, M may be between 4-6 and approximately 12 for gramicidin A.

Anisotropy can also be expressed as polarization P,

$$P = 3.r \; / \; [2 + r]$$

This is a term which was used for the calculations of M in the original work of Hoffman et al. (1981), and will also be used in these studies instead of the anisotropy.

2.7. DIFFERENTIAL SCANNING CALORIMETRY.

This technique is widely used to study physical transitions occurring to biomolecules into a range of temperatures (McElhaney, 1984). The DSC instrument contains two equal compartments, one containing the sample and the other empty as reference. In the absence of energy absorption by the sample, the differential heat flow between sample and reference compartment is constant or zero. As the phase transition of a physical proccess takes place, e.g. solid-liquid transition of lipids, protein denaturation, heat has to be applied or taken from the sample compartment in order to keep its temperature constant relative to that of the reference compartment. The DSC instrument measures the difference of energy flow through the two compartments, while the temperature in both compartments is raised at a steady rate to cover the phase transition.

In order to calculate the enthalpy H, the curves that correspond to the transition are defined above the base-line and integrated.

CHAPTER 3

FOURIER-TRANSFORM SPECTROSCOPIC STUDIES OF FIBRINOGEN AND PLASMIN-DERIVED FRAGMENTS.

3.1. INTRODUCTION.

The maintenance of hemostasis requires the active participation of platelets, and several plasma proteins such as fibrinogen. Fibrinogen is the soluble precursor of fibrin. Fibrinogen is converted into fibrin upon activation of thrombin by the clotting cascade enzymes. Fibrin forms insoluble meshworks which are the basis of the blood clot that seals damaged blood vessels.

Human fibrinogen is a blood glycoprotein with a molecular weight of 340 KDa, comprising two pairs of three polypeptide chains α, ß and G, in the form of a dimer (Doolittle, 1984). Despite the number of studies aimed at characterising crystals of fibrinogen and fibrin, there is no atomic structure model based on X-ray diffraction data (Cohen et al., 1983; Rao et al., 1991). However, a growing flow of biochemical and physical evidence has permitted the definition of a 'consensus' model, which is now widely accepted (Doolittle, 1973; Doolittle, 1984). This model (figure 3.1) consists of a triple α-helical coiled-coil which connects the two distal globular domains to a smaller central domain. From both distal domains, the carboxy-termini of the α-chains extend forming a polar appendage.

Each distal domain contains the binding sites 'A' and 'B', pre-existing in fibrinogen and with affinity for complementary sites 'a' and 'b', concealed in the central domain

Figure 3.1.

Schematic model of fibrinogen and fragments resulting from plasmin digestion, showing main domains and points of proteolytic attack in fibrinogen.

Data obtained from Doolittle, (1973); Doolittle, (1984).

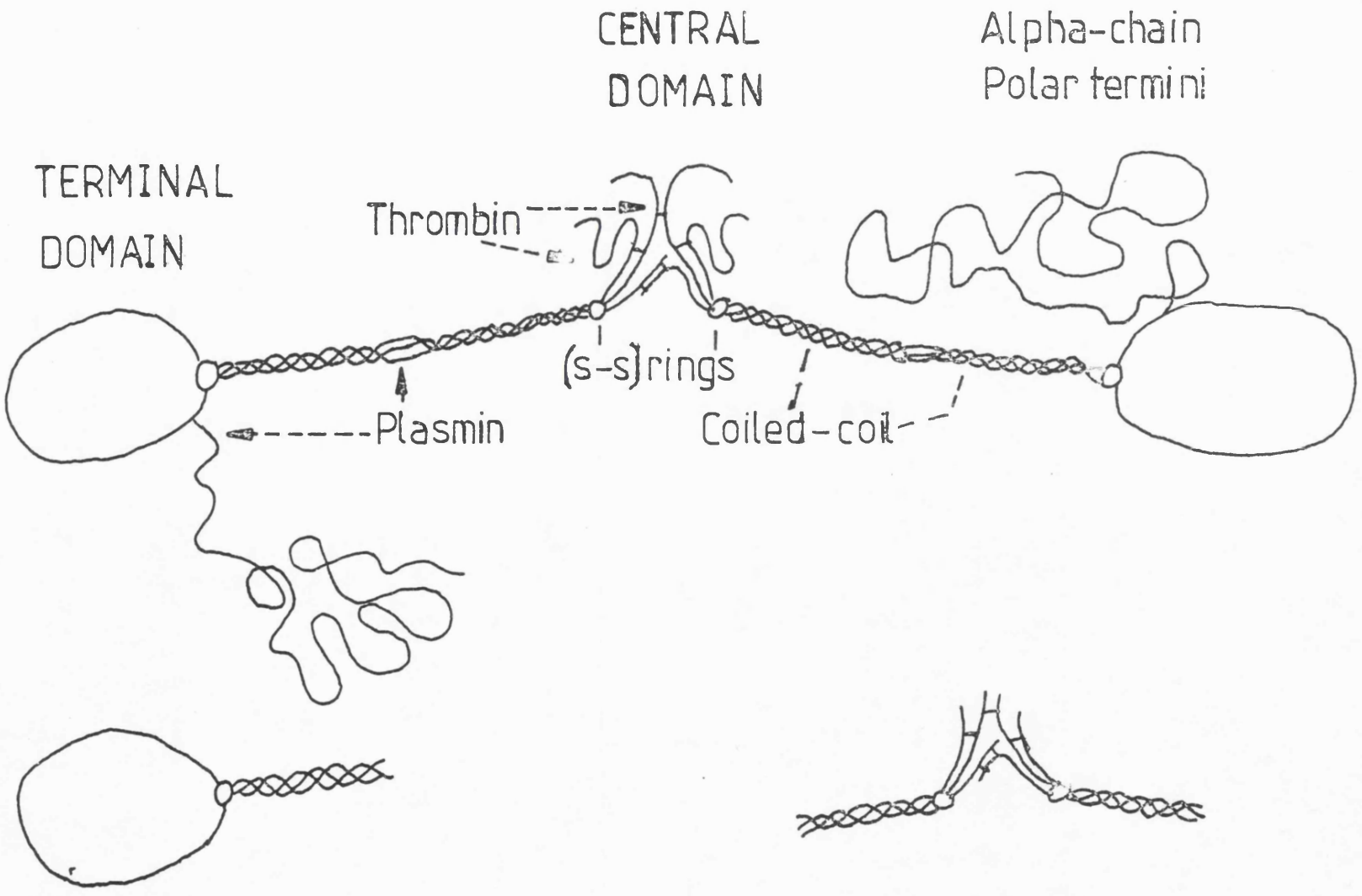
CENTRAL
DOMAIN
Alpha-chain
Polar termini
TERMINAL
DOMAIN
Thrombin
(s-s)rings
Plasmin
Coiled-coil
Fragment D (Mw=100,000)
Fragment E (Mw=45,000)

(Doolittle, 1973). These complementary sites are exposed by selective thrombin cleavage of peptides from the amino terminus of α and ß chains of fibrinogen. Fibrinogen is thus converted into fibrin monomers which self-polymerise forming insoluble clots that aggregate with platelets and other blood cells in the blood thrombuses.

The isolation and study of fragments that contain regions of fibrinogen has permitted the assignment of some features present in the fragments to their respective parts in the structure of fibrinogen. When fibrinogen is cleaved with plasmin in the presence of Ca^{2+} (Haverkate & Timan, 1977; Fowler et al., 1980), two major fragments are recovered: Fragment E (Mw 45 KDa) corresponding to part of the central domain and the coiled-coil, and Fragment D (Mw 100 KDa) which includes the whole distal domain and a portion of the coiled-coil. Both fragments play physiological roles in the regulation of fibrinogen synthesis in liver (Kessler & Bell, 1979). Fragment D conserves the sites 'A' and 'B' and inhibits the polymerisation of fibrin (Dray-Attali & Larrieu, 1977; Cierniewski et al., 1986). This indicates that the native structure of the distal domain of fibrinogen is conserved in fragment D (Mw 100 KDa). The integrity of the tertiary structure has been shown to be essential for the expression of the sites 'A' and 'B', as fragment D treated with 5M guanidine HCl loses affinity for fibrin and

does not inhibit fibrin-clot formation (Cierniewski et al., 1986). In the absence of Ca^{2+}, plasmin digestion of fibrinogen produces a smaller fragment D' (Mw 90 KDa), which contains the binding site 'B' (Laudano et al., 1983), but does not inhibit fibrin-clotting (Dray-Attali & Larrieu, 1977). The C-terminal portion of the G-chain (residues 303-411) is absent in Fragment D' (Mw 90 KDa). This C-terminal portion is thought to play an essential role in fibrin polymerization (Shimizu et al., 1992; Váradi & Scheraga, 1986).

Knowledge of the tertiary and secondary structure of the domains of fibrinogen is limited (Melved' et al., 1986; Rao et al., 1991). CD and Raman studies (Budzynski, 1971; Marx et al., 1979) of fibrinogen and its plasmin-derived fragments reported the presence of 35% and 35-40% α-helical content, respectively. Raman spectroscopy indicated the presence of smaller amounts of ß-sheet (10%) in fibrinogen than those shown by CD spectroscopy (20%).

The present study uses FT-IR spectroscopy to examine the secondary structure of fibrinogen and fibrin, fragment E (Mw 45KDa), fragment D (Mw 100KDa) and fragment D' (Mw 90KDa), obtained after digestion of fibrinogen with various proteases (plasmin and pepsin). This information is used to study and to deduce the secondary structure of the globular domains of fibrinogen.

3.2. MATERIALS AND METHODS.

3.2.1. Materials.

All reagents were of analytical grade and obtained from commercial sources. Streptokinase, pepsin, human fibrinogen (Type I, 95% of protein clottable) and human thrombin were supplied by Sigma U.K.. Plasminogen was purified from outdated plasma (Blood Bank, RFH), as described (Deutsch & Mertz, 1970). The purity of plasminogen was confirmed by SDS-PAGE, showing a single band at a molecular weight of 85 KDa.

3.2.2. Clotting studies.

Thrombin (0.5 NIH units/mg fibrinogen) was added to a solution of fibrinogen (50 mg/ml) in Tris saline pH 7.4 with either 0.01 M EGTA or 0.015 M $CaCl_2$. The solution was left to clot in the spectroscopic cell at 37°C, 20 minutes previous to FT-IR studies.

3.2.3. Purification of Fragment D (Mw 100 KDa) and Fragment E (Mw 45 KDa).

Fibrinogen (10mg/ml) was dissolved in Tris saline pH 7.4. All concentrations indicated are the final concentrations. Before the digestion $CaCl_2$ was added to a concentration of 25 mM and then the digestion was initiated by coadding plasminogen and streptokinase at a concentration of 10

μgr/ml and 5 units/μgr plasminogen, respectively. After six hours at 37°C, digestion was stopped adding 0.2 mM PMSF. Approximately a volume containing 100 mg digest was diluted in distilled water and Tris Acetate (ionic strength 0.1, pH 8.01) and applied overnight to an ion-exchange Q-Sepharose column (1.5 X 25 cm) equilibrated at 4°C with Tris Acetate buffer (ionic strength 0.1, pH 8.01). Fragments were eluted isocratically as previously described (Chen et al., 1972). Pools were concentrated by ultrafiltration and applied to a Sephacryl S-300 (1.5 X 55 cm) column or in the case of fragment E, to a Sephadex G-100 (1.5 X 55 cm) column, both equilibrated at 4°C in 0.05 M TrisCl / 0.15 M NaCl pH 7.4. Pools were dialysed at 4°C against distilled water and then freeze-dried.

The purity and molecular weight of the fragments were assessed by SDS-PAGE under non-reduced conditions (Hames and Rickwood, 1981). Both fragments D and E (fragment E_3 in Olexa et al. (1981)) were shown to be pure by SDS-PAGE (figure 3.2), and their molecular weights were approximately 100 KDa and 45 KDa, respectively. From 100 mg fibrinogen, typical yields were 10-25 mg fragment D and around 2-5 mg fragment E.

Figure 3.2.

SDS-PAGE gel (7% acrylamide concentration) of purified fragment E (Mw 45KDa), fragment D (Mw 100KDa) and fragment D' (Mw 90KDa).

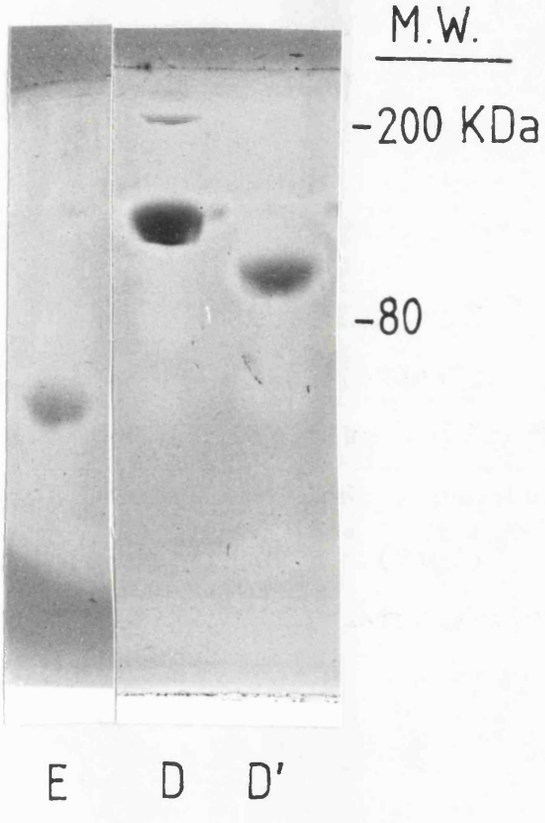
M.W.
-200 KDa
-80
E
D
D'

Figure 3.3.

(Centre). SDS-PAGE gel (10% acrylamide concentration) of timed digestions of fragment D (Mw 100KDa) with pepsin at pH 2.8.

(Left). Lane corresponding to purified coiled-coil fragment.

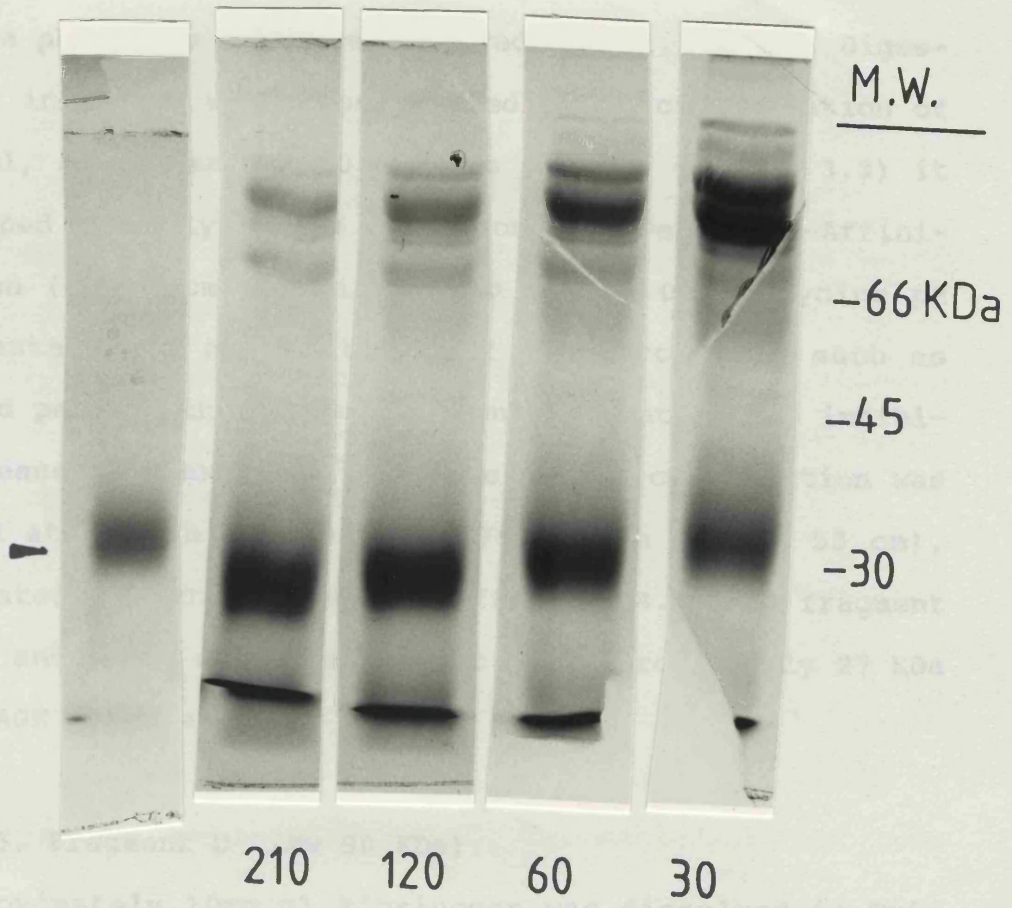
M.W.
-66 KDa
-45
-30
210
120
60
30

3.2.4. Coiled-coil portion of fragment D.

Fragment D (Mw 100 KDa) (10 mg/ml) was dissolved in 0.05 M Glycine pH 2.8 as described (Melved' et al., 1982). Digestion was initiated with pepsin added to a concentration of 50 μgr/ml, and after 80-180 minutes at 25°C (figure 3.3) it was stopped by applying the digest on to a Pepstatin-Affinity column (1 X 2 cm), equilibrated with 0.05 M Glycine pH 2.8. Pepstatin is an inhibitor of acid-proteases such as renin and pepsin; the disassociation constant of the inhibitor-protease complex is 10^{-8} M. The coiled-coil portion was purified at 4°C on a Sephadex G-75 column (1.5 X 55 cm), equilibrated with 0.2 M acetate buffer pH 4.4. The fragment was pure and had a molecular weight of approximately 27 KDa by SDS-PAGE (figure 3.3).

3.2.5. Fragment D' (Mw 90 KDa).

Approximately 10mg/ml Fibrinogen was dissolved in Tris saline buffer containing 2mM EGTA (a Ca^{2+} chelator). To initiate digestion Plasminogen (100 μg/ml) was coadded with streptokinase to a concentration of 5 units/μg plasminogen. After 8-12 hours at 37°C, PMSF was added to a concentration of 0.5 mM and Fragment D' was separated following the same procedure for Fragment D (Mw 100 KDa). Pools were concentrated and desalted on a column of Sephadex G-25 (2.5 X 30 cm) which was equilibrated with deionized water. Fragment D'

was pure, as judged from a single band at approximately 90 KDa on a SDS-PAGE gel (figure 3.2).

3.2.6. Infrared spectroscopy.

Proteins were dissolved at concentrations 2-3% in ^2H_2O or H_2O buffers containing Tris saline pH 7.4/ p^{2}H 7.4, or 0.2 M phosphate pH 3.5 (see section 2.5.1 for more details on sample preparation). For each sample 400 scans in H_2O or 100 in ^2H_2O were recorded at 4 cm^{-1} resolution, signal-averaged and apodized on a Perkin-Elmer 1750 FT-IR Spectrometer connected to a Perkin-Elmer Data Station.

Deconvolution and second derivative routines were used to narrow the widths of components in the amide I and II bands of the protein spectra (see sections 2.4.2 and 2.4.3). With the first routine, for most cases an estimated HWHH of 15 cm^{-1} was used and a K of 2-2.25. The secondary structure was quantified by factor analysis of the spectra (see section 2.2.4.2. for details) (Lee et al., 1990).

3.3. RESULTS.

3.3.1. Fibrinogen and fibrin.

The spectrum of fibrinogen in H_2O (figure 3.4A, lower trace) shows an amide I band at 1651 cm^{-1}, typical of proteins containing predominantly α-helical structure. The deconvolved spectrum (figure 3.4A, upper trace) indicates

that the amide I band is comprised of various components located at frequencies of 1686, 1667, 1653, 1642, 1631 and 1617 cm^{-1}, which arise from different types of secondary structure. The band at 1653 cm^{-1} has been shown to originate from α-helical and/or random structures (Jackson et al., 1989a). The band at 1631 cm^{-1} arises from ß-sheet structures (Jackson et al., 1989a; Susi, 1969), while the components at 1642 cm^{-1} could be attributed to either ß-sheet (Olinger et al., 1986) or ß-turn (type I or III) (Krimm & Bandekar, 1986). The band at 1617 cm^{-1} is unusually low for a ß-sheet structure but has been observed in other proteins (Byler & Susi, 1986). The component of the amide I band at 1667 is assigned to ß-turns and that at 1686 cm^{-1} to ß-turns and ß-sheet (Krimm & Bandekar, 1986). Aminoacid side-chains like those from Arg, Asn, Gln and Lys are known to absorb along the whole amide I band and their contribution is estimated to be around 15-20% of the total absorbance of the amide I band (Venyanimov & Kalnin, 1991). Quantification (Lee et al., 1990) of the secondary structure indicates that fibrinogen has 37% α-helix, 30% ß-sheet, 14% ß-turns and 16% unassigned structures. The spectrum of fibrinogen was not recorded as it was found to be unsoluble in ^2H_2O solution. (see table 3.1).

A similar range of secondary structures is observed in the spectra of fibrin clots made in the presence of 10 mM EGTA (figure 3.4B solid trace). In the presence of Ca^{2+} at

Figure 3.4.

(A). Absorption spectrum (bottom trace) of human fibrinogen in H_2O pH 7.4. Deconvolution of spectrum (top trace), using K=2.125 and HWHH=15 cm^{-1}.

(B). Absorption spectra of fibrin clot in the EGTA buffer solution (solid line); and absorption spectrum of fibrin clot in Ca^{2+} buffer solution (dotted line).

ABSORBANCE
1800
1700
1600
1500
WAVENUMBER (CM⁻¹)
A
0.05 A.U.
1686
1667
1653
1651
1642
1631
1617
1551
1551
ABSORBANCE
1800
1700
1600
1500
WAVENUMBER (CM⁻¹)
0.05 A.U.
B

Figure 3.5.

(A). Absorption spectrum (bottom trace) of Fragment E in H_2O pH 7.4. Deconvolution of spectrum (bottom trace), using K=2 and HWHH=15 cm^{-1}.

(B). Second derivative spectra of Fragment E, where the data range was 13 points. (Bottom trace). Spectrum of fragment E in H_2O. (Centre trace). Spectrum obtained after one hour in ^2H_2O pD 7.4, showing partial deuteration. (Top trace). Spectrum twelve hours later in ^2H_2O pD 7.4, showing complete deuteration.

ABSORBANCE
1800
1700
1600
1500
WAVENUMBER (CM-1)
A
1683
1670
1655
1655
1632
1616
1551
1552

ABSORBANCE/ WAVENUMBER2
1800
1700
1600
1500
WAVENUMBER (CM-1)
B
1685
1655
1650
1644
1677
1552
1552
1552

Table 3.1.

Percentages of secondary structures[a,b] obtained from the infrared spectra of the following proteins:

	FIBRINOGEN	**FIBRIN-EGTA**	**FIBRIN-Ca^{2+}**
α	37/33/36	37/38/35	31/33
ß	30/29/26	28/29/27	36/33
t	14/7/15	10/18/17	14/16
u	15/15/19	16/16/17	14/16

	FRAGMENT D	**FRAGMENT D'**	**FRAGMENT E**
α	34.5/35/36	41/40	51/53
ß	29.5/29/27	25/25	19/15
t	17/15/10	15/17	14/13
u	17/17/18	16/17	15/14

[a]Calculated using quantitative analysis of the amide I band of the protein in H_2O as described by Lee et al. (1990).

[b]α= α-helix, ß= ß-sheet, t= turns, u= unassigned structures.

15mM, the intensity of the amide I band at 1650 cm^{-1} (figure 3.4B dashed trace) becomes smaller relative to the intensity of the amide II band at 1549 cm^{-1}, possibly indicating aggregation. Quantitative analysis of Ca^{2+}-clot indicates that the content in ß-sheet increases slightly (7%) with some reduction of the intensity of bands at 1650-5 cm^{-1} that originate from α-helical/random structures. (see table 3.1).

3.3.2. Fragment E.

The spectrum of fragment E (figure 3.5A lower trace) in H_2O shows an amide I band maximum at 1655 cm^{-1}, typically observed in α-helical proteins. The deconvolved spectrum (figure 3.5A upper trace) also indicates the presence of a band at 1632 cm^{-1} that arises from ß-sheet structures, the bands at 1670 and 1683 cm^{-1} are assigned to ß-turns (type II) and ß-sheet (Krimm & Bandekar, 1986). Quantitative analysis of the secondary structure indicates that fragment E contains 50% of α-helical structures, 19% of ß-sheet, 14% of turn structures and 15% unassigned structures. (see table 3.1).

The second derivative spectra of fragment E in ^2H_2O (figure 3.5B central trace) shows the main amide I band component at 1650 cm^{-1}. The amide II band at 1552cm^{-1} shows a reduction in intensity upon $H/^2H$ exchange. The amide I band of fragment E recorded after complete amide $H/^2H$ exchange appears at 1644 cm^{-1} (figure 3.5B upper trace) 9 cm^{-1} down in frequency as compared to the frequency in H_2O

(figure 3.5B lower trace). This suggests that random structures are predominant in fragment E (Jackson et al., 1989a; Susi, 1969), which is in disagreement with the previous quantitative analysis indicating a conformation rich in α-helical structure. Part of fragment E (figure 3.1) is predicted to be a coiled-coil with its α-helical structure exposed to the solvent (Doolittle et al., 1978). An FT-IR study of calmodulin, a protein with solvent-exposed α-helices, shows a ten cm^{-1} shift in the frequency of the amide I band upon $H/^2H$ exchange (Jackson, 1990; Jackson et al., 1991).

3.3.3. Fragment D.

The spectrum of fragment D in H_2O (figure 3.6A lower trace) shows the amide I band at 1652 cm^{-1}, which is usually observed in proteins with α-helical structures. The deconvolved spectrum (figure 3.6A upper trace) reveals a band at 1631 cm^{-1}, assigned to ß-sheet structures, and another at 1643 cm^{-1} which can be attributed to ß-sheet (Jackson et al., 1989a; Olinger et al., 1986) or ß-turn (type I or III) structures (Krimm & Bandekar, 1986). The components observed at 1670 and 1689 cm^{-1} may originate from ß-turn or ß-sheet structures and also to some extent from side-chains of certain aminoacids (Venyaminov et al., 1991). Quantification of the secondary structures present in fragment D indicates 34.5% α-helix, 29.5% ß-sheet, 17% turns and 17.5% unassigned (see table 3.1).

Figure 3.6.

(A). Absorption spectrum (bottom trace) of Fragment D (Mw 100KDa) in H_2O pH 7.4. Deconvolution of spectrum (top trace), using K=2.25 and HWHH=15 cm^{-1}.

(B). Absorption spectrum (bottom trace) of Fragment D in ^2H_2O. Deconvolution of spectrum (top trace), with K=2.125 and HWHH=15 cm^{-1}.

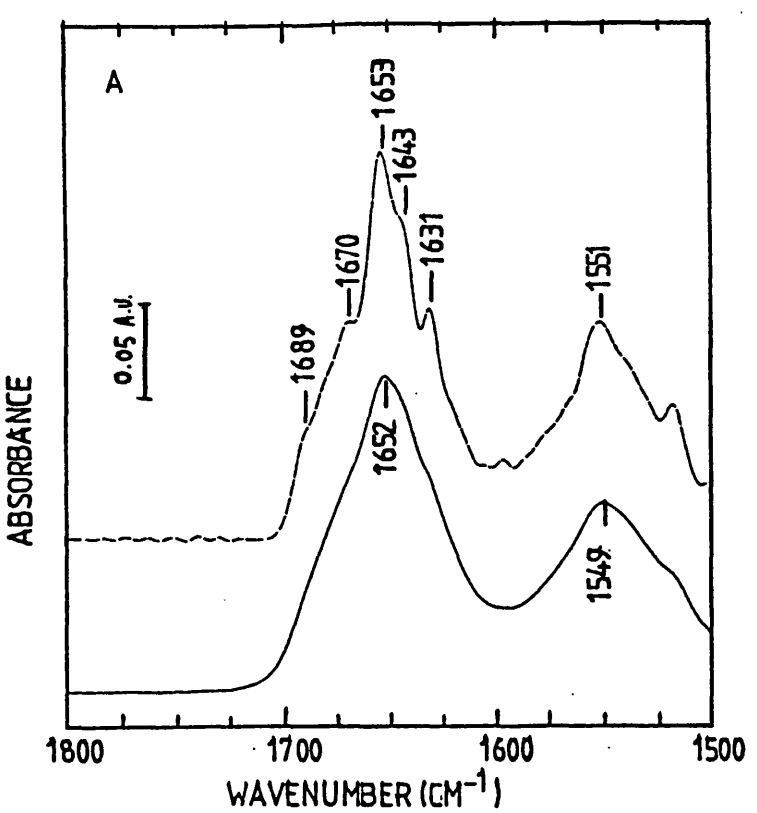
A
0.05 A.U.
1689
1670
1653
1643
1631
1652
1551
1549
ABSORBANCE
1800
1700
1600
1500
WAVENUMBER (CM^{-1})

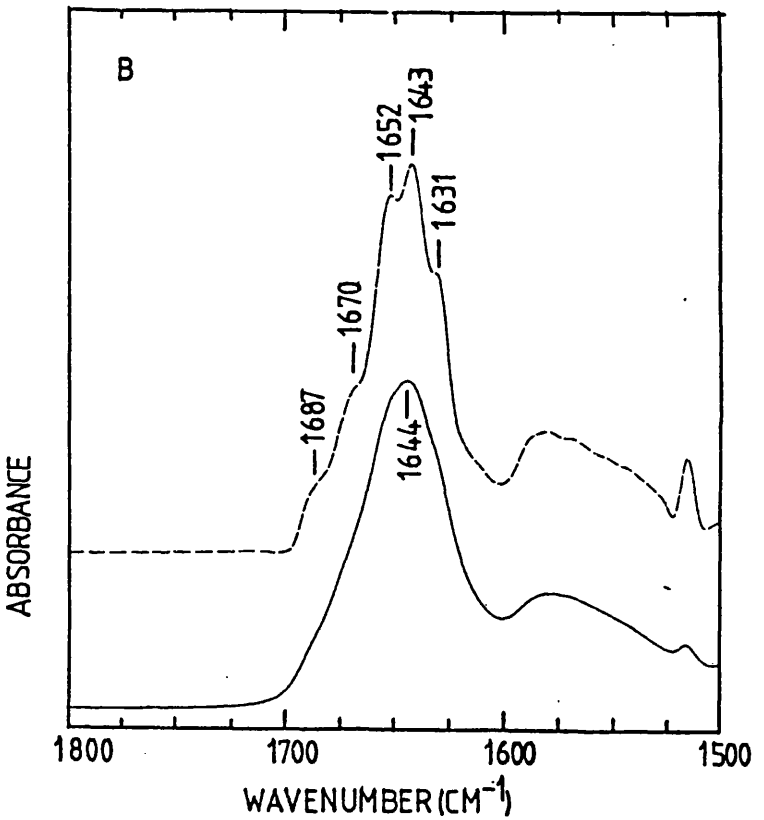
B
1687
1670
1652
1643
1631
1644
ABSORBANCE
1800
1700
1600
1500
WAVENUMBER (CM^{-1})

structures. Quantitative data of fragment D, obtained from plasmin-digested fibrin clots, indicated similar percentages of secondary structure.

The spectrum of fragment D in ^2H_2O solution (figure 3.6B lower trace) shows a weak amide II band at 1549 cm^{-1}, indicative of an almost complete $H/^2H$ exchange of the amide protons. No changes upon Ca^{2+}-binding were observed in the rate of reduction of the amide II band (spectra not shown). The amide I band maximum appears at 1644 cm^{-1} (figure 6B, lower trace), which indicates an 8 cm^{-1} shift from the frequency of the amide I maximum observed in H_2O (figure 6A). This shift would suggest the presence of some random structures in fragment D as the frequency of these bands is known to shift from 1650-5 cm^{-1} in H_2O to 1640-5 cm^{-1} in ^2H_2O (Susi, 1969). Fragment D is predicted to contain a coiled-coil domain (figure 3.1) similar to that of fragment E. This suggests that the amide I maximum shift is caused to some extent by the presence of solvent-exposed α-helical structures (Jackson, 1990; Jackson et al., 1991).

The deconvolved spectrum of fragment D in ^2H_2O (figure 3.6B upper trace) shows two main components of the amide I band located at 1652 and 1643 cm^{-1}. The first is attributed to α-helical structures, and the second originates from random and solvent-exposed α-helical structures of the coiled-coil domain. The other components appear at the same

Figure 3.7.

Absorption spectrum (bottom trace) of coiled-coil portion in H_2O pH 3.5.

Deconvolution of spectrum (top trace), using K= 2 and HWHH= 15 cm^{-1}.

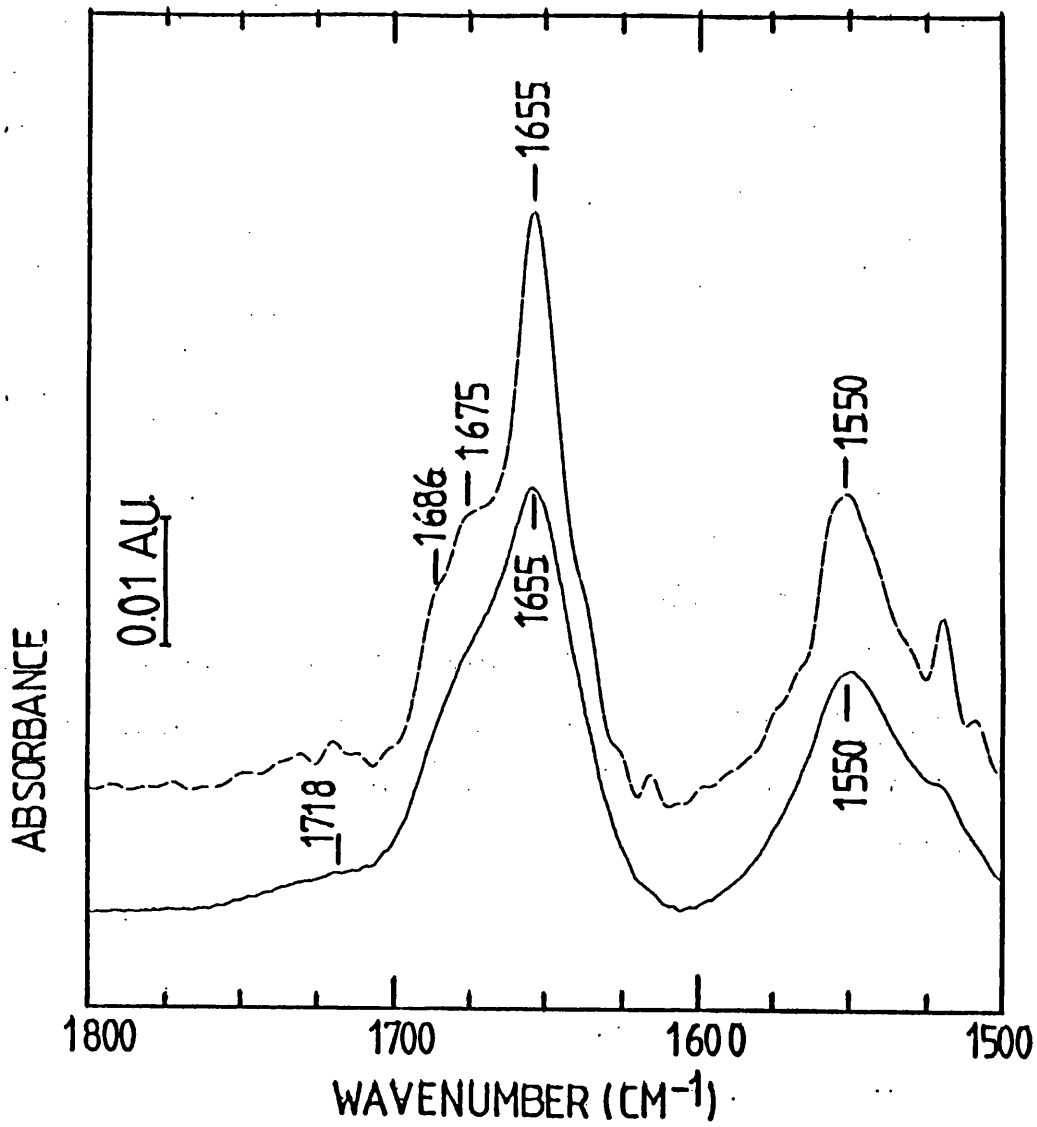
1655
1686
1675
1550
0.01 A.U.
1655
1718
1550
ABSORBANCE
1800
1700
1600
1500
WAVENUMBER (CM^{-1})

Figure 3.8.

Second derivative spectra of Fragment D in ^2H_2O recorded at different times of exposure to a temperature of 55°C (from the bottom to the top spectrum).

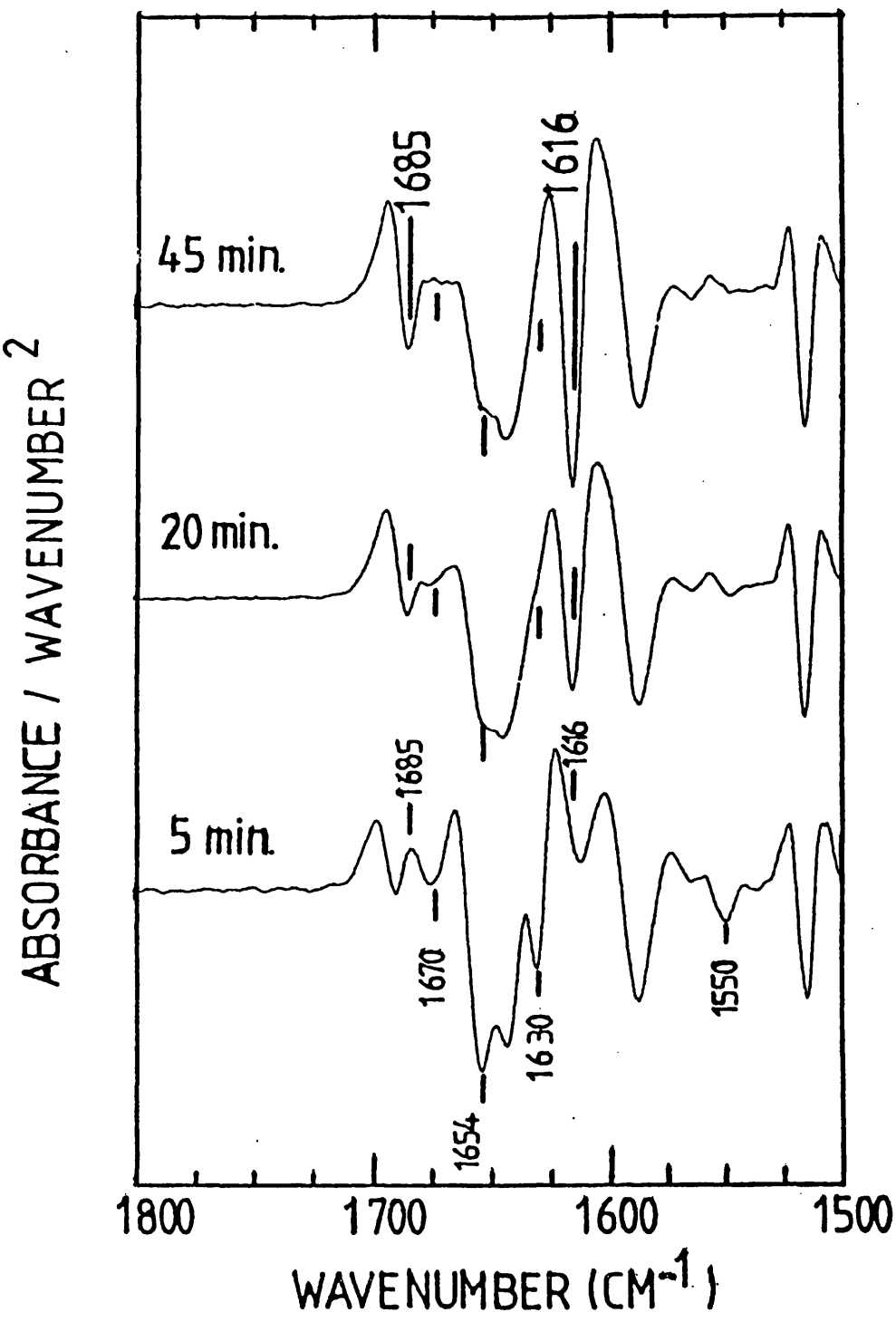
45 min.
20 min.
5 min.
1685
1616
1685
1616
1670
1654
1630
1550
1800
1700
1600
1500
WAVENUMBER (CM-1)
ABSORBANCE / WAVENUMBER 2

frequencies as those in the amide I band in H_2O (figure 6A).

3.3.4. The coiled-coil portion.

At pH < 3, the globular domain of bovine fragment D denatures (Melved' et al., 1982) whereas the coiled-coil portion is stable and can be recovered after pepsin digestion of fragment D at pH 2.8 (figure 3.3). The coiled-coil portion (Mw 27 KDa) (figure 3.7 lower trace) of human fragment D shows a narrow amide I band with its maximum at 1654 cm^{-1}. Quantification of the secondary structure indicates a percentage of approximately 70% α-helix and some ß-turn structures as indicated by the bands at 1670 and 1686 cm^{-1} (figure 3.7 upper trace). The band at 1718 cm^{-1} is assigned to the carboxylic acid side-chains of Asp and Glu (Venyanimov et al., 1991). The spectrum of the coiled-coil at p^2H 3 was not recorded because of the slow rate of $H/^2H$ exchange at acid pH.

3.3.5. Thermal denaturation of the globular domain of fragment D.

The globular domain of fragment D denatures above a temperature of 55°C (Privalov & Melved', 1982), whereas the coiled-coil portion is stable. The second derivative spectra of fragment D in ^2H_2O at 55°C (figure 3.8) shows initially the presence of the bands at 1670, 1654 and 1630 cm^{-1} that correspond to the native structure of the protein. The

spectra obtained following exposure to 55°C for 20 min and for 45 min reveal that the intensities of the bands present in the native protein are markedly reduced. This is accompanied by the appearance of bands at 1616 and 1685 cm^{-1} attributed to ß-sheet structures which are typically observed upon unfolding and aggregation of denatured proteins (Jackson et al., 1989a). These changes in the spectra are associated to the denaturation and unfolding of the globular domain of fragment D, therefore this provides qualitative information on those structures present in the globular domain of fragment D (figure 3.1).

3.3.6. The globular domain.

Fragment D contains two domains: the coiled-coil portion (Mw ≈ 27 KDa) and the globular domain (Mw ≈ 73 KDa) (Privalov & Melved', 1982; Melved' et al., 1982). The approximate spectrum of the globular domain can be obtained by subtraction of the spectrum of fragment D in H_2O (figure 3.6A lower trace) with the contribution of the spectrum of the coiled-coil portion in H_2O (figure 3.7 lower trace). To carry out the subtraction, firstly, the areas of the amide I bands between 1700-1600 cm^{-1} were normalized to 100 arbitrary units in both spectra. Then the area of the amide I band in the spectra of the coiled-coil portion was weighted down to 27 arbitrary units to account for its percentage in molecu-

Figure 3.9.

(A) Adjusted spectrum of fragment D in H_2O.

(B) Spectrum of the globular domain of fragment D, after subtraction of weighted spectrum of coiled-coil portion (see Results and Discussion).

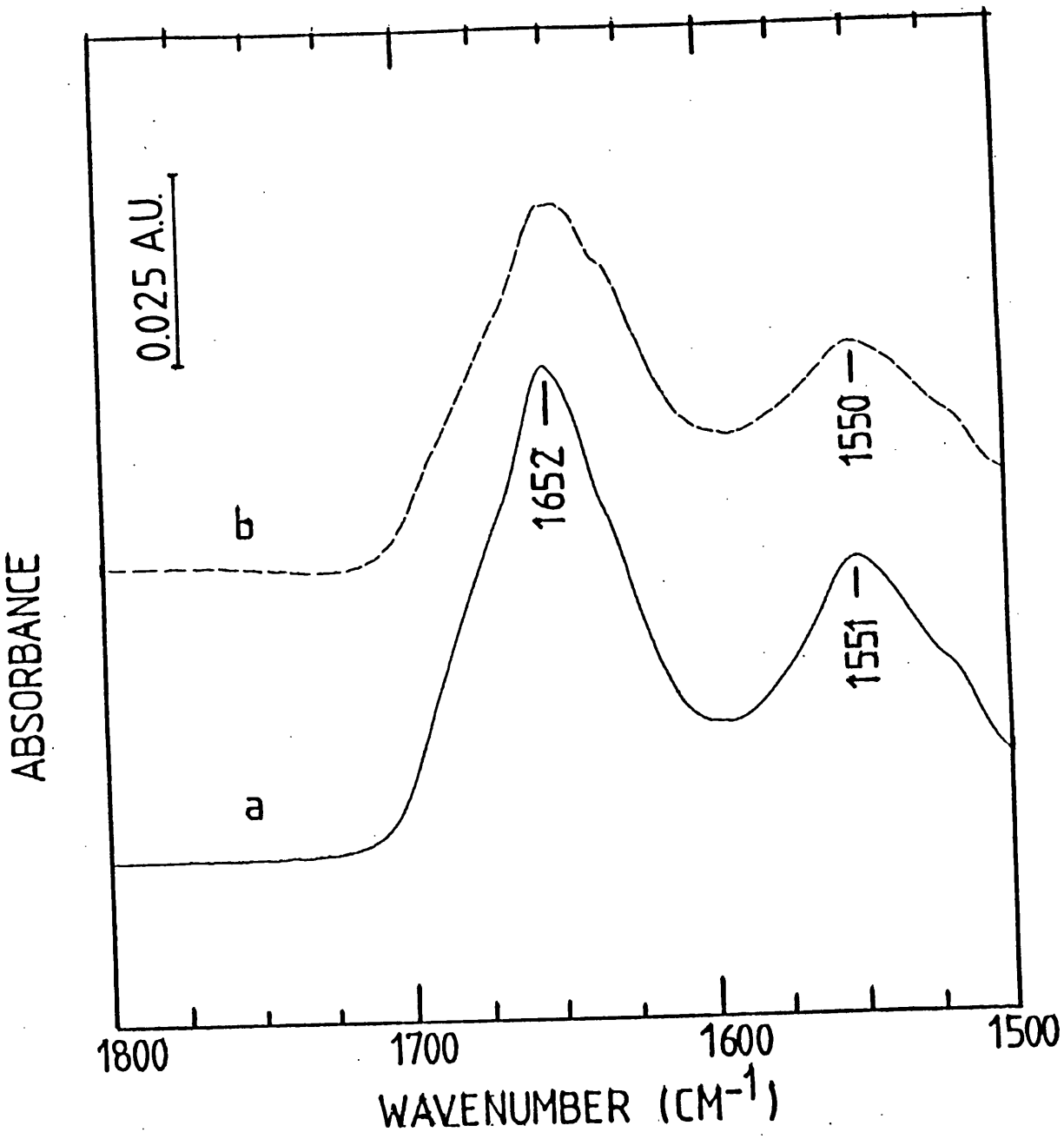
0.025 A.U.
b
a
1652
1550
1551
ABSORBANCE
1800
1700
1600
1500
WAVENUMBER (CM-1)

Figure 3.10.

(A) Spectrum of globular domain of fragment D (Mw 100KDa).

(B) Deconvolved spectrum, using K=2 and HWHH=15 cm^{-1}.

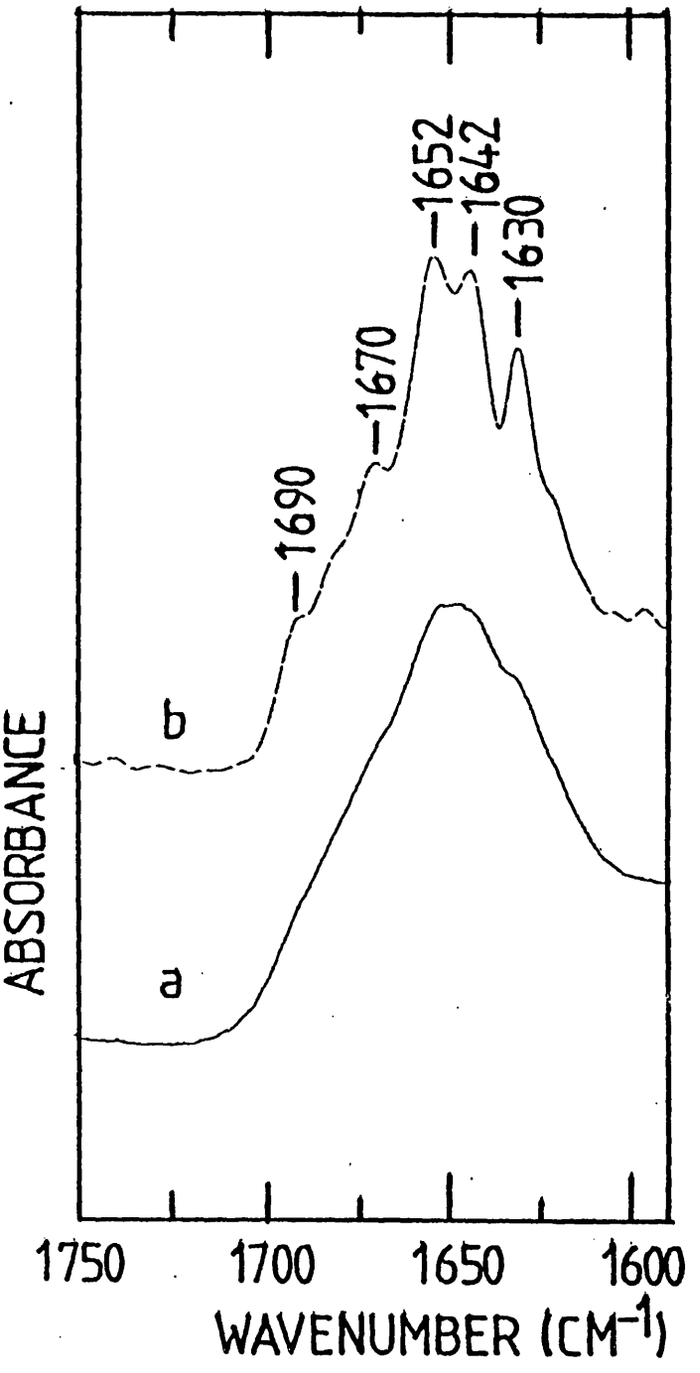
1652
1642
1630
1670
1690
b
a
ABSORBANCE
1750
1700
1650
1600
WAVENUMBER (CM-1)

lar weight (27%) in fragment D. The normalized spectrum of fragment D (figure 3.9A) was then subtracted with the weighted spectrum of the coiled-coil (not shown) to give the spectrum shown in figure 3.9B. This spectrum would therefore approximate that of the globular domain.

To make the subtraction, several assumptions have been made: (1) the amide I absorption (1700-1600 cm^{-1}) is proportional to the molecular weight of the respective fragments, which implies that the amide I bands and the contributions from each band component are additive, (2) the amide I band comprises only the region 1700-1600 cm^{-1} and (3) the spectrum and structure of the isolated coiled-coil portion is similar to that present when bound to fragment D. Quantification by factor analysis (Lee et al., 1990) of the spectrum of the globular domain (figure 3.9B) indicates a content of secondary structure of 21% α-helix, 43% ß-sheet, 15% ß-turns and 15% unassigned structures.

The deconvolved spectrum (figure 3.10A) shows components of α-helix at 1652 cm^{-1}, ß-sheet and some turns possibly between 1642-1630 cm^{-1} and others from ß-turns and/or ß-sheet at 1670-90 cm^{-1}. These components can be also observed in the deconvolved spectrum of fragment D in H_2O and ^2H_2O solution (figures 3.6A and 3.6B).

Figure 3.11.

(A) Spectrum of fragment D' (Mw 90KDa) in H_2O solution.

(B) Deconvolved spectrum where K= 2.25, HWHH= 15 cm^{-1}.

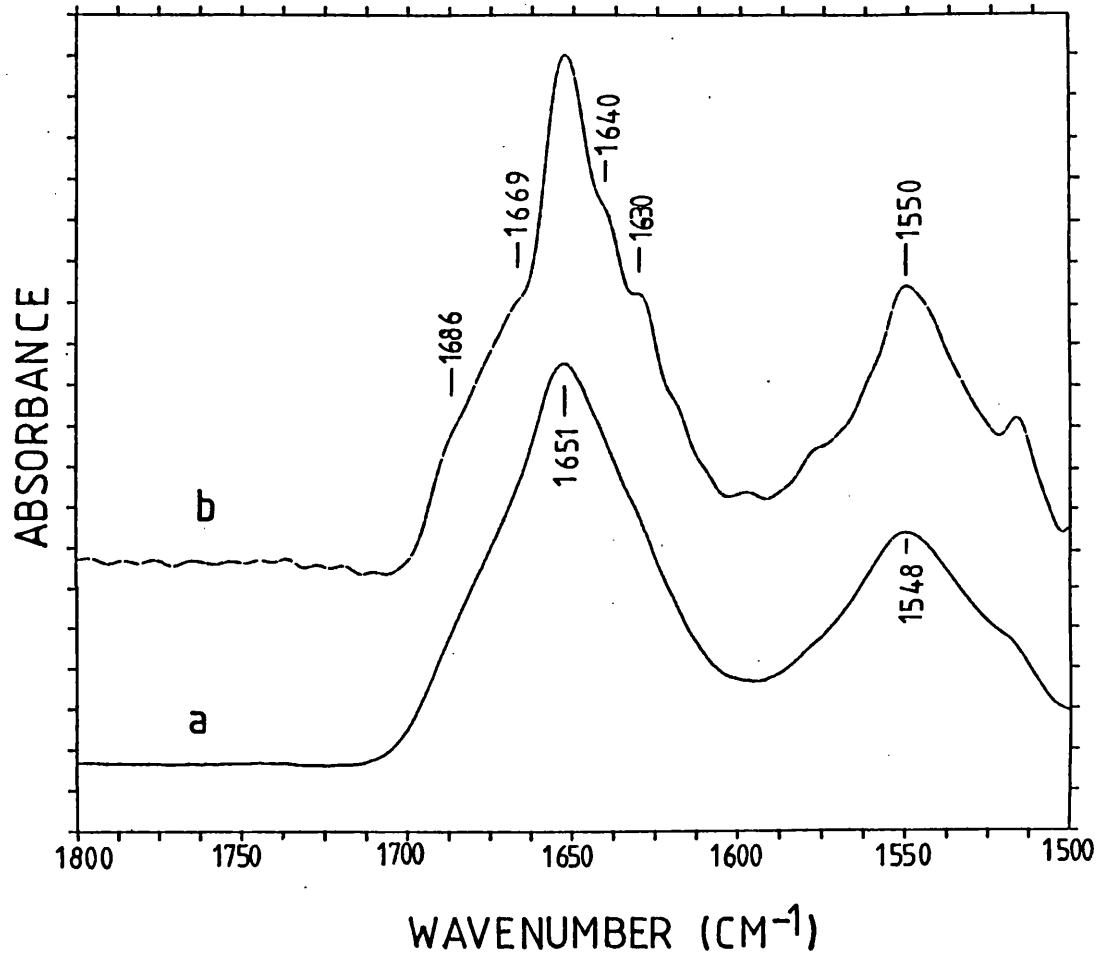
ABSORBANCE
b
a
1686
1669
1640
1630
1651
1550
1548
1800
1750
1700
1650
1600
1550
1500
WAVENUMBER (CM-1)

Figure 3.12.

(A) Spectrum of fragment D' (Mw 90KDa) in $^{2}H_{2}O$.

(B) Deconvolved spectrum, using K=2 and HWHH=15 cm^{-1}.

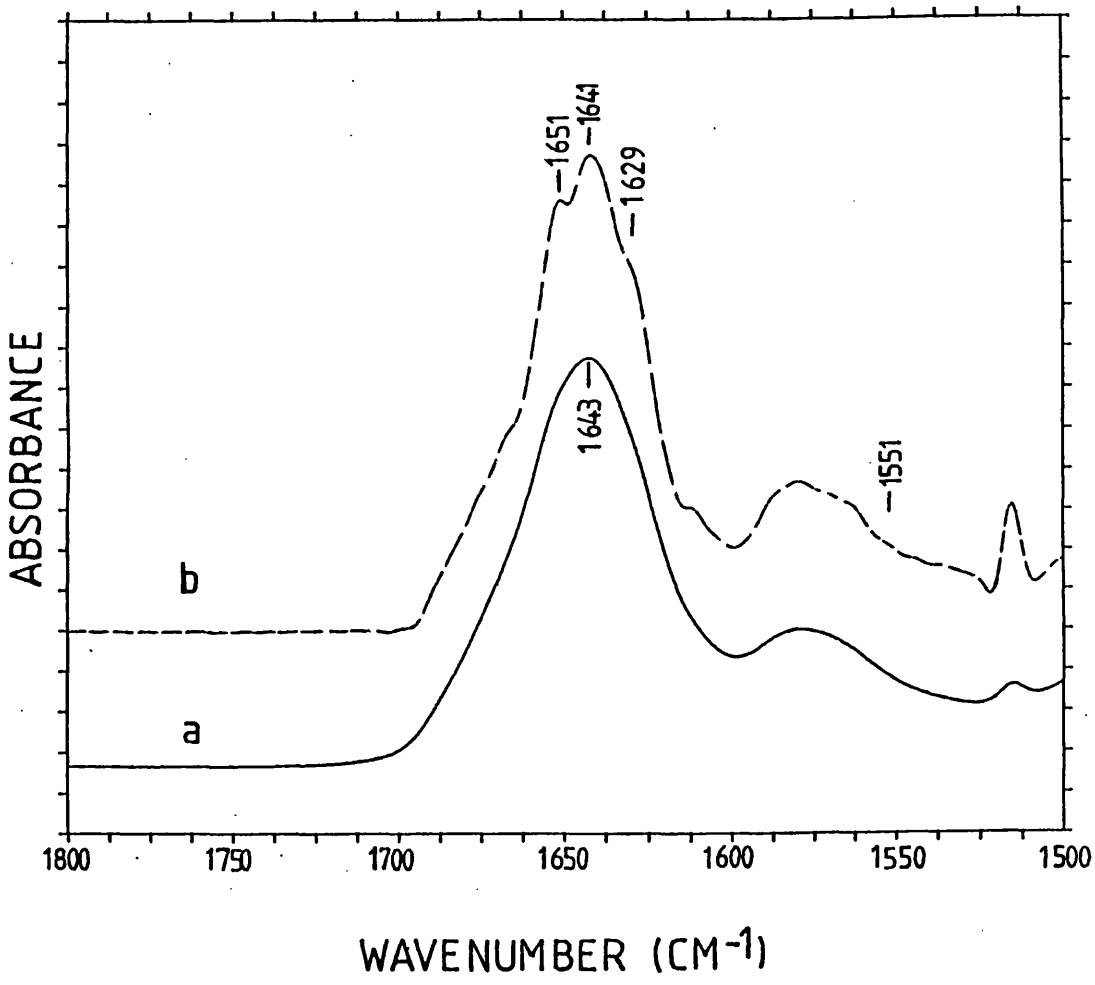
ABSORBANCE
1651
1644
1629
1643
1551
b
a
1800
1750
1700
1650
1600
1550
1500
WAVENUMBER (CM-1)

3.3.7. Fragment D' (Mw 90 KDa).

The spectrum of fragment D' (figure 3.11A) in H_2O shows an amide I maximum at 1651 cm^{-1}, indicative of a conformation predominantly α-helical structure. The deconvolved spectrum (figure 3.11B) reveals components in the amide I band at 1686, 1669, 1651, 1640 and 1630 cm^{-1}, similar to those of fragment D (figure 3.6A upper trace). Secondary structures values for fragment D' (Mw 90 KDa) are 40% α-helix, 26% ß-sheet, 17% turns and 17% unassigned structures. These values are not statistically different from those of Fragment D (Mw 100 KDa) (see table 3.1).

The spectrum of fragment D' in ^2H_2O (figure 3.12A) shows an amide I band maximum shifted to a lower frequency at 1643 cm^{-1}. The deconvolved spectrum of fragment D' (figure 3.12B) shows similar bands at 1651, 1641 and 1629 cm^{-1} to those found in the spectrum of fragment D in ^2H_2O in figure 3.6B. This is indicative that the conformations in fragment D and D' are similar. The reduction of the intensity of the amide II band upon $H/^2H$ exchange was found to be fast and complete within 15 min.

3.4. DISCUSSION.

3.4.1. Fibrinogen and fibrin.

These FT-IR studies attempt to gain insight into the secondary structure of fibrinogen and its distal and central

domains (figure 3.1). The infrared spectrum shows, according to the factor analysis method (Lee et al., 1990), that fibrinogen is an α-helical (37%) protein, but with important contributions of ß-sheet structures (30%). These data agree with previous CD studies (Budzynski, 1971; Kloczewiak et al., 1976), which indicated values of 35% of α-helical structure and 20% ß-sheet structure. Raman spectroscopy reported a lower content of ß-sheet (10%) (Marx et al., 1979). The high α-helical content of fibrinogen can be partially attributed to the coiled-coil that connects the central domain to the two distal domains (figure 3.1). This coiled-coil is predicted to amount 20-25% of α-helical structure in fibrinogen according to primary sequence analysis (Doolittle et al., 1978), the remaining being possibly present in the domains of fibrinogen.

The fibrin clots prepared in the presence of $CaCl_2$ (figure 3.4B solid trace), show an increase in the content of ß-sheet at the expense of some α-helical/random structures and a reduction in the ratio of the intensities of the amide I to the amide II band. An increase in the ß-sheet content has also been observed by Raman spectroscopy (Marx et al., 1979) and is thought to be associated with the formation of thick fibres that give rise to opaque clots (Doolittle, 1973). The spectrum of the fibrin EGTA-clot obtained in the absence of Ca^{2+} ions are similar to the

spectrum of fibrinogen. These EGTA clots are transparent and possibly comprised of thinner fibres than in the opaque Ca^{2+}-clots. As the fibrin clots only show detectable alterations in the amide I band when prepared in the presence of Ca^{2+} and not in its absence, they probably occur as a consequence of the formation of thick fibres and large aggregates.

Plasmin-cleavage of fibrinogen results in the appearance of fragments, E and D, bearing domains of the original molecule (figure 3.1) (Fowler et al., 1980). Plasmin-cleavage may cause changes in the conformation upon removal of parts of the polypeptidic chain, as probably occurs in the case of fragment E (Olexa et al., 1981). Fragment D pre serves the functional activity of the distal domain of fibrinogen (Dray-Attali & Larrieu, 1977; Cierniewski et al., 1986) and therefore it implies that its structure is intact. However immunological studies of exposure of epitopes using antibodies have detected changes in fragment D as compared to fibrinogen (Plow et al., 1983; Cierniewski & Budzynski, 1987). These changes were interpreted as an increased exposure of epitopes upon removal of the α-chains (see figure 3.1).

3.4.2. Fragment E.

Factor analysis of the amide I band of fragment E show the presence of 50% α-helical structure, indicating a percentage higher than 35% reported by CD studies (Budzynski, 1971). This disagreement may arise from the use of preparations of fragment E subjected to various degrees of proteolysis; and also by interference in the CD measurement of ellipticity from disulphur groups of fragment E (Doolittle, 1984). The shift in $^{2}H_{2}O$ solution (figure 3.5B central and upper traces) of the amide I band is attributed to the α-helical coiled-coil portions of this fragment. This shift has been observed in other proteins such as calmodulin (Jackson, 1990) and is associated with the presence of solvent-exposed helical regions (Susi et al., 1969). The carbonyl groups of the α-helices are solvated by the $^{2}H_{2}O$ molecules, which compete for hydrogen-bonding with the N-^{2}H molecules (Jackson, 1990). As a consequence, the infrared frequency appears at a lower position similar to those shown by random structures in proteins (Jackson et al., 1989a; Susi, 1969).

Most of the α-helical segments in fragment E can be attributed to the coiled-coil pre-existing in the original fibrinogen molecule (Doolittle, 1984). Other secondary structures have been suggested to occur in fragment E (Budzynski, 1971). Quantification of the secondary structure

indicates the presence of some ß-strands (19%) and turn structures (14%), previously not detected by CD spectroscopy (Budzynski, 1971). These structures are probably located in the disulphur-bond rich region of Fragment E (figure 3.1) that serves to interconnect the two pairs of three polypeptides originally present in the central nodule of fibrinogen (Doolittle, 1984).

3.4.3. Fragment D.

The spectrum of fragment D (figure 3.6A lower trace) shows an amide I band similar to that observed in fibrinogen (Figure 3.4A lower trace). As the contribution of fragment D is equivalent to almost two thirds of the original fibrinogen molecule, fragment D is expected to dominate the spectrum of fibrinogen (Doolittle, 1984). The high content of ß-sheet in fragment D as compared to that in fragment E suggests that most of the ß-sheet structure of fibrinogen is present in fragment D. Two components at 1630 and 1643 cm^{-1} have been assigned to ß-sheet. The relative high frequency of the band at 1643 cm^{-1}, present also in fibrinogen, can be attributed to ß-sheet with a twisted plane such as the ß-strands of aprotinin (Haris, 1989), and also to the presence of short and distorted ß-strands such as in ribunoclease A (Olinger et al., 1986). Theoretical predictions (Krimm & Bandekar, 1986) suggest that ß-turn type I or III structures may absorb between 1645-1640 cm^{-1}. The presence of 35% α-

helical content agrees with CD spectroscopic studies (Budzynski, 1971) which reported 40% α-helical content in this fragment.

The shift of the amide I band maximum in the spectrum of fragment D in ^2H_2O (figure 3.6B lower trace) is attributed to the presence of random structures and possibly solvent-exposed α-helical structures of the coiled-coil domain. The band at 1652 cm^{-1} indicates the presence of α-helical structures typically observed in the spectra of globular proteins in ^2H_2O (Byler & Susi, 1986). These α-helical segments may correspond to structures of the globular domain of fragment D (figure 3.1).

3.4.4. Domains of fragment D.

Fragment D contains two domains of different thermal stability (figure 3.1) according to calorimetric studies (Privalov & Melved', 1982). The coiled-coil portion has been isolated and shows a high α-helical content (70%) in agreement with previous CD studies of the coiled-coil of bovine fragment D (Melved' et al., 1982). The amide I band at 1654 cm^{-1} is identical to the frequency of the amide I band observed for fragment E (figure 3.5A lower trace). This similarity may reflect the nature of the α-helical structures of the coiled-coil that seems to be common to both fragments.

The globular domain of fragment D has been shown to denature at 55°C, whereas the coiled-coil portion remains intact at temperatures up to 75°C (Privalov & Melved', 1982). FT-IR studies of the thermal denaturation of fragment D at 55°C (figure 3.8) show a reduction in the intensity of α-helical, ß-turn and ß-sheet associated bands, indicating that these structures are present in the globular domain. Quantification of the secondary structure from these spectra is not possible as the sample contains components corresponding to the denatured protein and the native protein.

The percentages of secondary structures in the globular domain can be evaluated from those percentages of fragment D and those of its coiled-coil portion (see Results). Fragment D contains 34.5% of helical structure. The molecular weight of the coiled-coil portion corresponds to almost a quarter of the molecular weight of fragment D. Therefore, a quarter of 70% α-helical content measured in the coiled-coil portion would account for only a percentage of 19% α-helix in fragment D. The remaining 15% of α-helical structures must be present in the globular domain of Fragment D. On the other hand, as the coiled-coil portion contains no ß-sheet, all the ß-sheet of fragment D (29%) must be in the globular domain. This would indicate that the latter domain is twice richer in ß-sheet structures than in α-helical structures.

This deduction is confirmed when compared to the percentages of the secondary structure of the globular domain predicted by factor analysis of the spectra of the globular domain (figure 3.10A). The assumptions made to derive the subtracted spectrum are justified to some extent. Firstly the amide I band taken from 1700-1600 cm^{-1} has been shown to be representative of the secondary structures present in a protein (Lee et al., 1990). Second, the α-helical content measured for the coiled-coil agrees with previous results of the coiled-coil portion of bovine fragment D (Melved' et al., 1982). However the proteolytic cleavage may result in minor changes of conformation when compared to the conformation of the coiled-coil present in fragment D. Third, Byler & Susi (1986) showed that the percentages of secondary structures are approximately proportional to the areas of the components present under the amide I band envelope of proteins. Whilst that conclusion can be correct for the proteins examined by Byler & Susi (1986), there is evidence from studies with copolymers of aminoacids such as polylysine that the absorptivities may not be equal for all secondary structures (Jackson et al., 1989b).

3.4.5. Fragment D'.

Differences in the spectra of fragment D (Mw 100 KDa) and fragment D' (Mw 90 KDa) are expected to reflect the structural features absent in fragment D' and present in the G-chain between residues 303-411 in the original fragment D. The percentages of secondary structures in fragment D' are similar to those of fragment D, indicating that the removal of the polypeptide G-chain (Mw 10KDa) does not result in significant changes in the secondary structure. The slight differences observed in the comparison of the two spectra are not so marked as to suggest an indication of the predominant secondary structure of the missing structures of the G-chain (Shimizu et al., 1992). The high rate of amide $H/^{2}H$ exchange suggests that fragment D' has a less compact structure than that of fragment D, possibly caused by the removal of the G-chain segment.

3.5. SUMMARY.

The secondary structure of human fibrinogen and its plasmin-fragments have been studied by FTIR spectroscopy. The percentages of secondary structure in fibrinogen are 37% α-helix, 30% ß-sheet and 14% turns, in good agreement with CD spectroscopic studies. The spectra of fibrin clots formed in Ca^{2+}-containing buffer have a lower amide I/amide II ratio than fibrin clots in the presence of the quelator EGTA, which is interpreted as being due to aggregation.

Plasmin-digested fragments of fibrinogen were isolated and studied. Fragment E (Mw 45 KDa) contains 50% α-helix, attributed to its solvent-exposed coiled-coil domain, with minor contributions of ß-strands and turn structures. Fragment D (Mw 100 KDa) shows 35% α-helix, 29% ß-sheet and 17% turn secondary structures. Of the two domains present in Fragment D, the coiled-coil portion (Mw 27 KDa) was isolated and shows a percentage of 70% in α-helical structures. The thermolabile globular domain is estimated to be twice richer in ß-sheet structures than α-helical structures.

The secondary structure of Fragment D' (Mw 90 KDa) has been shown to be similar to Fragment D. Fragment D' shows a solvent-accessible structure as indicated by the rapid rate of $H/^{2}H$ exchange.

CHAPTER 4.

BIOPHYSICAL STUDIES OF THE PF1 AND FD COAT PROTEINS IN THE PHAGE, IN DETERGENT MICELLES AND IN PHOSPHOLIPID MEMBRANES.

4.1. INTRODUCTION.

Filamentous phages are the thinnest and longest viruses known, consisting of a single-stranded DNA encapsulated by 2000-7000 copies of a 5 KDa coat protein in a characteristic filament particle (Marvin & Wachtel, 1975; Day et al., 1988). Depending on the strain, the viruses measure 6 nm in diameter by 1000-2000 nm long, and contain about 6-10% (w/w) DNA and no lipid.

During the life cycle of the phages the coat proteins have to adapt to two different environments, the bacterial membrane and the phage. During the synthesis of the viral components inside the bacteria, the coat proteins are encoded as membrane proteins with a signal sequence (Smilowitz et al., 1972; Webster & Cashman, 1973) which is removed by the host signal-peptidase. Phage assembly seems to take place at points of the inner bacterial membrane where the coat proteins and the DNA cluster as the filament particles are extruded out to the external media.

On the basis of the structure of the viruses and the homology of the aminoacid sequence of the coat proteins, two classes of filamentous phages can be distinguished: class I that correspond to the fd, M13, f1 strains and class II to the Pf1 and Pf3 strains (Day et al., 1988). The aminoacid sequence of the coat proteins, such as those of the Pf1 and fd phages (table 4.1), shows a pattern of an acidic N-termi-

TABLE 4.1 .

Aminoacid sequence of the fd coat protein.

Ala-Glu-Gly-Asp-Pro-Ala-Lys-Ala-Ala-Phe$_{10}$-Asp-Ser-Leu-Gln-Ala
Ser-Ala-Thr-Glu-Tyr$_{20}$-Ile-Gly-Tyr-Ala-Trp-Ala-Met-Val-Val-Ile$_{30}$
Val-Gly-Ala-Thr-Ile-Gly-Ile-Lys-Leu-Phe$_{40}$-Lys-Lys-Phe-Thr-Ser
Lys-Ala-Ser$_{48}$

Aminoacid sequence of the Pf1 coat protein.

Gly-Val-Ile-Asp-Thr-Ser-Ala-Val-Glu-Ser$_{10}$-Ala-Ile-Thr-Asp-Gly
Gln-Gly-Asp-Met-Lys$_{20}$-Ala-Ile-Gly-Gly-Tyr-Ile-Val-Gly-Ala-Leu$_{30}$
Val-Ile-Leu-Ala-Val-Ala-Gly-Leu-Ile-Tyr$_{40}$-Ser-Met-Leu-Arg-Lys-
Ala$_{46}$

Data obtained from Day et al. (1988).

nal segment, a basic C-terminus and a 20-residue hydrophobic region in the centre of the sequence.

Neutron and X-ray diffraction studies of oriented phages (Marvin & Wachtel, 1975; Day et al., 1988) indicate that the coat proteins exist as α-helical subunits parallel to the phage axis, with the solvent-exposed N-termini covering the hydrophobic region of adjacent coat proteins in a array mimicking scales in fish. The arrangement of the α-helical subunits forms left-handed spirals around the filamentous particle, with 4.5-5.5 spirals per turn (Day et al., 1988).

In the bacterial membrane, the hydrophobic segment is thought to span the bilayer with the C-termini facing the cytoplasmic side and the N-terminus the periplasmic side (Wickner, 1975). CD spectroscopic studies indicate that the α-helical content of the Pf1 and the fd coat proteins is reduced markedly upon solubilisation in detergent micelles or reconstitution in lipid aqueous suspensions as compared to the phage (Schiksnis et al., 1987; Leo et al., 1987). The tertiary structure of the Pf1 coat protein in DPC detergent micelles has been determined using 2-D $^{15}N/^{1}H$-NMR spectroscopy. The Pf1 coat protein, in this detergent micelle, is a monomer and adopts an arrangement of two stable α-helical segments (Shon et al., 1991; Schiksnis at al., 1987). With the assumption that this structure was conserved in lipid membranes, solid-state NMR spectroscopy of $^{2}H/^{15}N$-labelled

residues of the Pf1 protein was used to deduce the degree of motion and the orientation of the two helical stretches adopted by the protein in the membrane. These studies led to Shon and coworkers (1991) to propose a model for the Pf1 protein in the phospholipid membrane where the hydrophobic region (about 24 residues) forms a membrane-spanning α-helix whilst the amino-terminal region (residues 1-14) is arranged as an amphipathic α-helix lying parallel to the lipid bilayer plane.

The conformation of the M13 coat protein has been studied in SDS micelles by NMR spectroscopy (Henry & Sykes, 1992). The sequence of the M13 protein is identical to the fd protein, except for a replacement of Asp11 to Asn (Day et al., 1988). The M13 coat protein in the micelle exists in a similar conformation to that of the Pf1 protein in DPC micelles (Henry & Sykes, 1992). In the micelle, the M13 coat protein forms a dimer with both hydrophobic regions juxtaposed in a parallel fashion. Solid-state $^{2}H/^{15}N$-NMR studies of the fd protein in the lipid membrane indicate a conformation that is rigid between residues Ala6-Phe41 and mobile in both N- and C-termini (Leo et al., 1987).

The coat protein of the filamentous phages, especially the fd and Pf1 proteins, are used extensively as models for the determination of the structure and the dynamics of

membrane proteins in membrane-mimicking environments such as detergent micelles and phospholipid aqueous systems (Schiksnis et al., 1987; Gallusser & Kuhn, 1990). Owing to their small molecular weight, it is possible to study basic features of the structure and dynamics of the exoplasmic and the membrane-spanning domains of membrane proteins. Herein, FT-IR spectroscopy is used to study the conformation of the Pf1 and fd coat proteins in the phage, in detergent micelles and reconstituted in a lipid membrane environment. Internal reflectance FT-IR spectroscopy is used to study the orientation of the secondary structure of the two coat proteins within the lipid bilayer. Other biophysical techniques such as polarization of the fluorescent probe DPH and calorimetry are used to examine the degree of lipid chain perturbation caused by the Pf1 coat protein when embedded within the lipid bilayer.

4.2.MATERIALS AND METHODS.

All reagents were of analytical grade and obtained from commercial sources. DMPC was purchased from Fluka and DPPC supplied by Lipid products.

4.2.1. Culture and purification of filamentous phages.

Host cells *Pseudomonas aeruginosa* strain K and bacteriophage Pf1 samples were kindly provided by Dr. R.N. Perham (Cambridge, UK), bacteriophage fd was prepared in Dr. S.

Opella's lab (Philadelphia, U.S.A.). 1-L TY medium culture of *Pseudomonas aeruginosa* strain K grown to early log phase ($O.D._{600}$=0.25), were infected with Pf1 phage at m.o.i. 15 (Schiksnis et al., 1987). About 12-18 hours later, bacteria were removed by low-speed centrifugation. Solid NaCl was added to the supernatant up to a concentration of 0.5 M, which after 6-10 hours was clarified. Addition of PEG 8,000 to a final concentration of 5%, precipitated the phage which was then recovered by centrifugation. Virus purification was carried out by equilibrium sedimentation in 0.4 gr/ml CsCl in a Beckmann SW15 at 35,000 rpm for 18 hours. The viscous layer of virus was separated drop-wise and dialysed three times against TrisEDTA buffer pH 8. The concentration of Pf1 phage was calculated by UV spectroscopy using an extinction coefficient of 2.07 $mg.cm^{-1}$ at 270 nm (Day & Wiseman, 1976). Yields of Pf1 phage were usually about 100mg.

4.2.2. ^{13}C-labelling of serine sites of Pf1 protein.

^{13}C is incorporated at all serine sites of the Pf1 coat protein by infecting cultures of bacteria grown in M9 mineral media (Miller, 1972) supplemented with natural aminoacids, except the ^{13}C-labelled L-Serine which was purchased from Cambridge Isotope Labs. In a separate experiment, the level of incorporated serine in the Pf1 phage was determined with ^{14}C-serine. It was estimated that the serine

supplemented to the mineral media was being incorporated at 65-75% of all serine sites present per mg of Pf1 phage. Serine is present at two positions (6, 10) of the amino-terminus and at position 40 near the carboxy-terminus (table 4.1) (Day et al., 1988).

4.2.3. Preparation of the phage samples.

For FT-IR studies in H_2O, phage samples were prepared by precipitation with 5 % PEG 0.5 M NaCl and then resuspended in the appropriate volume. For studies in ^2H_2O several precipitations and resuspension steps were performed in ^2H_2O solutions until H_2O was removed. This was checked by the absence of H-O-D infrared bands at 3400 cm^{-1} in the transmission spectrum of the solution.

4.2.4. Preparation of the coat protein in detergent micelles and in lipid vesicles.

Phage samples (2 mg/ml) were solubilised in 20 mg/ml SDS for 60 minutes at 37°C. For studies of the coat protein in lipid membranes, DMPC was first dissolved in organic solvent, dried and dispersed in buffer by strong vortexing at 30°C. To reconstitute the coat proteins into lipid vesicles, two methods were used: (i) Phage samples (1 mg/ml) and aqueous suspensions of DMPC (2.5-5 mg/ml) were sonicated in a pear-shaped flask intermittently in a MTE sonication bath at a temperature of 30-33°C, until the solution was translu-

cent and (ii) 1 mg/ml phage and 2.5-5 mg/ml DMPC were solubilised separately in sodium-deoxycholate solution (DOC) (5 and 15 mg/ml, respectively) for 60 minutes at 37°C, then the two solutions were mixed and the detergent was removed by dialysis.

Incorporation of the coat protein in the lipid vesicles was checked by centrifugation on a sucrose gradient. All samples of the coat protein in detergent micelles and in phospholipid suspensions were freeze-dried for their examination by FT-IR spectroscopy.

4.2.5. Digestion of the Pf1 protein in lipid vesicles.

Several proteases were used to probe the solvent-exposed segments of the Pf1 coat protein in the lipid vesicles. Separate assays were carried out using reconstituted protein/lipid systems with the proteases papain, elastase, chymotrypsin and trypsin, at 100:1 (w:w) protein:protease ratio. Mixtures were sonicated briefly to ensure access of the protease to all sites of the coat protein in the aqueous lipid systems, as described for fd protein/lipid systems (Leo et al., 1987). Samples were kept at 33°C for 3 hours, heated at 100°C briefly and then solubilised in SDS detergent solution to be analysed by SDS-PAGE using the Tricine:Tris buffered system (Hames and Rickwood, 1981; Schägger & Jagow, 1987).

4.2.6. Infrared spectroscopy.

Samples were rehydrated to give a final concentration of protein of 3-4 % in H_2O and 2-2.5 % in ^2H_2O buffer (see section 2.5.1 for more details). The cell was mounted on a thermostated vertical cell holder with the temperature set at 30°C. For each sample 400 scans in H_2O or 100 in ^2H_2O, were recorded at 4 cm^{-1} resolution, signal-averaged and treated in a Perkin-Elmer 1750 FT-IR spectrometer connected to a Perkin-Elmer Data Station.

For transmission polarization studies, phage aliquots of 100 μl (2-4 %) were oriented on a rectangular CaF_2 window by manually stroking with a sharp needle, whilst the liquid was being simultaneously dried with a current of nitrogen gas, as described by Fritzsche et al., (1987) in their studies of the fd phage. The film was enclosed in a transmission cell using a teflon spacer of 1 mm and a CaF_2 window, and were mounted on a fixed vertical cell holder. A KRS-5 grid polarizer was used to polarize the infrared radiation and the parallel beam was made to coincide with the direction of stroking.

To deconvolve the original difference spectra of the protein, in all cases a HWHH=12 cm^{-1} was used and a K=2 (see section 2.4.2). The degree of $H/^2H$ exchange was estimated by measuring the amide I band to amide II band intensity ratio with respect to the ratio with the spectra of the

protein in H_2O (see section 2.2.3.5. for more details) (Rath et al., 1991a; Lee et al., 1987). The secondary structure was quantified by factor analysis of the spectra (see 2.2.4.2. for more information) (Lee et al., 1990).

4.2.7. Attenuated total internal reflectance.

Thin films were formed by spreading suspensions of lipid vesicles onto a Germanium crystal (angle of incidence of 45°) and drying with a current of N_2 gas. The Germanium crystal was installed on a vertical ATR accessory. Some 500-2000 scans were signal-averaged per spectra on a Mattson FT-IR spectrometer Series 4060, equipped with a TGS detector. Spectra of the germanium crystal with and without film were recorded separately as single beam spectra and ratioed to give the reflectance spectra. The intensities of absorption in the ATR spectra are shown as *Absorbance = 2-log(Ri/Ro)*, where *Ri* and *Ro* correspond to final and initial reflectance, respectively. The dichroic character of the infrared bands of the terminal methyl groups of the lipid acyl chains at 2874 and 1200 cm^{-1} served as an indicator of the degree of perpendicular orientation of the lipid molecules in the film (for details see section 2.2.2.1. and 2.5.2) (Fringeli & Gunthard, 1981).

4.2.8. Differential scanning calorimetry.

Calorimetric data were recorded using a Perkin-Elmer DSC-7 differential calorimeter following the procedure described by Gomez-Fernandez et al. (1980). Scanning rates of 4°C/min and sensitivities of 1 mcal/s were used. Samples were prepared by detergent dialysis method which was followed by two cycles of centrifugation and resuspension to ensure the elimination of traces of the detergent. Samples were hermetically sealed in Perkin-Elmer aluminium 'volatile' sample pans. Satisfactory performance of the instrument was checked using pure DMPC and DPPC aqueous suspensions.

The enthalpies were determined by integrating the areas associated with the phase transition. After the measurements the phospholipid content of the pans were determined by solubilising the pan contents in 6 % SDS at 70°C and analysing the phosphate content as described by Bartlett (1959). Pf1 protein content was measured by UV spectroscopy at 270 nm by comparison with solutions of Pf1 phage in 6 % SDS.

4.2.9. Fluorescence polarization studies.

Fluorescence polarization measurements of the DPH probe (figure 2.11) in aqueous lipid/protein systems were made using a Perkin-Elmer Fluorimeter MPF-4B. The temperature of the sample was thermostatically controlled and set at 37°C.

The fluorescent probe DPH (an aliquot of a 10 mM solution in tetrahydrofuran) and lipid were added to the organic solvent solution, before drying, to give a probe:lipid molar ratio of 1:500.

In the fluorescence polarization experiment the sample (25-50 μgr lipid/ml) was excited with a polarized beam and the components of the emission parallel or perpendicular to the direction of the excitation beam were measured. The polarization of the emitted fluorescence *P* was determined as:

$$P = (Ipar - Iperp \cdot G) / (Ipar + Iperp \cdot G),$$

where *Ipar* and *Iperp* were the intensities of the parallel and perpendicular components of the fluorescence and *G* is a correction factor for the instrumental response of the two components of the emission (Lakowicz 1983).

The values of polarization were approached to a exponential curve of the type $P=1-e^{-MX}$ (Hoffman et al., 1981). *M* is an empirical quantity of the approximate number of lipid molecules or probes which fit around the perimeter of the intrinsic molecule embedded in the membrane (for details see section 2.6.3). To derive *M*, the polarization values *P* for each sample had to be transformed. The values were normalised relative to a minimum value of *0* for the polarization value of the pure lipid ($P_o=0.25$) and a maximum value of *1* for the estimated maximum. It was estimated that 95% of

maximum polarization was reached at $P=0.375$. For the calculation of M, curves of the form $P=1-e^{-MX}$ for several values of M were fitted to the experimental values.

4.3. RESULTS.

4.3.1. The Pf1 coat protein in the phage.

Figure 4.1 shows the FT-IR transmission spectrum of Pf1 phage when present in H_2O solution. The coat protein represents 95 % of the phage mass and 99 % of the total protein of Pf1 phage, whilst only some 5 % of the phage mass corresponds to the DNA (Day et al., 1988). The infrared spectrum is hence dominated by the contribution of the coat protein subunits in the filamentous phage. The amide I band is positioned at 1652 cm^{-1}, which corresponds to α-helical structure (Jackson et al., 1989a). The deconvolved spectrum (figure 4.1) reveals a small component at 1675 cm^{-1}, which is attributed to ß-turn structures (Krimm & Bandekar, 1986; Jackson et al., 1989a). Quantitative analysis of the secondary structure by factor analysis of the amide I band (Lee et al., 1990) indicates an α-helical content of approximately 90-100% of the protein in the Pf1 filamentous phage, in agreement with previous reports (Day et al., 1988). In ^2H_2O solution (not shown), some reduction of the amide II' band intensity occurs over a period of two hours, indicating that part of the structure of the coat protein in the phage is

Figure 4.1.

Absorption FT-IR spectrum of the Pf1 coat protein in the phage in H_2O (solid trace) and its deconvolved spectrum (dashed trace) using K=2 and HWHH=12 cm^{-1}.

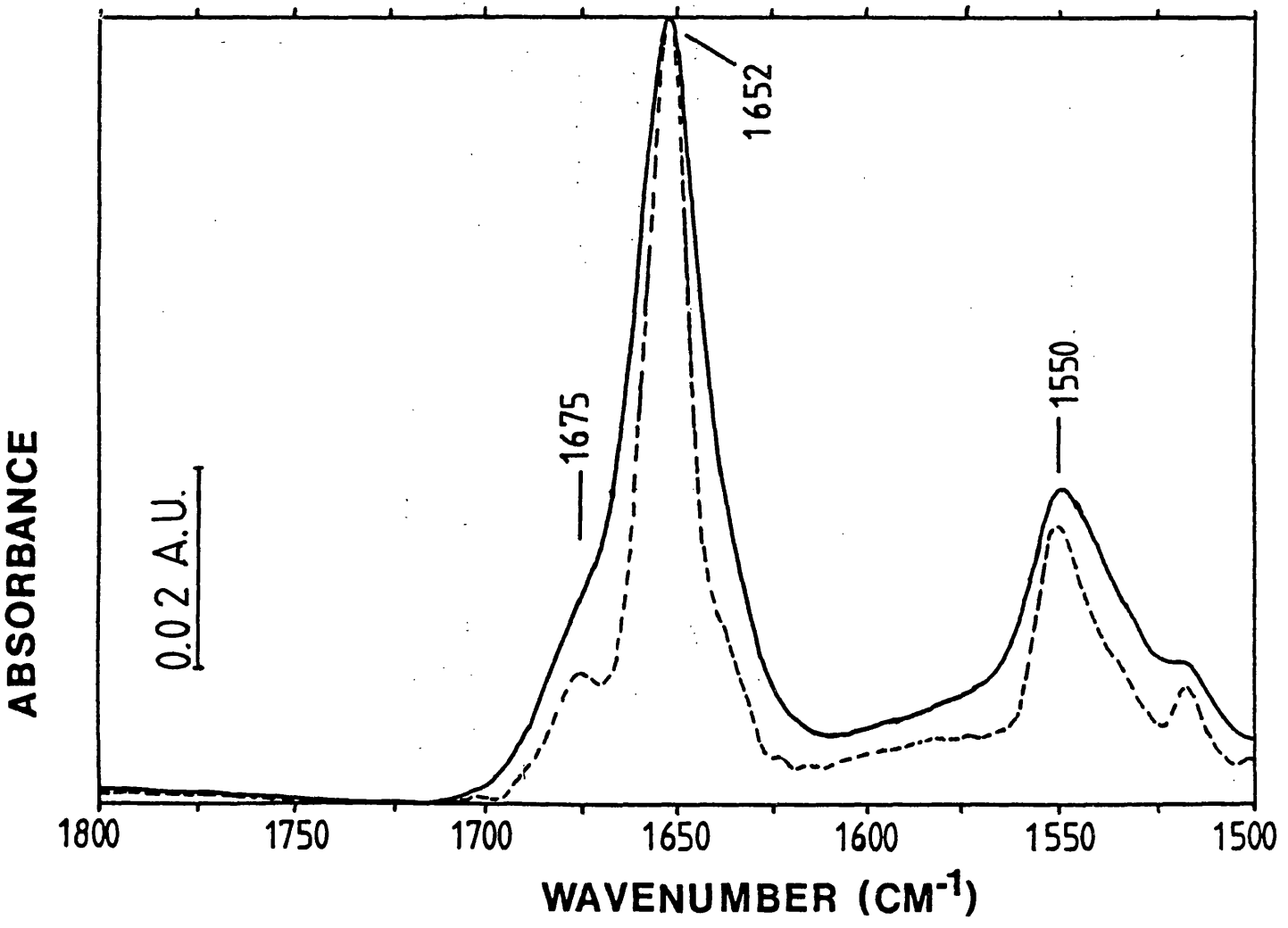
ABSORBANCE
0.02 A.U.
1675
1652
1550
1800
1750
1700
1650
1600
1550
1500
WAVENUMBER (CM-1)

Figure 4.2.

Transmission FT-IR spectra of oriented films of Pf1 phage, obtained with beams polarized parallel (solid trace) and perpendicular (dashed trace) to the direction of the axis of the phage. (A) Spectrum between 4000-1000 cm^{-1} and (B) spectrum between 1800-1500 cm^{-1}.

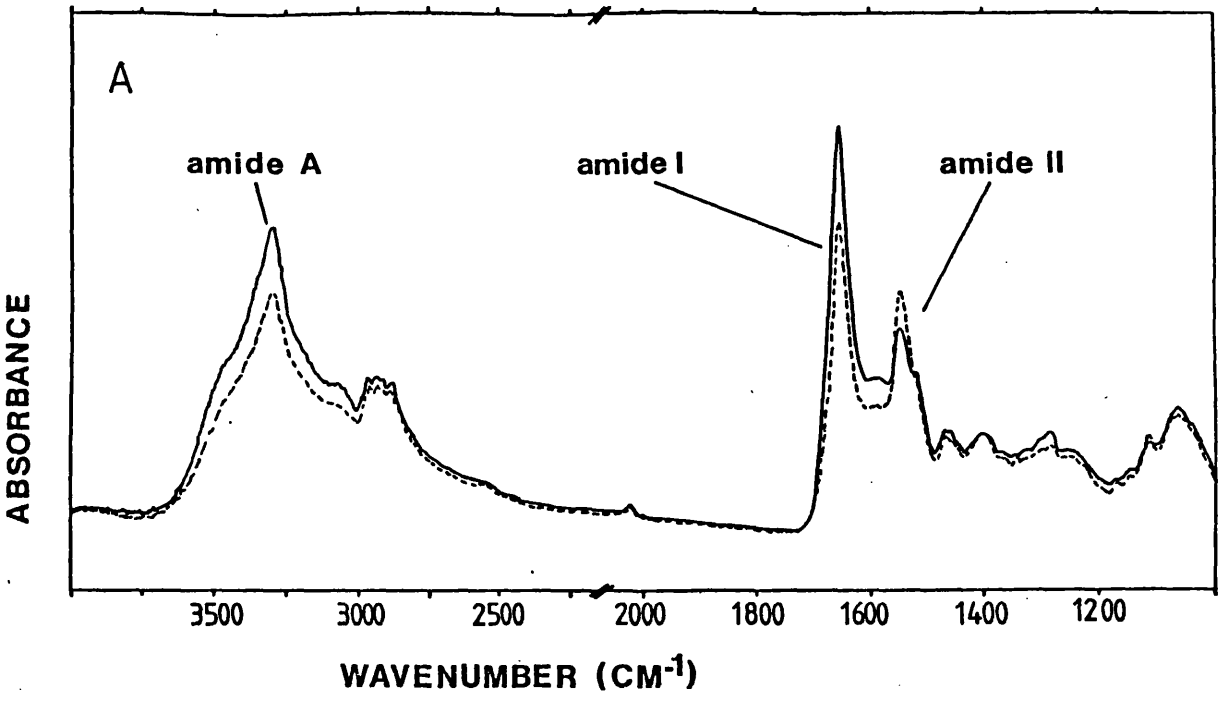
A
amide A
amide I
amide II
ABSORBANCE
3500
3000
2500
2000
1800
1600
1400
1200
WAVENUMBER (CM-1)

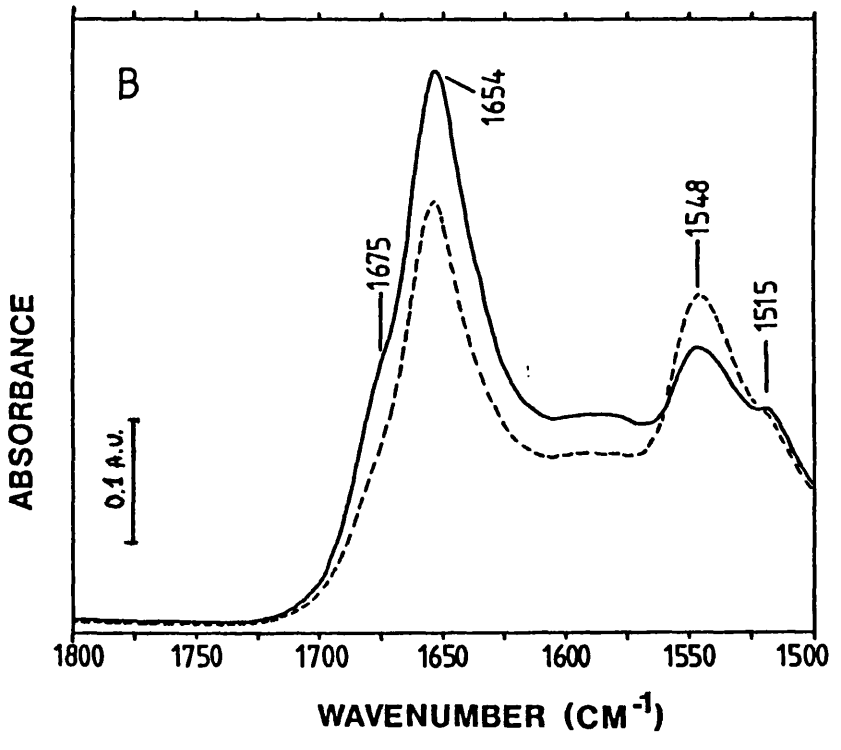
B
1654
1675
1548
1515
0.1 A.U.
ABSORBANCE
1800
1750
1700
1650
1600
1550
1500
WAVENUMBER (CM-1)

available for $H/^2H$ exchange to occur.

Figure 4.2A shows the transmission spectrum of oriented dried films of the Pf1 phage, recorded with polarized infrared radiation. The parallel polarized beam follows the direction of the stroking and thus the direction of the axis of the Pf1 phage. With the parallel beam, there is an enhancement of various bands: the amide A band at 3200 cm^{-1} which originates mainly from N-H stretching vibrations (Susi, 1969) and the amide I band at 1654 cm^{-1}; a reduction is observed in the amide II band. In the spectra recorded with perpendicularly polarized beam, the amide A and amide I bands are reduced and only the amide II band is enhanced. Except the a minor change at the amide III band at 1300-1270 cm^{-1}, the remaining bands exhibit no changes in intensity. This pattern in the infrared bands is consistent with the helices being aligned parallel to the axis of the phage. The amide I and II bands region (figure 4.2B) reveals that the bands at 1675 cm^{-1} and 1515 cm^{-1} show an increase in intensity with the parallel polarized beam. The band at 1515 cm^{-1} originates from vibrations of tyrosine residues (Venyaminov & Kalnin, 1991).

4.3.2. The Pf1 coat protein in detergent micelles.

The FT-IR spectra of the Pf1 coat protein in SDS micelles in H_2O solution is shown in figure 4.3A, in compari-

Figure 4.3.

(A) Transmission FT-IR spectra of the Pf1 coat protein in H_2O, in SDS detergent micelles (solid trace) and in the phage (dashed trace).

(B) Transmission FT-IR spectrum of the Pf1 coat protein in SDS detergent micelles in ^2H_2O solution (solid trace) and its deconvolved spectrum (dashed trace).

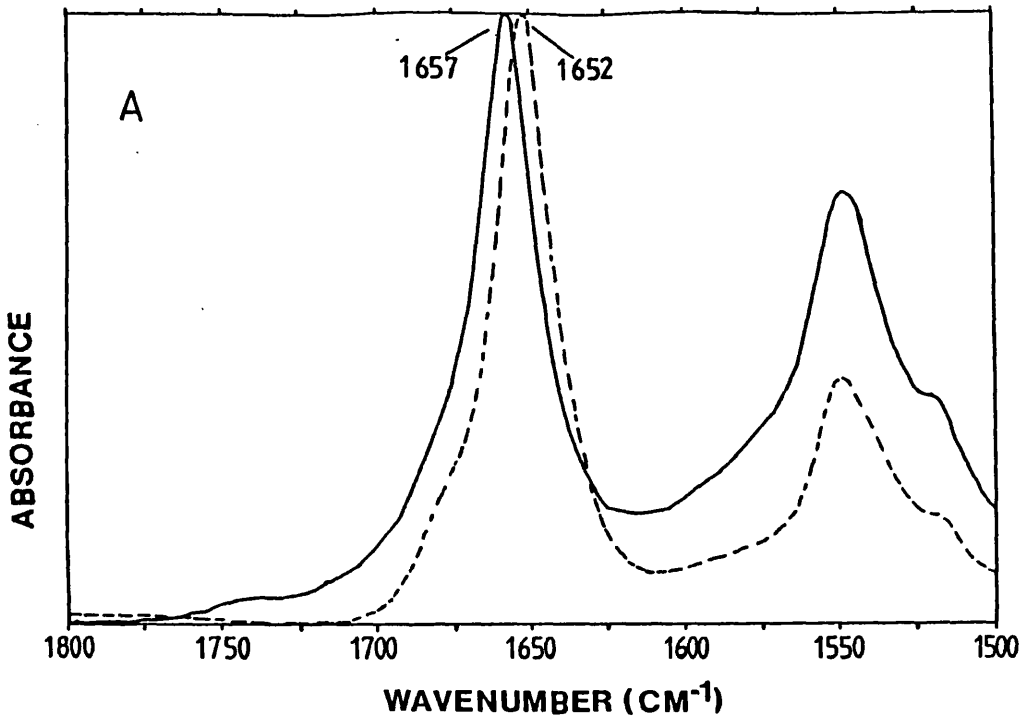
A
1657
1652
ABSORBANCE
1800
1750
1700
1650
1600
1550
1500
WAVENUMBER (CM-1)

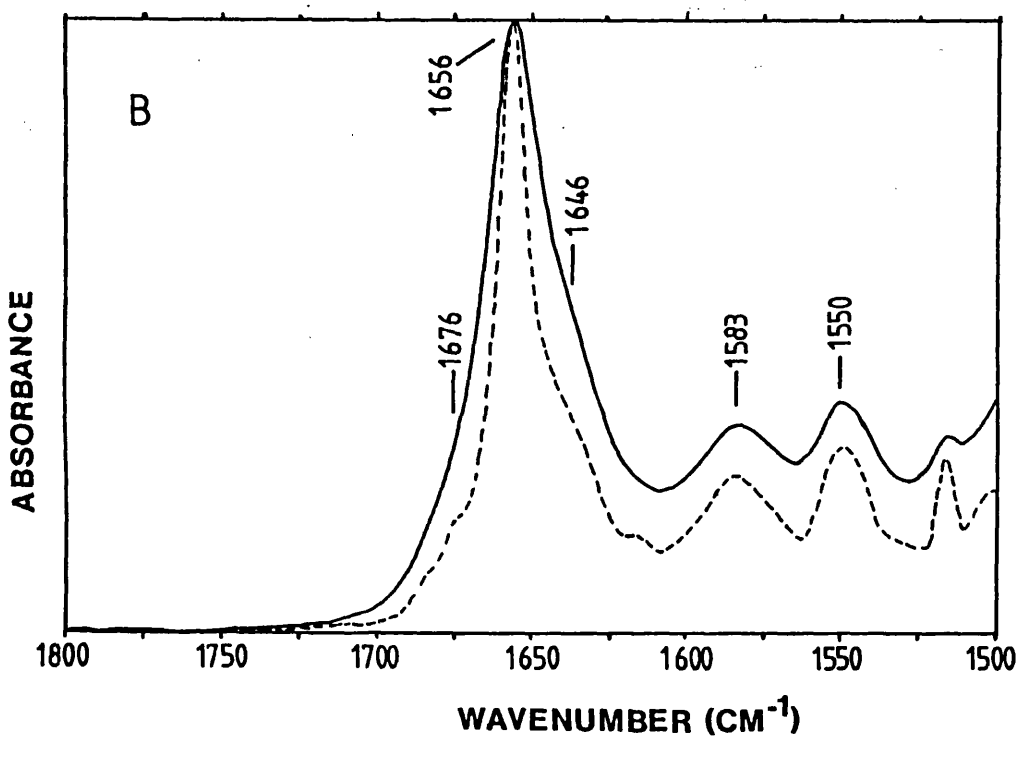
B
1656
1646
1676
1583
1550
ABSORBANCE
1800
1750
1700
1650
1600
1550
1500
WAVENUMBER (CM-1)

Figure 4.4.

(A). Transmission FT-IR spectra of the coat protein in DPC detergent micelles in H_2O (solid trace) and in the phage (dashed trace).

(B) Transmission FT-IR spectrum of the Pf1 coat protein in DPC detergent micelles in ^2H_2O (solid trace) and its deconvolved spectrum (dashed trace).

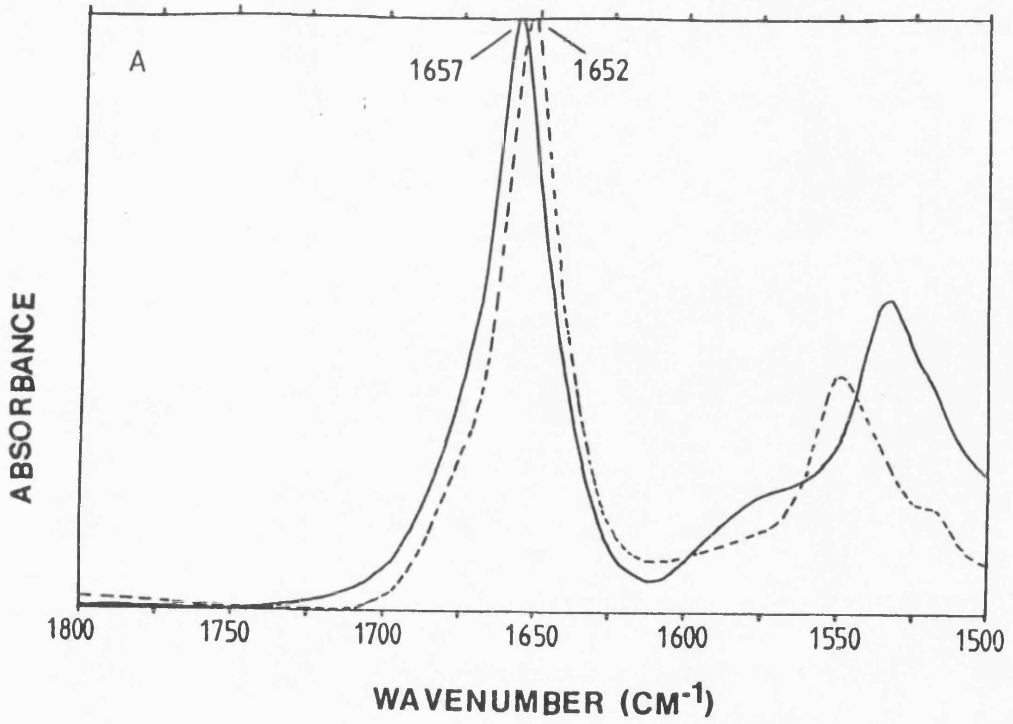
A
1657
1652
ABSORBANCE
1800
1750
1700
1650
1600
1550
1500
WAVENUMBER (CM-1)

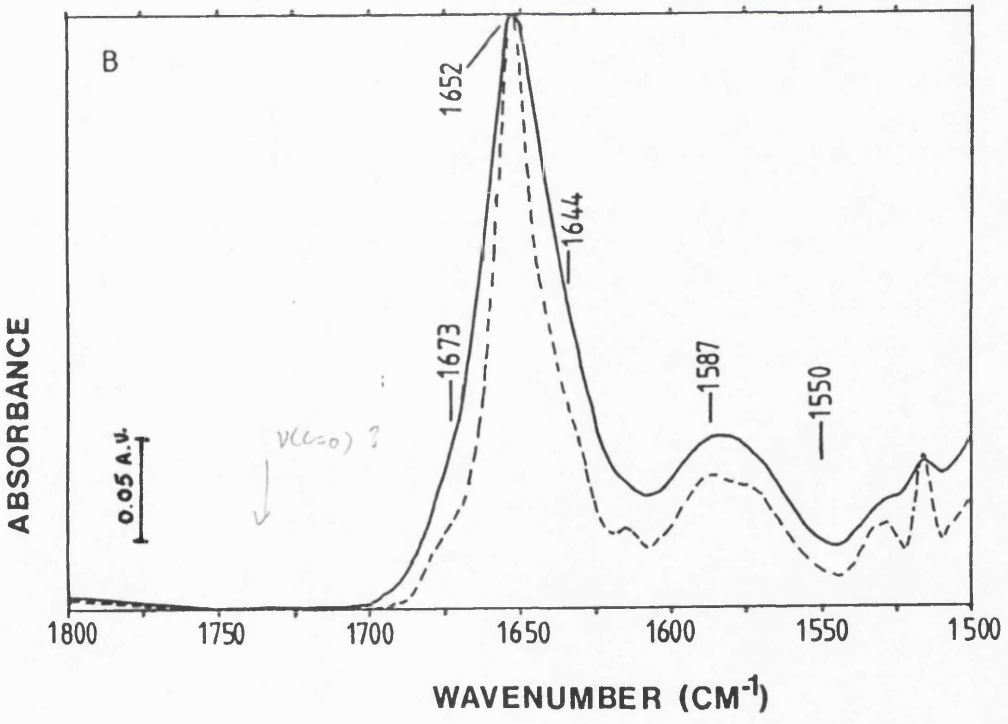
B
1652
1644
1673
1587
1550
0.05 A.U.
ν(C=O) ?
ABSORBANCE
1800
1750
1700
1650
1600
1550
1500
WAVENUMBER (CM-1)

son with the spectrum of the phage. The Pf1 protein in SDS micelles gives rise to an amide I band with a similar band-shape to that observed with the phage. The frequency of the amide I band shifts from 1652 cm^{-1} in the phage to 1657 cm^{-1} in SDS micelles and DPC micelles (figure 4.4A). This higher amide I frequency is indicative of a weaker hydrogen-bonding occurring in the α-helical structures of the coat protein in the detergent micelle. Quantification of the secondary structure by factor analysis (Lee et al., 1990) indicates that the protein in SDS and DPC micelles have a percentage of α-helix of approximately 90-100%.

The ratio of the intensity of the amide I band to the amide II band is higher with the protein in the phage than that occurring with the protein in the detergent micelles. The low position of the amide II band of the protein in DPC micelles is atypical and no possible explanation has been found out.

In SDS micelles using ^2H_2O solution (figure 4.3B) the amide I band of the protein is broader and appears at 1656 cm^{-1}. In the deconvolved spectrum (figure 4.3B) a small band at 1630-45 cm^{-1} is observed which appears to originate from a shift of band components present under the main amide I band at 1657 cm^{-1} with the protein in H_2O (figure 4.3A). These type of structures are assigned to random-structures (Jackson et al., 1989a). The intensity of the amide II band

shows a partial decrease as a result of H/^{2}H exchange, indicating that some of the amide protons are accessible to the solvent and exchange rapidly. Further exchange is slow and is not complete after 24 hours. Comparison of the ratio of the amide II/amide I band intensity with that of the protein in H_2O indicates that these slow-exchanging amide protons corresponds to approximately 30-40% of the total peptidic bonds. This agrees with studies on H/^{2}H exchange of the coat protein in SDS micelles using ^{1}H-NMR spectroscopy (Schiksnis et al., 1987). The slow-exchanging amide protons were suggested in this case to correspond to an eleven aminoacid-long hydrophobic part of the Pf1 coat protein (Schiksnis et al., 1987).

The amide I band of the coat protein in DPC micelles in ^2H_2O (figure 4.4B) appears at 1652 cm^{-1}. The deconvolved spectrum shows a weak band at 1644 cm^{-1}, indicative of the presence of some random structures as observed in SDS micelles. The band at 1585 cm^{-1} probably corresponds to the presence of traces of carboxylic groups of EDTA buffer. The intensity of the amide II band shows a marked decrease as a result of H/^{2}H exchange, indicating that almost all amide protons of the coat protein in the DPC micelle are readily accessible to the solvent. This can possibly be due to a solvent accessible conformation of the DPC micelle as compared to that in the SDS micelle (Tanford, 1980).

4.3.3. The Pf1 coat protein in a membrane environment.

The spectra of the reconstituted Pf1 coat protein in aqueous lipid systems and the coat protein in the phage are shown in figure 4.5A. The spectrum of the protein reconstituted by sonication or deoxycholate-detergent dialysis method show an identical infrared spectra. In the spectrum of aqueous lipid/protein suspensions three bands are observed, the first one at around 1740 cm^{-1} corresponds to the stretching vibrations of carbonyl groups of the acyl-esters of the phospholipid. The amide I band maximum of the protein is observed at 1658 cm^{-1} and its contour is similar to that in the phage, though slightly broader due to the presence of the band associated with the lipid ester group. The shape and frequency of the amide I band are similar to those observed with the coat protein in SDS or DPC micelles, indicative that the protein secondary structures are similar in the micelles and in the membrane. The percentage of α-helical structure determined by factor analysis (Lee et al., 1990) is approximately 90-100%, similar to that observed in the protein in the phage and detergent micelles.

In ^2H_2O solution (figure 4.5B) the amide I band maximum of the protein in the lipid membrane appears at 1658 cm^{-1}. Deconvolution of the spectrum indicate that additional bands are present at 1630-40 cm^{-1}, which are attributed to random structures (Jackson et al., 1989a). Comparison of the ratio

Figure 4.5.

(A). Transmission FT-IR spectra of the Pf1 coat protein in H_2O in DMPC vesicles (solid trace) and in the phage (dashed trace).

(B). Transmission FT-IR spectrum of the Pf1 coat protein in DMPC vesicles in ^2H_2O (solid trace) and its deconvolved spectra (dashed trace).

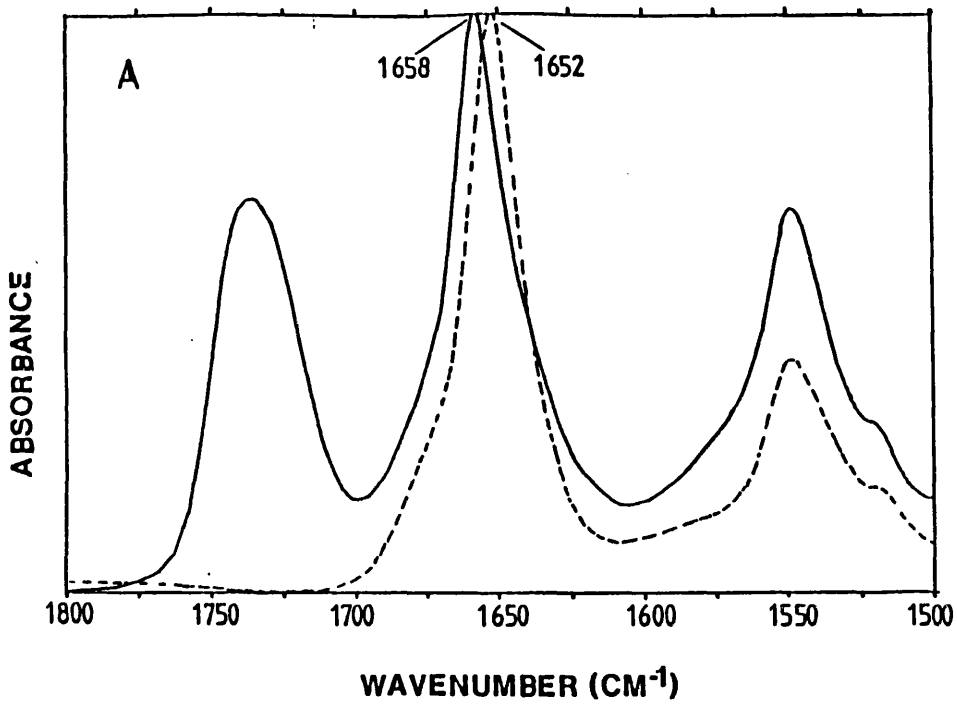
A
1658
1652
ABSORBANCE
1800
1750
1700
1650
1600
1550
1500
WAVENUMBER (CM-1)

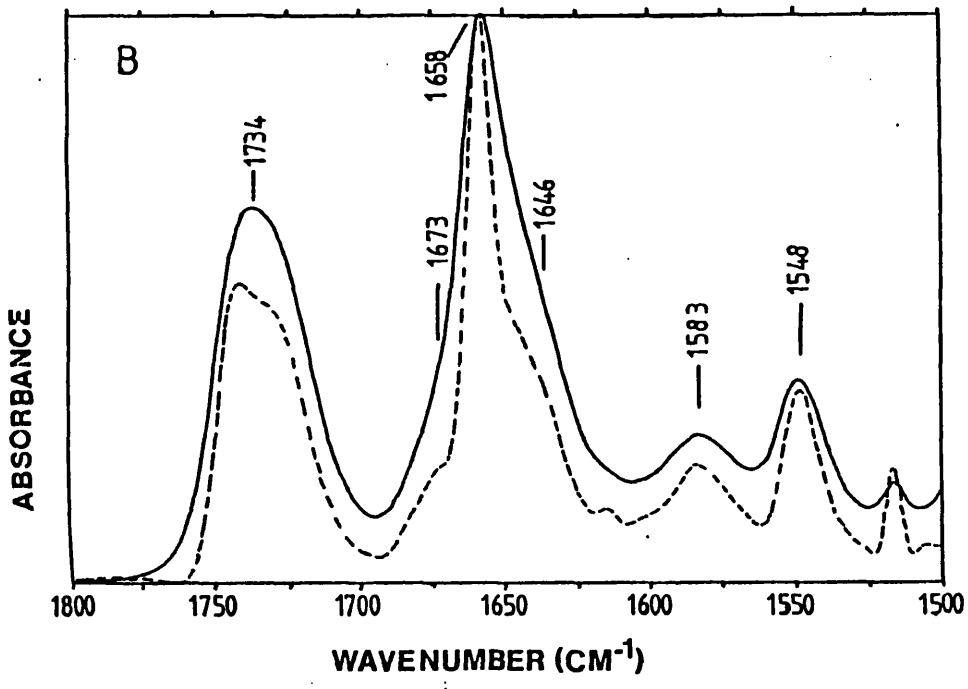
B
1734
1658
1673
1646
1583
1548
ABSORBANCE
1800
1750
1700
1650
1600
1550
1500
WAVENUMBER (CM-1)

Figure 4.6. SDS-PAGE gel of (from Left to Right lane):

Molecular weight markers: (1) SBA 66KDa and Pf1 coat protein 5KDa, (2) cytochrome C 13KDa and insulin chain A 3KDa; (3) and (4) controls of Pf1 coat protein from lipid suspensions; samples treated with proteases (5) papain, (6) elastase, (7) chymotrypsin and (8) trypsin (see methods).

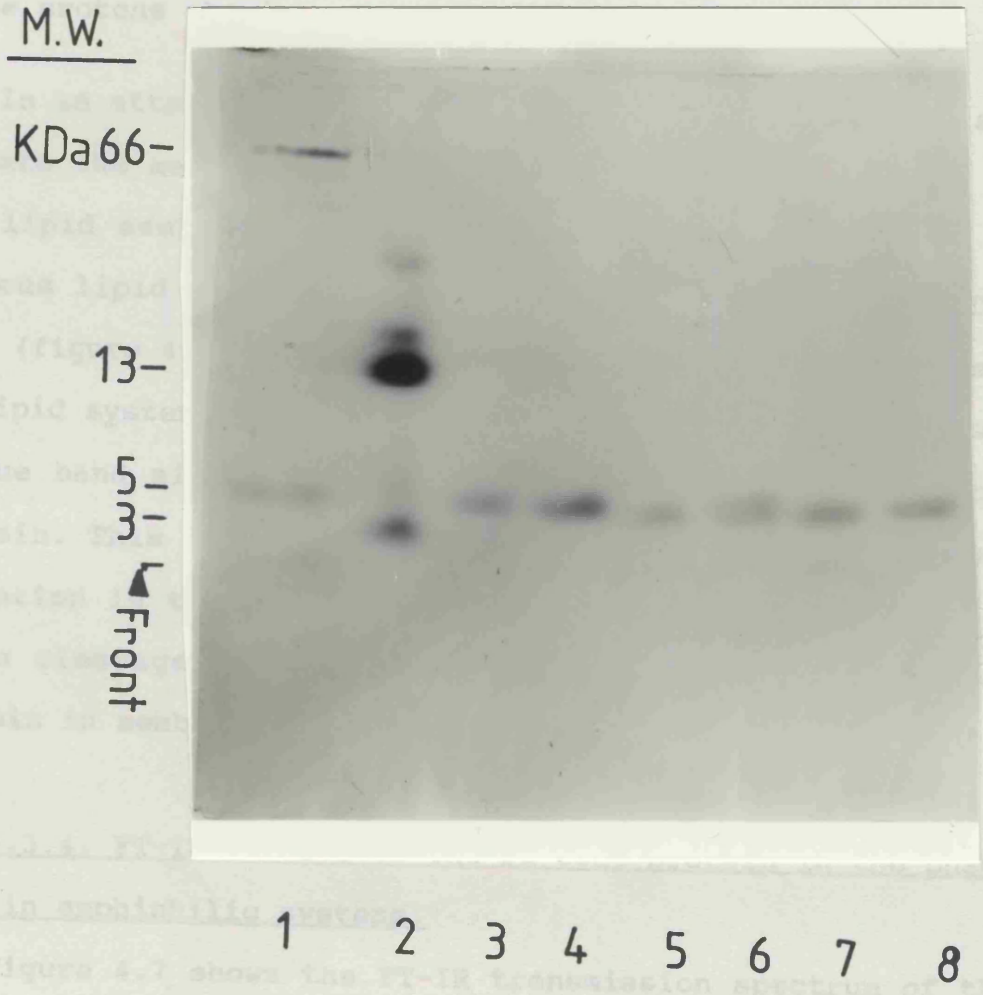
M.W.
KDa 66-
13-
5-
3-
Front
1
2
3
4
5
6
7
8

of the amide I/amide II band intensities to that observed in the H_2O spectrum indicates that approximately 60% of the amide protons undergo rapid $H/^2H$ exchange and the remaining amide protons showing slow exchange.

In an attempt to cleave the solvent-exposed segments and isolate the membrane spanning-domain of the coat protein in the lipid membrane, the reconstituted Pf1 coat protein in aqueous lipid suspensions was treated with proteases. SDS-PAGE (figure 4.6) of solubilised samples of the coat protein in lipid systems that have been exposed to proteases shows a unique band similar to the band observed in the untreated protein. This indicates that the Pf1 protein adopts a conformation in the membrane which is not accessible to protease cleavage, contrary to what is observed with the fd protein in membranes (Chamberlain et al., 1978).

4.3.4. FT-IR studies of the fd coat protein in the phage and in amphiphilic systems.

Figure 4.7 shows the FT-IR transmission spectrum of the fd phage as observed in H_2O solution and ^2H_2O. The amide I band is seen at 1651 cm^{-1} with a component at 1675 cm^{-1}. Quantitative analysis of the amide I band in H_2O indicates that the percentage of α-helical structure in the fd phage is approximately 90-100%.

Figure 4.7.

Transmission FT-IR spectrum (solid line) of the fd coat protein in the phage, in (A) H_2O and (B) ^2H_2O.

Deconvolved spectra (dashed trace) obtained with K=2 and HWHH=12 cm^{-1}.

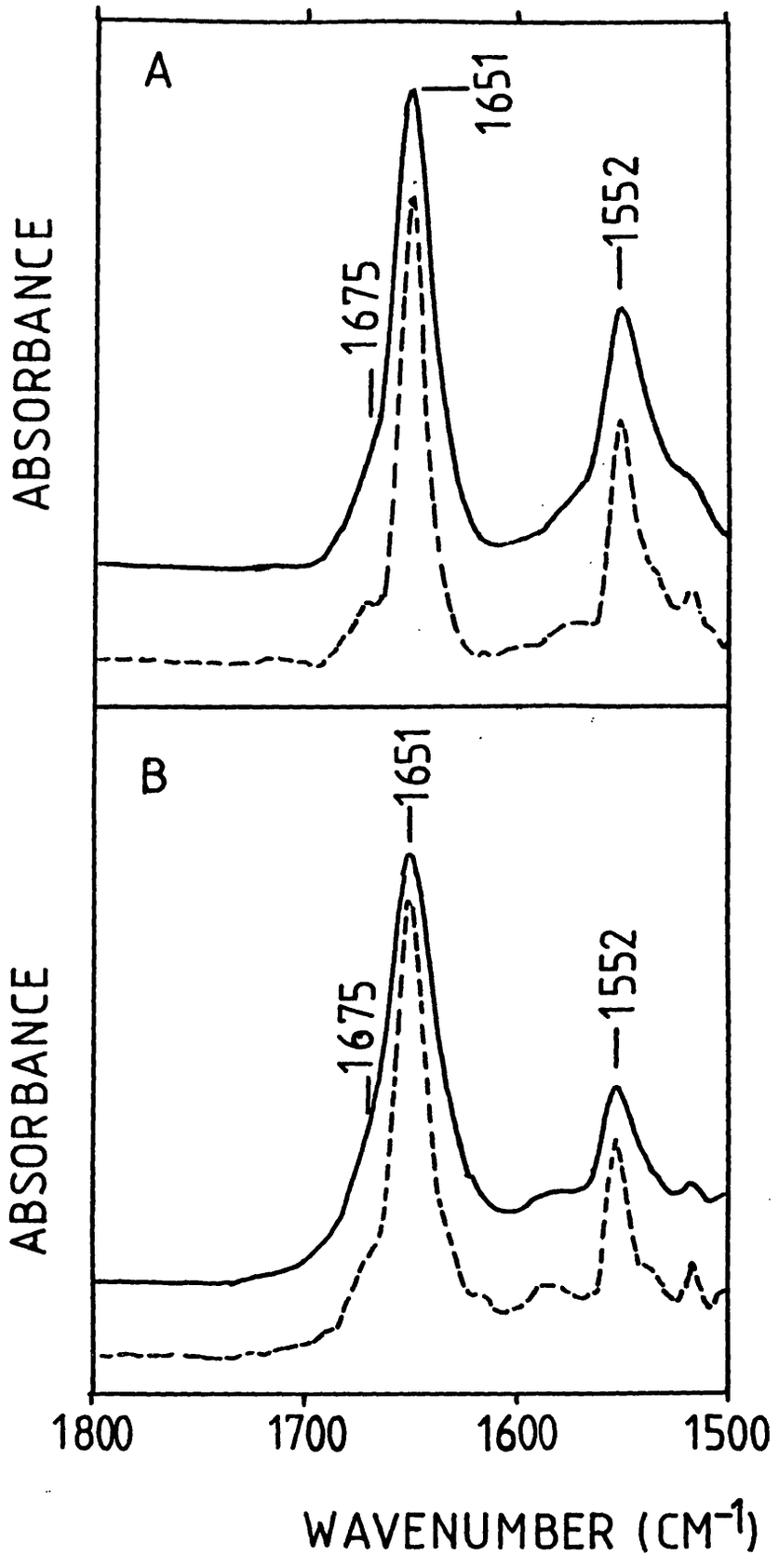
A
1651
1675
1552
ABSORBANCE
B
1651
1675
1552
ABSORBANCE
1800
1700
1600
1500
WAVENUMBER (CM-1)

Figure 4.8.

Transmission FT-IR spectra (solid trace) of the fd coat protein in SDS detergent micelles in (A) H_2O and (B) ^2H_2O solution.

Deconvolved spectra (K=2, HWHH=12 cm^{-1}) indicated in dashed trace.

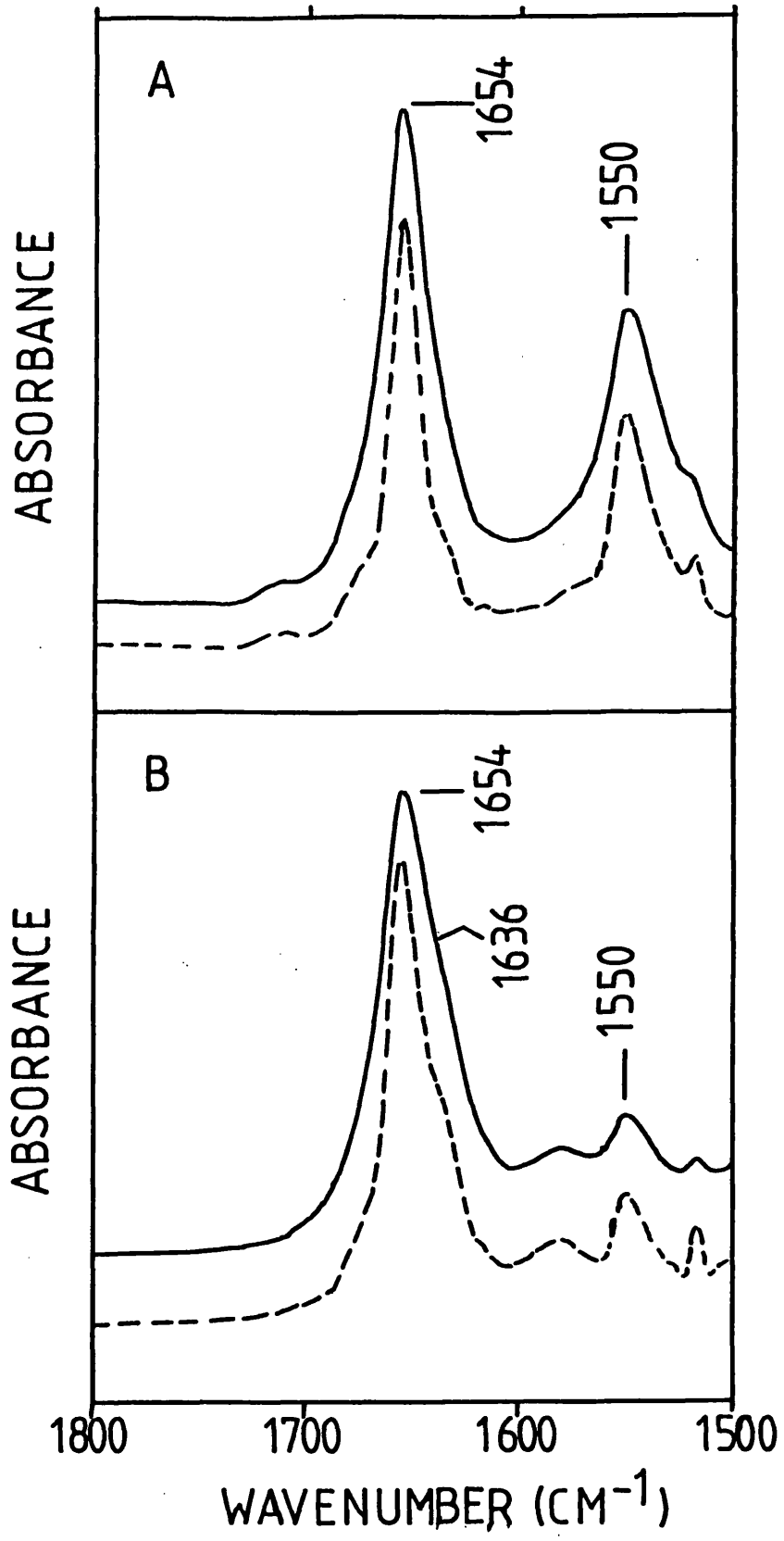
A
1654
1550
ABSORBANCE
B
1654
1636
1550
ABSORBANCE
1800
1700
1600
1500
WAVENUMBER (CM-1)

The amide I band of the fd coat protein in SDS micelles in H_2O and ^2H_2O (figure 4.8) appears at 1654 cm^{-1} with a bandshape similar to that observed in the amide I band in the fd phage. The presence of weak band above frequencies of 1670 cm^{-1} and another band at 1630 cm^{-1}, indicates the presence of non-helical structures. These may arise from ß-turn structures (Krimm & Bandekar, 1987). The higher frequency of the amide I band may originate from a weaker hydrogen-bonding of the α-helical structure of the coat protein in the micelle. Quantitative analysis shows that the percentage of α-helix in the detergent micelle is similar to that observed in the phage.

In ^2H_2O a weak component centred at 1636 cm^{-1} indicates the existence of bands shifted upon ^2H exchange as compared to the spectrum in H_2O (figure 4.7A). These bands are assigned to random structures (Jackson et al., 1989a). The low frequency of the band at 1636 cm^{-1} is probably due to the overlap with the band at 1630 cm^{-1} observed in H_2O. The amide II band shows a reduction of intensity upon $H/^2H$ exchange as compared with the amide II band in H_2O. Analysis of the ratio of the amide II/amide I band intensities suggests that 60% of the amide protons in the coat protein exchange rapidly, the remaining undergoes slow $H/^2H$ exchange until completion.

Figure 4.9.

Transmission FT-IR spectrum (solid trace) of the fd coat protein in DMPC vesicles in $^{2}H_{2}O$.

Deconvolved spectrum (K=2, HWHH=12 cm^{-1}) shown in dashed trace.

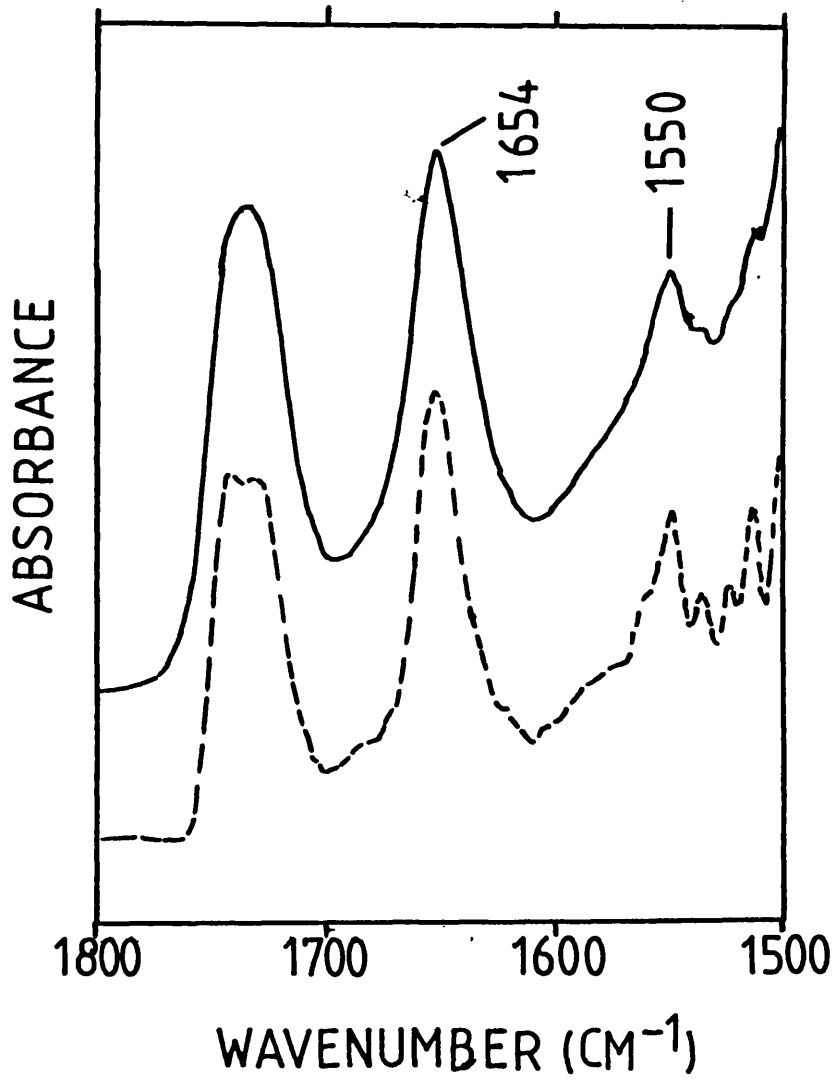
1654
1550
ABSORBANCE
1800
1700
1600
1500
WAVENUMBER (CM^{-1})

The spectrum of the fd coat protein in lipid vesicles in ^2H_2O is shown in figure 4.8B. The coat protein was reconstituted only by the deoxycholate-detergent dialysis method, as the sonication procedure resulted in the appearance of bands between 1640-1615 cm^{-1} in the infrared spectra, which were possibly resulting from protein aggregation. The band corresponding to the carbonyl group of the lipid ester appears at 1734 cm^{-1}. The amide I band maximum of the coat protein appears at 1654 cm^{-1}, which is similar to the frequency of the amide I band observed in the SDS micelle. The amide II band shows a reduction in intensity upon $H/^2H$ exchange, indicative that some of the amide protons of the fd proteins in the membrane are accessible to the solvent for exchange to occur.

P89 "THEORY" (SOLID FILM?)

4.3.5. Internal reflectance infrared studies.

Figure 4.10 shows the infrared spectra of lipid films with reconstituted Pf1 coat protein recorded with polarized beams. The amide I and II bands are located at frequencies similar to those observed in aqueous suspensions (see figure 4.5A). The amide I band at 1657 cm^{-1} is more intense in the spectra recorded with the beam polarized perpendicular to the plane of the lipid film. The amide II band shows similar areas (ratio 1.2-1.3) in the perpendicularly and parallel polarized spectra. The ratios of the amide I band areas is

Figure 4.10.

ATR infrared spectra of Pf1 coat protein in lipid films, obtained with beams polarized perpendicular (solid trace) and parallel (dashed trace) to the plane of the film.

ABSORBANCE
0.1 A.U.
1734
1657
1545
1800
1750
1700
1650
1600
1550
1500
WAVENUMBER (CM-1)

Figure 4.11.

ATR infrared spectra of films of purple membrane, obtained with beams polarized perpendicular (solid trace) and parallel (dashed trace) to the plane of the film.

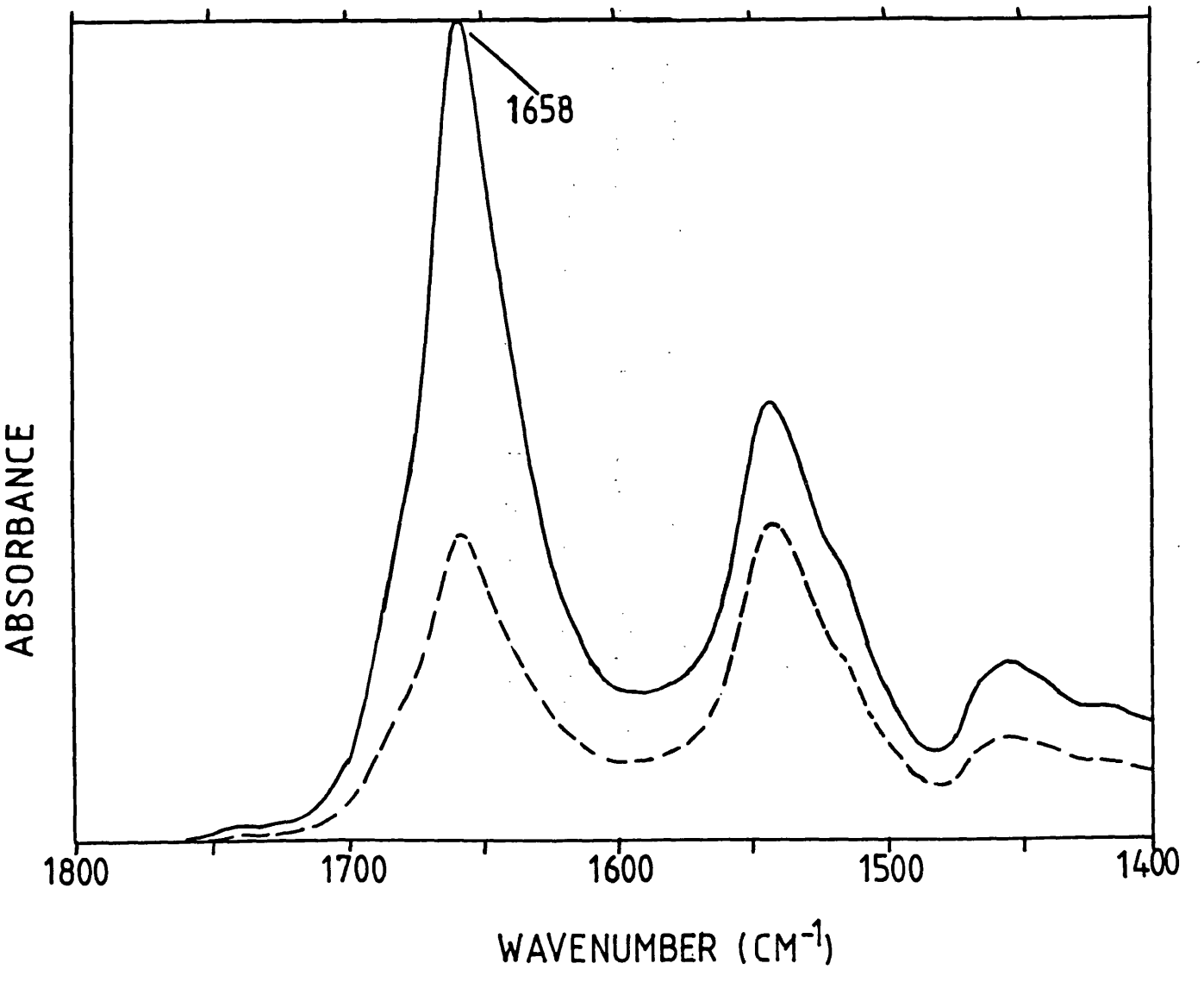
1658
ABSORBANCE
1800
1700
1600
1500
1400
WAVENUMBER (CM-1)

Figure 4.12.

ATR infrared spectra of fd coat protein in lipid films, obtained with beams polarized perpendicular (solid trace) and parallel (dashed trace) to the plane of the film.

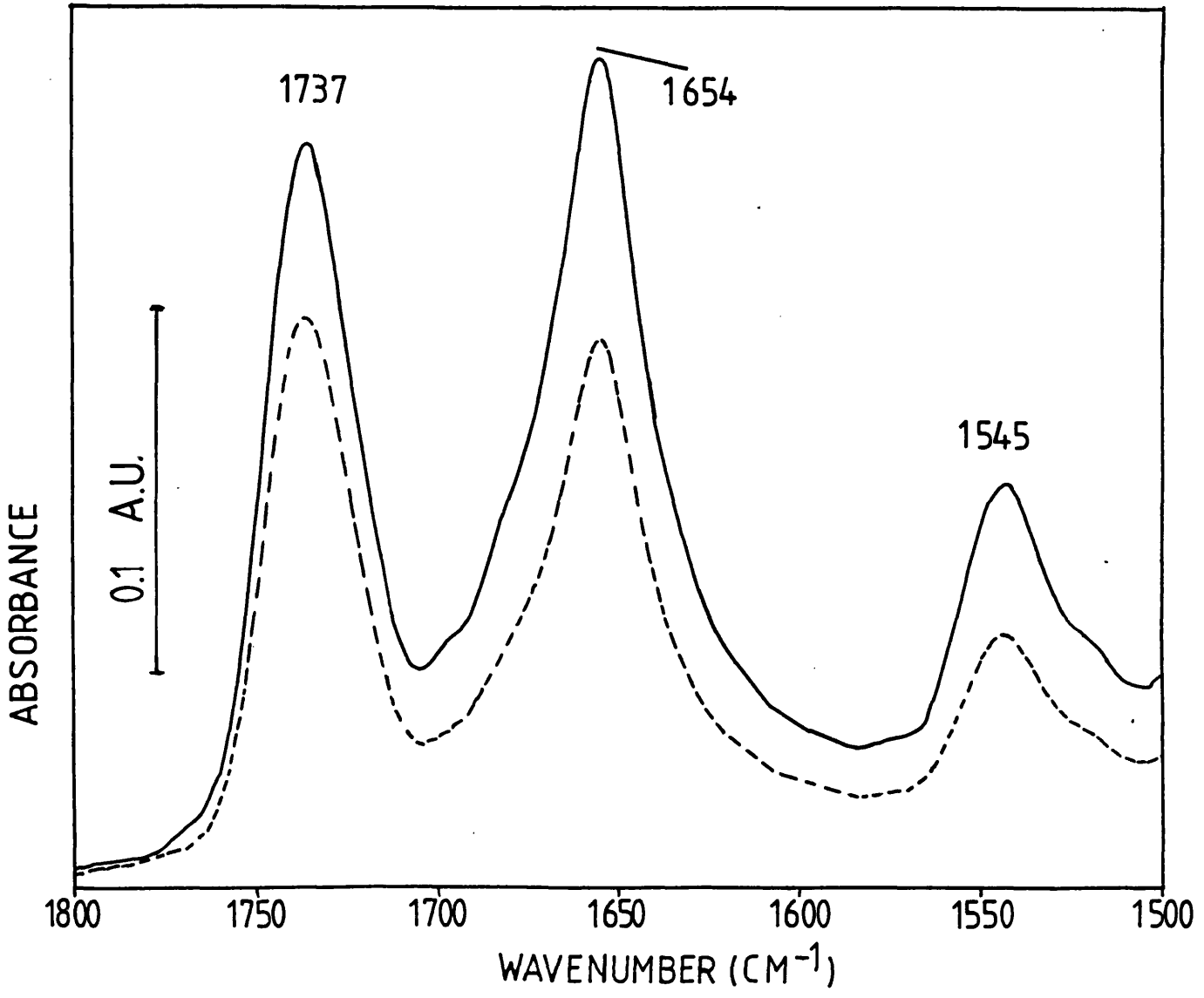
1737
1654
1545
0.1 A.U.
ABSORBANCE
1800
1750
1700
1650
1600
1550
1500
WAVENUMBER (CM^{-1})

Table 4.2

Estimated dichroic ratios for isotropically oriented molecular structures in lipid films cast on an ATR crystal.

DICHROIC RATIO	CONDITIONS	AUTHORS
1.2	----	Brauner et al.(1987) Weaver et al.(1991)
1	Thin film (d≤dp)	Mirabella (1985)
1-2	Thin film (d≤dp)	Buchet et al.(1991)
2	Thick film (d>>dp)	Mirabella (1985)
2	Thick film (d>>dp)	T.-M.-Saroga (1988)

In the ATR studies of fd or Pf1 protein/lipid samples (section 4.3.5), films of thicknesses 3-40 $\mu gr/cm^2$ were used. The corresponding dichroic ratios for the amide I band did not vary significantly with the thickness of the film.

2.3-2.5, which is similar to those reported in ATR studies of bacteriorhodopsin in films of purple membrane (Yang et al., 1987) and in our lab (figure 4.11).

The ATR-IR spectra of lipid films with reconstituted fd coat protein (figure 4.12) has been recorded with polarized beams, perpendicular and parallel to the plane of the lipid film. The ratios of the areas of the protein bands determined from the two spectra are 1.4-1.5 for the amide I at 1654 cm^{-1} and 1.5-1.6 for the amide II band at 1545 cm^{-1}, indicating that the average α-helical structure with respect to the plane of the lipid film is oriented randomly or distributed equally on the perpendicular and parallel directions with respect to the plane of the lipid film. Values of the DR for random orientation of alamethicin in a membrane with an aqueous environment were shown to be 1.55 for both amide I and II bands (Fringeli & Fringeli, 1979; Fringeli, 1977). Other DR values for isotropically oriented structures have been reported (see Table 4.2).

4.3.6. Internal reflectance infrared studies of ^{13}C-labelled Pf1 coat protein.

^{13}C-isotopic labelling of the aminoacid Ser was used to separate the components of the amide I band corresponding to aminoacids present in the amino-terminal region from the rest of the amide I band of the Pf1 coat protein (see methods). For the ^{13}C-serine labelled Pf1 protein the amide

Figure 4.13.

ATR infrared spectra of ^{13}C-serine labelled Pf1 protein in lipid films, obtained with beams polarized perpendicular (solid trace) and parallel (dashed trace) to the plane of the film.

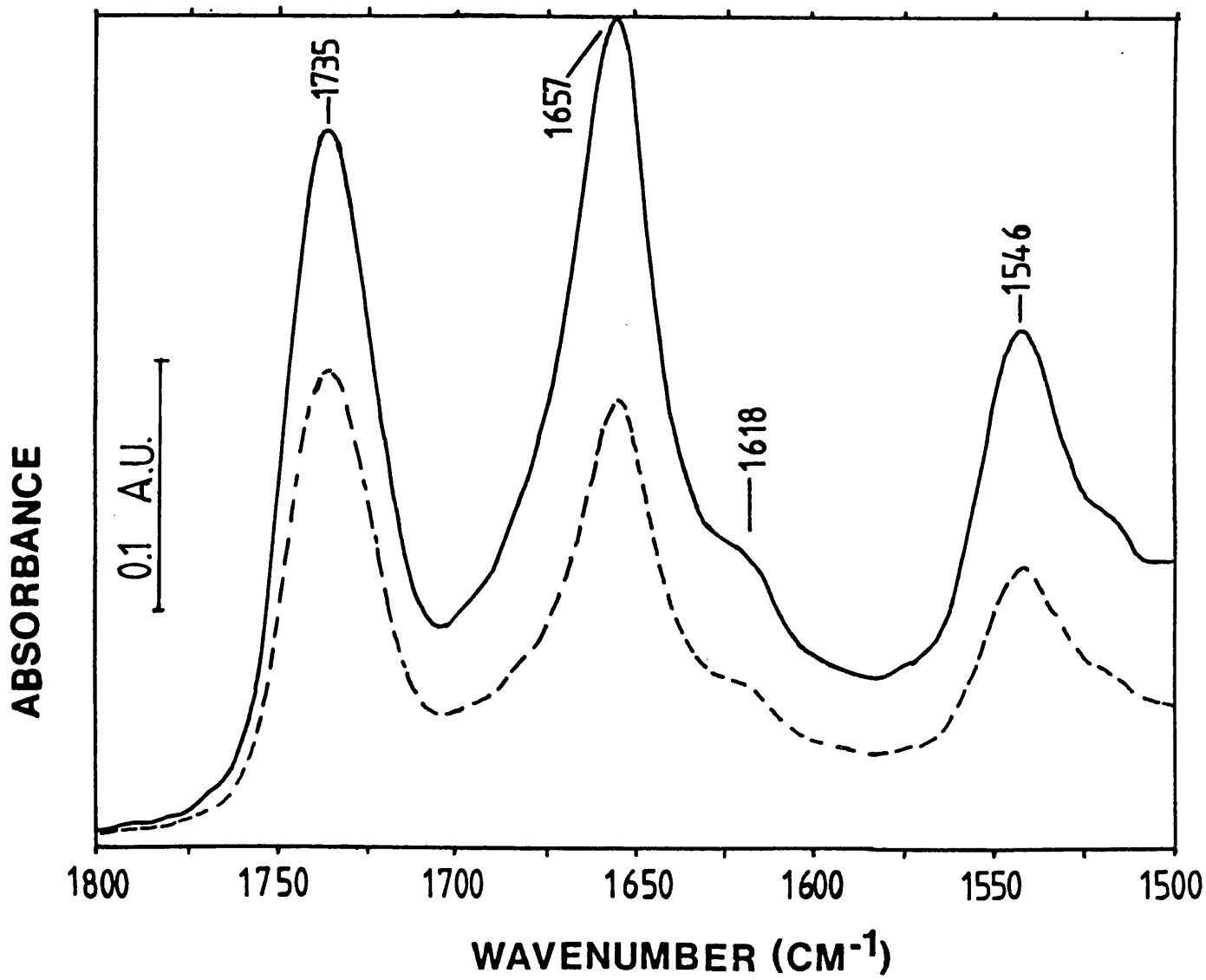
1735
1657
1618
1546
0.1 A.U.
ABSORBANCE
1800
1750
1700
1650
1600
1550
1500
WAVENUMBER (CM-1)

I band shows two components, a band at 1658 cm^{-1} corresponding to the original band (see figure 4.10) and a second one at 1618 cm^{-1} corresponding to the isotopically ^{13}C-shifted amide I. The frequency of this ^{13}C-band corresponds to the 40 cm^{-1}-shifted frequency of ^{12}C-amide of a α-helical structure at 1658 cm^{-1} (Blume et al., 1988; Haris et al., 1992), which is therefore attributed to α-helical structure.

Polarized ATR measurements of oriented lipid films with the ^{13}C-Ser Pf1 protein are shown in figure 4.13. The amide I band at 1657 cm^{-1} shows an enhancement of intensity with the perpendicularly polarized beam, similar to that observed with the unlabelled protein (see figure 4.10). The band at 1618 cm^{-1} shows a comparable increase in intensity when studied with a beam polarized perpendicular to the plane of the lipid film. This increase in intensity was checked by curve-fitting analysis of the spectra between 1700 and 1500 cm^{-1}. This indicates that the α-helical residues of the serine groups have a net orientation perpendicular to the plane of the lipid film.

DR? 2.5?

4.3.7. Fluorescence depolarization. (Theory p 48)

Figure 4.14 shows the values of polarization *P* using the fluorescent probe DPH obtained with DMPC suspensions containing increasing concentrations of the Pf1 coat protein.

Figure 4.14.

Plot of *P* values of the probe DPH in Pf1 protein/DMPC aqueous suspensions.

Best-fit (dashed trace) obtained with an exponential curve of the form $P = 1 - e^{-MX}$ for $M = 5$ (see methods).

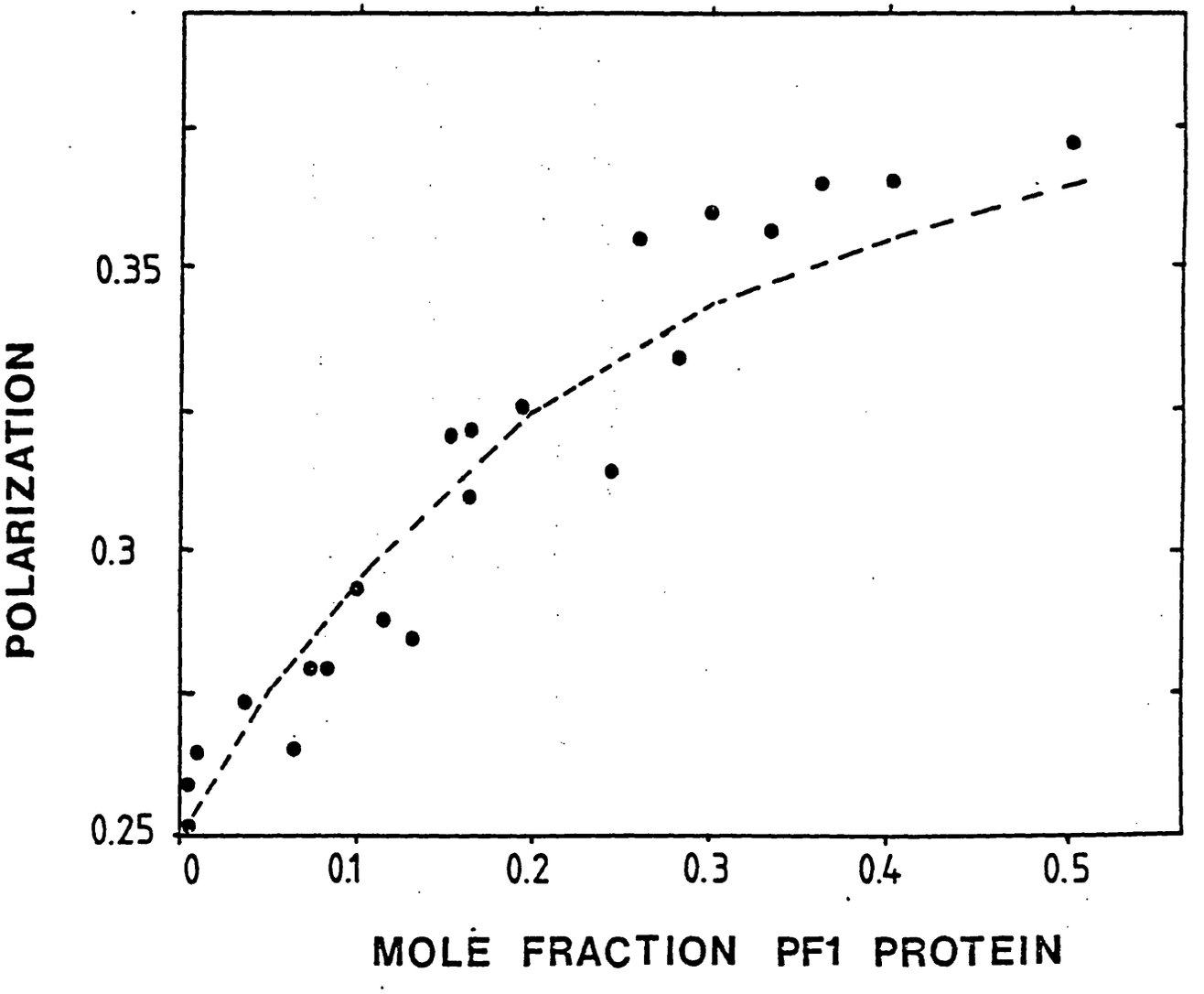
POLARIZATION
0.35
0.3
0.25
0
0.1
0.2
0.3
0.4
0.5
MOLE FRACTION PF1 PROTEIN

Figure 4.15.

Calorimetric heating curves of aqueous suspensions of pure DMPC (top) and lipid/protein Pf1 (from top to bottom).

The measured lipid sample was approximately 2 μmoles. The scale for the curve obtained with pure DMPC aqueous suspension has been halved.

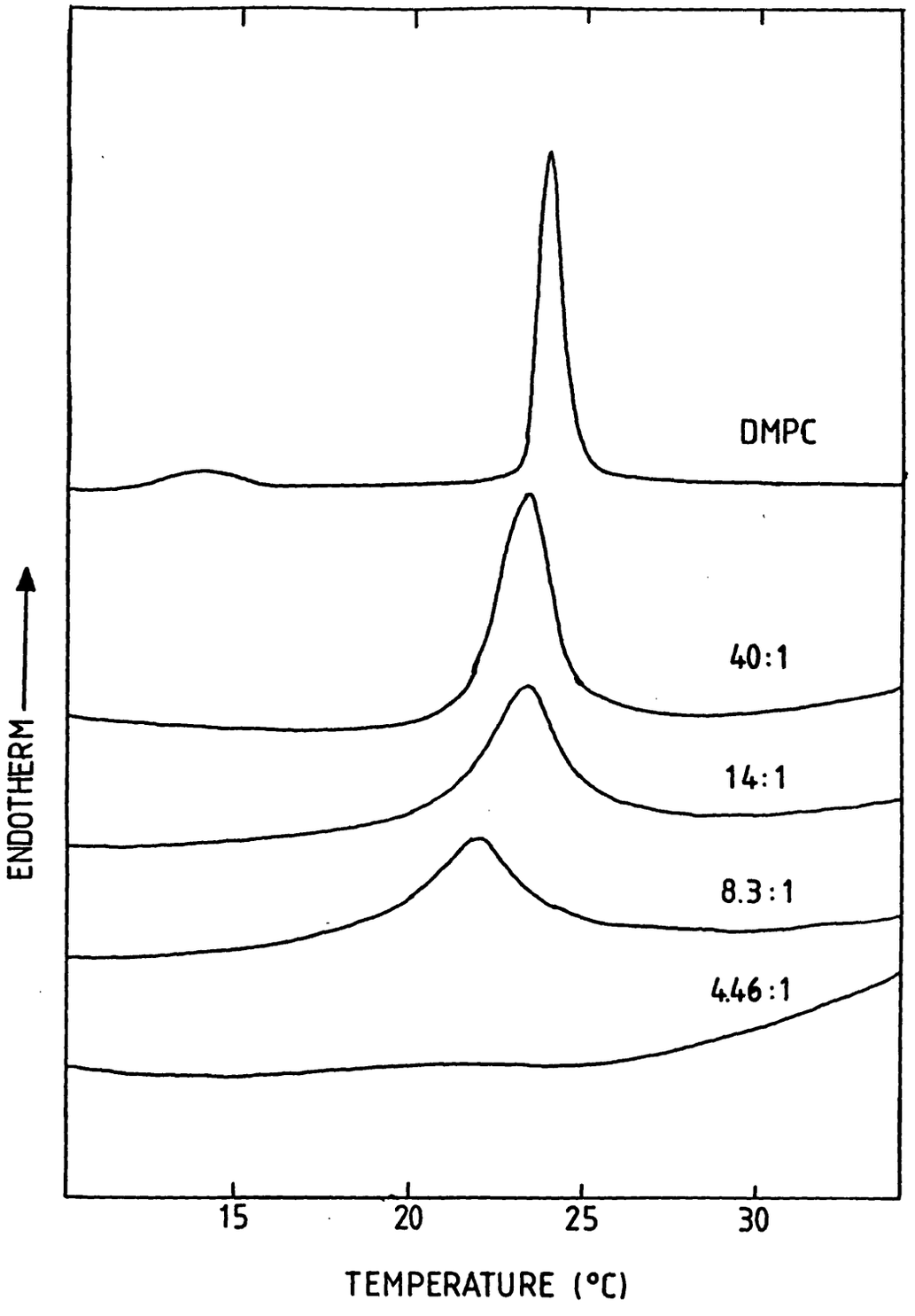
DMPC
40:1
14:1
8.3:1
4.46:1
ENDOTHERM
15
20
25
30
TEMPERATURE (°C)

Figure 4.16.

Plot of the molar enthalpies of the phase transition of the lipid in Pf1 coat protein/DMPC aqueous suspensions.

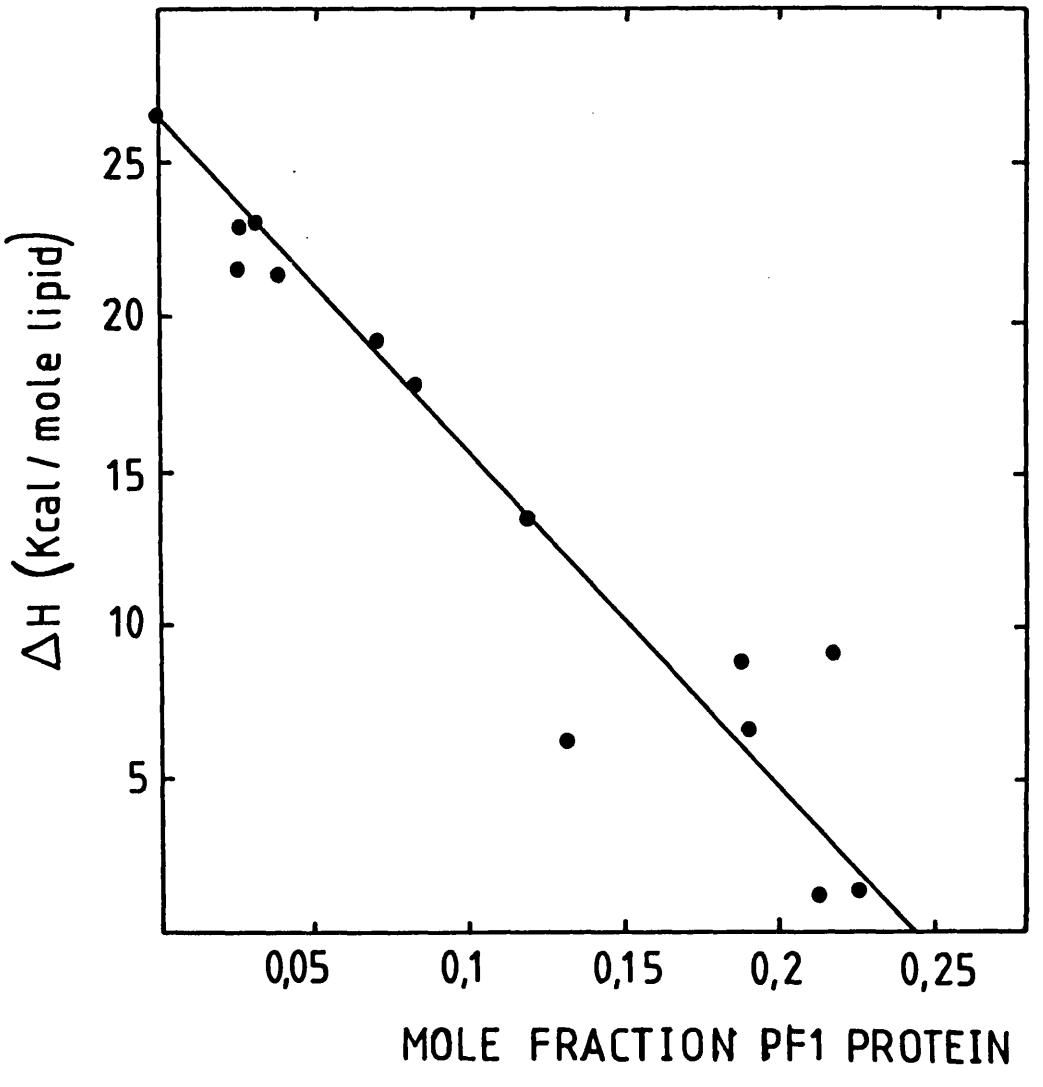
ΔH (Kcal / mole lipid)
25
20
15
10
5
0,05
0,1
0,15
0,2
0,25
MOLE FRACTION PF1 PROTEIN

At low protein/lipid concentrations, the introduction of the coat protein in the lipid bilayer causes a linear increment in the polarization of the DPH probe, indicating that the presence of the protein restricts the motion of the probe. At high protein:lipid ratios the polarization values reach a limit in a similar manner to the polarization curves obtained with other aqueous lipid systems containing cytochrome oxidase, gramicidin A and cholesterol (Hoffman et al., 1981). Hoffman et al. (1981) showed that these curves can be fitted to exponential curves of the form $P= 1-e^{-MX}$, where M corresponds to the number of DPH chains that can contact the protein in the lipid bilayer. A curve constructed for $M=5$ is shown in figure 4.14, which gives a best fit ($r^2=0.9$) for the experimental values. Curves obtained with $M=4$ *or* 6 gave a correlation coefficient of $r^2=0.85$.

4.3.8. Calorimetric studies of the Pf1 coat protein reconstituted into phospholipid aqueous systems.

The effect of the presence of the Pf1 protein on the lipid chain organisation was also investigated by DSC (figure 4.15). The phase transition of the pure DMPC suspension exhibits a narrow peak, indicative of a highly cooperative phase transition. The incorporation of the coat protein causes a a marked reduction of the enthalpy of the phase transition of the lipid, indicative of the insertion of the protein within the lipid bilayer. This reduction in enthalpy

was linearly dependent on the protein/lipid ratio of the DMPC suspension (figure 4.16). The value of the protein/lipid ratio at which the phase transition enthalpy reaches zero was extrapolated to a value of 0.24, corresponding to a lipid:protein molar ratio of approximately 4.1:1 (figure 4.16). This is the amount of lipid molecules withdrawn from the cooperative transition per molecule of Pf1 coat protein present in the lipid membrane suspension.

4.4. DISCUSSION.

4.4.1. The coat protein in the phage.

These FT-IR spectroscopic studies (figure 4.1 and 4.7) show that the Pf1 and the fd phage contain 90-100% α-helical structure and provide evidence of the existence of some non-helical structures.

The transmission polarization studies of oriented films of the Pf1 phage (figure 4.2) and the fd phage (spectrum not shown) indicate that the α-helical segments are oriented in the direction of the phage filament. The band at 1675 cm^{-1} has been assigned to ß-turn structures (Krimm & Bandekar, 1986; Jackson et al., 1989a). The transmission polarization studies of the Pf1 phage films show that this band at 1675 cm^{-1} has a net orientation parallel to the direction of the axis of the phage. It is plausible that the infrared band at 1675 cm^{-1} originates from a loop-connector structure

(Asp14-Asp18) present in the coat protein subunits in the Pf1 phage as proposed by Nambudripap et al. (1990). In most known secondary structures, e.g. α-helix, 3_{10}-helix, ß-sheet in proteins and peptides (Krimm & Bandekar, 1986), the direction of the vibrational transition moments of the peptidic groups coincide with the axis of the α-helix and 3_{10}-helix and is perpendicular to that exhibited by the ß-sheet. However in a ß-turn this is different since most are comprised of paired amide bonds (ß-sheet like) and non-bonded amide groups which vary in their dihedral angles, giving randomised orientations (Bandekar & Krimm, 1979). Therefore no defined orientation for a ß-turn can be deduced from our polarization studies of the oriented films of the Pf1 phage.

In agreement with Raman spectroscopy (Day et al., 1988) the parallel orientation of the tyrosine band at 1515 cm^{-1} provides evidence that the benzene ring planes are aligned with the filamentous axis. Tyrosine residues are found in positions 25 and 40 in the aminoacid sequence of the coat protein. The alignment of the tyrosine sidechains may arise from a restricted motion due to the stacking with the DNA bases or from space constraints in the interior of the filamentous phage (Nakashima et al., 1975; Day et al., 1979).

4.4.2. The coat proteins in detergent micelles and lipid membranes.

FT-IR spectroscopy techniques enable a direct comparison to be made of the three structural forms of the Pf1 and fd coat proteins: in detergent micelles, artificial membranes and filamentous phage. Previous studies using CD spectroscopy have indicated that the Pf1 and fd coat proteins in detergent micelles and in lipid membranes are predominantly α-helical with perhaps some reduction in the content of α-helical structure as compared with that present in the phage (Schiksnis et al., 1987; Chamberlain et al., 1978). The amide I band maximum in the detergent micelles and in the lipid membrane reveals a frequency of 1656-58 cm^{-1} for the Pf1 protein and 1654 cm^{-1} for the fd protein. This is indicative of the presence of a weaker hydrogen-bonding in the α-helical structures of the protein in detergent micelles and membrane systems. A similar difference in frequencies is observed with soluble proteins when compared to membrane proteins. The amide I band frequency of the former proteins at 1654-1651 cm^{-1} is usually lower than that observed with membrane proteins at 1658-1656 cm^{-1} (Haris & Chapman, 1992).

The frequency of the amide I band maximum at 1654 cm^{-1} of the fd protein in the SDS micelle is indicative of a stronger hydrogen-bonding in the α-helical structure of the fd protein as compared to the Pf1 protein. Unlike the Pf1

protein, the fd and the M13 coat proteins form non-dissociable dimers in detergent micelles (Makino et al., 1975; Henry & Sykes, 1992). The α-helical segments of the M13 protein in the micelle were suggested to adopt a parallel orientation (Henry & Sykes, 1992) with respect to each other. The lower frequency of the amide I maximum of the fd protein in the micelle may be attributed to the interaction between the individual monomers in the dimer-SDS complex. In the lipid membrane, the bandshape and frequency of the fd coat protein are similar to those observed in the detergent micelle, suggesting that the fd protein in the micelle and the lipid bilayer forms a similar α-helical structure, possibly as a dimer.

Recent NMR spectroscopic studies of the Pf1 protein in DPC detergent micelles indicate the existence of a monomer in the micelle, formed by two stable α-helical segments (Shon et al., 1991) in the micelle. These studies maintain that the tertiary structure of the protein in the micelle is conserved in the lipid membrane. The similarity of the FT-IR spectra and the secondary structure of the coat protein in DPC detergent micelles and in phospholipid membrane systems in H_2O lends support to the suggestion of Shon et al. (1991).

The rate of amide H/^{2}H exchange of the Pf1 and fd coat protein in SDS micelles agrees with previous findings made by H-NMR spectroscopy (Schiksnis et al., 1987; Henry & Sykes, 1992). The percentage of non-exchangeable amide protons of about 30-40 %, determined by the change in the amide I/II ratio, corresponds well with the percentage deduced from the H-NMR studies. These slow-exchanging amide protons encompass the segments between aminoacid residues Leu30-Tyr40 of the Pf1 protein which adopt α-helical structure in SDS micelles (Schiksnis et al., 1987). The rapid rate of H/^{2}H exchange of the Pf1 protein in the DPC micelle can be caused by an open structure or a rapid dynamics of the DPC molecules in the micelle as a result of exchange with the DPC monomers in the solution.

NMR spectroscopic studies of the H/^{2}H exchange of the M13 coat protein in SDS micelles show similar results (Henry & Sykes, 1992). In the M13 protein the slow-exchanging amide protons correspond to an α-helical segment between the residues Met28-Phe42.

The rapid H/^{2}H exchange of some of the amide protons of both fd and Pf1 protein in the phospholipid membrane indicates that part of the protein is accessible to the solvent. The remaining amide protons undergo slow-exchange, indicating the existence of structures not accessible to the solvent for exchange to occur. The rate of H/^{2}H exchange of

the fd and Pf1 protein in the phospholipid membrane is therefore similar to the H/^{2}H exchange observed in SDS micelles. The H/^{2}H slow-exchanging structures of the protein in the membrane may correspond to the hydrophobic α-helical structures of the proteins deeply buried within the lipid membrane. The exchange properties of bacteriorhodopsin studied by FT-IR spectroscopy show a similar slow exchange of the hydrophobic α-helices embedded within the lipid bilayer (Lee et al.,(1987) Earnest et al., 1990).

4.4.3. The tertiary structure of the fd protein in the lipid bilayer.

The fd protein in the lipid bilayer contains 90-100% percentage of α-helical structure. The polarized ATR-IR studies suggest that the α-helical structures of the fd coat protein in the lipid bilayer adopt a structure randomly oriented with respect to the plane of the membrane. This may also indicate that part of the α-helical structure of the coat protein is parallel and the other is perpendicular with respect to the plane of the lipid bilayer. Owing to the existence of the 20-25 residue hydrophobic region, it is reasonable to assume that the fd coat protein must span the lipid bilayer once. To satisfy an orientation with the α-helical structures averaged in the parallel and perpendicular directions, the rest of the coat protein would possibly

have to adopt an α-helical structure parallel to the plane of the lipid bilayer.

Solid-state ^{2}H-NMR studies of the motion of residues of the protein in the lipid membrane indicate that of the 48 residues of the fd protein, the region between aminoacids Ala6-Phe41 is rigid, whilst both N-termini (residues 1-5) and C-termini (residues 41-48) are mobile (Leo et al., 1987). This suggests that the structures corresponding to the N-termini (residues 1-5) and the C-termini (residues 41-48) may adopt an orientation other than parallel with respect to the plane of the lipid bilayer. The ATR-IR results could be explained by the fact that when the lipid film is in a dried state the mobile segments of the protein, detected in solution by NMR, are laying parallel to the plane of the lipid bilayer. The relative differences in rigidity in the N-termini suggested by solid-state ^{2}H-NMR (Leo et al., 1987) could also be interpreted as due to another type of interaction such as dimerization or aggregation under the conditions of high concentration necessary for the measurements by solid-state NMR spectroscopy.

4.4.4. The tertiary structure of the Pf1 coat protein in the lipid bilayer.

The secondary structure of the Pf1 protein in the SDS and DPC micelles has been shown to be remarkably similar to that in the DMPC aqueous suspensions. Based on solid-state

^{15}N-NMR studies of the coat protein in DMPC aqueous suspensions, Shon et al. (1991) proposed that an α-helical domain occurs with its axis perpendicular to the plane of the membrane and that another domain, corresponding to the amino-terminus (residues 1-14) lies parallel to the surface of the lipid bilayer. They propose that the latter α-helical domain is amphipathic with its hydrophobic face immersed between the lipid molecules and its hydrophilic face exposed to the water.

The fluorescence polarization studies indicate that the number of DPH probe molecules *M* that may contact simultaneously the Pf1 coat protein in the membrane is approximately *4-6*. Recent electron-spin resonance spectroscopic studies of reconstituted rhodopsin in fluid lipid systems, where the protein exists in a monomeric form, indicate that 22 lipid molecules can surround the perimeter of a monomer of rhodopsin (Ryba & Marsh, 1992). A monomer of rhodopsin is predicted to have seven transmembrane α-helices. Extrapolation of the number of lipids surrounding the perimeter of a monomer of rhodopsin of 3 nm diameter to that of a single transmembrane α-helix of 1 nm diameter gives an approximate value of *6-7* lipids for the perimeter of an α-helix. Hence the number of DPH molecules or lipids being perturbed is consistent with the presence of only one single α-helix in the lipid membrane.

The calorimetric studies also suggest strongly that the Pf1 coat protein is present in the membrane as a single α-helical membrane-spanning domain. This suggests that the amino-terminal region of the Pf1 protein may not interact with the lipid molecules in the fashion proposed by Shon et al. (1991).

The high dichroic ratio which is observed with the Pf1 coat protein in the lipid film indicates that the protein has an α-helical structure which is predominantly perpendicular to the plane of the lipid bilayer.

Isotopic-^{13}C-labelling of the aminoacids serines at the amino-terminal region of the Pf1 coat protein shows that these serines form part of an α-helical stretch of the Pf1 coat protein. The polarization studies of the ^{13}C-serines band at 1618 cm^{-1} indicate that the amide groups of these aminoacids, and possibly the encompassing amino terminus, have an orientation predominantly perpendicular to the plane of the membrane. The presence of another ^{13}C-labelled serine at a position near the carboxy-terminus of the protein (Table 4.1) however complicates the analysis of spectra of the ^{13}C-amide bands of these serine residues. Nonetheless, the interpretation is still applicable to the extent that a dichroic ratio of 2.5 would be very unlikely to originate from components which are parallel or randomly oriented to

the plane of the lipid bilayer.

The studies of the tertiary structure of the Pf1 and fd proteins in the lipid bilayer indicate that their conformations are different. Unlike for the Pf1 protein, these studies suggest that the structure of the fd protein in the lipid bilayer is similar to the model of Shon and coworkers (1991) for a coat protein monomer in the membrane.

4.5. SUMMARY.

FT-IR spectroscopy shows that suspensions of the Pf1 and fd filamentous phages give rise to amide I bands indicative of a high content of the α-helical structure. Oriented films of the Pf1 phage studied by polarized FT-IR transmission spectroscopy show that the α-helical structures as well as the tyrosine residues (band at 1515 cm^{-1}) are both aligned along the axis of the phage.

When present in SDS detergent micelles or in lipid aqueous systems, the FT-IR spectra of the Pf1 and fd proteins show amide I bands at 1657-8 cm^{-1} and 1654 cm^{-1} respectively, also indicative of a predominantly α-helical structure. $H/^{2}H$ amide proton exchange studies of the coat proteins in micelles or membranes are consistent with a proportion of the protein being exposed to the solvent and the remainder being embedded in the lipid bilayer. The presence of a band at 1630-40 cm^{-1} is indicative of the presence of random structures.

Polarized FTIR-ATR spectra of the Pf1 coat protein in lipid films indicate that the average α-helical structures of the protein are oriented perpendicular to the plane of the lipid membrane. In contrast, the arrangement of the α-helical structures of the fd coat protein in the lipid bilayer seems to be balanced with segments oriented perpen-

dicular and parallel with respect to the plane of the lipid bilayer.

The fluorescence polarization results and DSC studies of the gel-liquid phase transition of the lipid in Pf1 protein/lipid systems are consistent with a perturbation expected from a single helix spanning the lipid bilayer once. FTIR-ATR studies of the ^{13}C-amide labelled serines of the Pf1 coat protein suggests that the amino-terminal region adopts an orientation perpendicular with respect to the plane of the lipid bilayer.

CHAPTER 5

FOURIER-TRANSFORM INFRARED SPECTROSCOPIC ANALYSIS OF HUMAN C-REACTIVE PROTEIN AND RELATED PROTEINS.

5.1. INTRODUCTION.

Human C-reactive protein (CRP) is an acute-phase blood protein synthesised in liver, in response to bacterial infection, tissue necrosis and various pathological conditions (Koj, 1974). CRP binds and precipitates cell wall C-polysacharide of bacteria of the Pneumococci family (Tillett & Francis, 1930).

One of the binding sites in the bacterial polysacharide was identified as the phosphoryl-choline (PC) group (Volanakis & Kaplan, 1971). PC is widely found in bacterial wall carbohydrates and also in cell phospholipids and sphingolipids. It has been shown that CRP can directly bind to natural membranes, after treatment with phospholipase A_2 or after the addition of lysolecithin (Narkates & Volanakis, 1982). This binding occurs by interaction of the binding PC site of CRP with the PC group of the lysolecithin. Binding of CRP to lipid membranes also occurs when galacto-cerebrosides and stearylamine are included in the lipid composition (Richards et al., 1977). Unlike the PC-binding site, the binding of CRP to the latter membranes does not require the presence of Ca^{2+} in solution (Mold et al., 1981). This interaction is thought to occur through the putative binding site for galactose and polycations (histones and polylysine) present in CRP.

Progress in the study of the function of human CRP and homologous proteins has been hindered by the lack of a atomic model based on X-ray diffraction data (DeLucas et al., 1987). According to CD spectroscopy, CRP contains 34% α-helix and 45% ß-sheet (Young & Williams, 1978). EM studies indicate that human CRP protein appears as cyclic pentamers (Osmond et al., 1977), comprised of identical subunits of Mw 21 KDa (Oliveira et al., 1979). The pentamers can be dissociated into its monomers only under denaturing conditions with 5M guanidinium chloride. These cyclic pentamers have a tendency to form decamers and oligomeres of higher order.

Human CRP shows strong homology to human serum amyloid precursor component (SAP), and only distant homologies to one domain (CH_2) of IgG (Liu, T.-Y. et al. 1982). CRP contains two Ca^{2+} binding sites per subunit which are present in the region between residues 133-147. This region is homologous to the sequence of the Ca^{2+}-binding sites of EFH hand proteins such as parvalbumin and troponin (Kinoshita et al., 1989). CD spectroscopic studies indicate that CRP undergoes a change of conformation upon Ca^{2+}-binding that allows the interaction with PC groups (Young & Williams, 1978). Ca^{2+}-binding increases the thermostability of the protein (Potempa et al., 1983). Immunomicroscopy studies have shown that the PC binding sites of the five subunits are located on one face of the pentamer (Roux et al., 1983).

The aim of this chapter is to study human CRP using FT-IR spectroscopy in order to obtain information on the secondary structures present. The influence of the ligands such as Ca^{2+}, PC and the C-polysacharide, upon the stability and the conformation of CRP is studied by following the reduction of intensity of the amide II band that occurs upon $H/^{2}H$ exchange.

5.2. MATERIAL AND METHODS.

Reagents were obtained from Sigma UK, chromatography products were supplied by Pharmacia UK and human ascites fluids was kindly provided by Dr. S. Gillespie (London). Limulus CRP was obtained from SIGMA U.K..

5.2.1. Purification of human CRP.

Human CRP was purified from human ascites fluids, as described by Oliveira et al. (1980) using affinity chromatography on phosphorylcholine-Sepharose 4B (synthesised as described by Oliveira et al., 1980), ion-exchange chromatography on cellulose DE-52 and gel-exclusion chromatography on Sepharose CL-6B. The presence of human CRP in eluates was checked by immuno-competitive ELISA against CRP-conjugated to peroxidase and its purity was assessed using SDS-PAGE electrophoresis (figure 5.1) (Hames and Rickwood, 1981). In non-reduced conditions, CRP appeared as a single

Figure 5.1.

SDS-PAGE gel (12% acrylamide concentration) of human CRP in non-reduced conditions (2) and reduced conditions (3). (1) Mw markers SBA 66 KDa and CRP 22 Kda. (4). Purified human CRP.

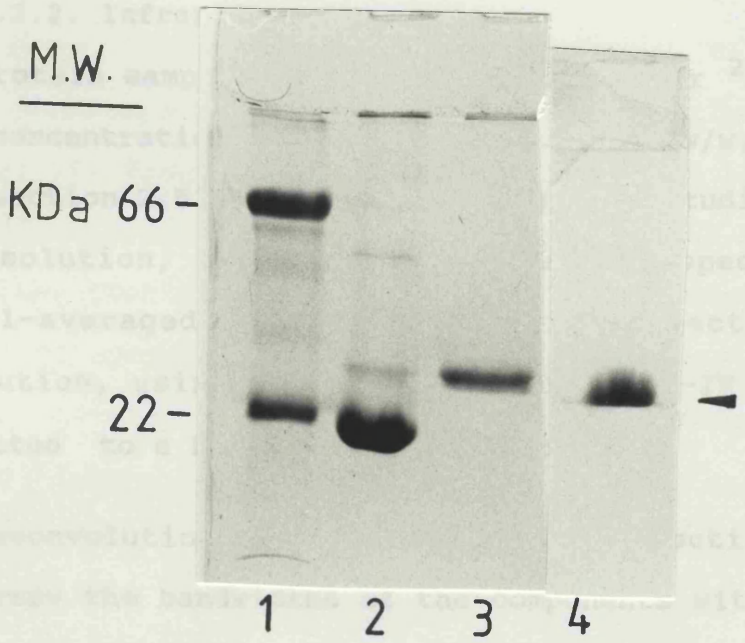
M.W.
KDa 66-
22-
1
2
3
4

band at 21 KDa and at 24 KDa in reduced conditions (Oliveira et al., 1979). Pools of CRP were dialysed against Tris saline buffer containing 5mM EDTA or were desalted on a Sephadex G-25 (2.5 x 25) column and subsequently freeze-dried.

5.2.2. Infrared spectroscopy.

Protein samples were hydrated in H_2O or ^2H_2O buffer to give concentrations of 2.5-3% and 1.5-2.5% w/w, respectively (see section 2.5.1 for more details). For studies in H_2O and ^2H_2O solution, 400 and 100-50 scans, respectively, were signal-averaged and transformed into spectra at 4 cm^{-1} resolution, using a Perkin-Elmer 1750 FT-IR Spectrometer connected to a Perkin-Elmer Data Station.

Deconvolution and second derivative routines were used to narrow the bandwidths of the components within the amide I band of the difference spectra of proteins (see section 2.4.2 and 2.4.3). The percentages of the secondary structure were quantified by factor analysis of the spectra of the protein in H_2O solution (see section 2.2.4.2) (Lee et al., 1990). The second derivative spectrum of human SAP was kindly recorded by J. Hadden (unpublished results, (a)).

5.3. RESULTS.

5.3.1. Human CRP.

The amide I band maximum of CRP in H_2O appears at 1634 cm^{-1}, indicative of a ß-sheet rich protein (figure 5.2 solid trace). The deconvolved spectrum (figure 5.2 dashed line) shows the main band at 1634 cm^{-1}, attributed to elements of ß-sheet structure (Byler & Susi, 1986). The band at 1650 cm^{-1} is assigned to α-helical structures (Jackson et al., 1989a), its frequency is slightly lower than the bands of α-helical segments (1652-56 cm^{-1}) typical of water soluble proteins (Haris & Chapman, 1992). Above a frequency of 1660 cm^{-1}, the deconvolved spectra does not clearly resolve the individual components. The second derivative spectrum of CRP in H_2O (figure 5.3) reveals two components, one at 1692 cm^{-1} and the other at 1672 cm^{-1}. ß-turn I and II structures are known to give rise to bands in this region (Krimm & Bandekar, 1986) and may also originate from high-frequency components that arises from ß-sheet segments (Byler & Susi, 1986; Susi & Byler, 1987).

The amide II band maximum of CRP appears at 1537 cm^{-1} (figure 5.2), showing after deconvolution a single component at 1537 cm^{-1}. Assignments of secondary structure from the amide II band are unreliable, however an amide II band at 1535 cm^{-1} has been observed in the ß-sheet-rich copolymer of ß-polyalanine (Krimm & Bandekar, 1986).

Figure 5.2.

Absorption spectrum of Human CRP in H_2O (solid trace).

Deconvolved spectrum obtained with F=2 and W=14 (dashed line).

ABSORBANCE
0.02 A.U.
1686
1670
1650
1634
1537
1800
1750
1700
1650
1600
1550
1500
WAVENUMBER (CM-1)

Figure 5.3.

Second derivative spectrum of CRP in H_2O

ABSORBANCE / WAVENUMBER 2
WAVENUMBER (CM-1)
1800
1750
1700
1650
1600
1550
1500
1692
1672
1650
1634
1536
1520

Figure 5.4.

Fitting of absorption spectrum of Human CRP: original spectrum (solid line) and calculated by CIRCOM (dashed line)

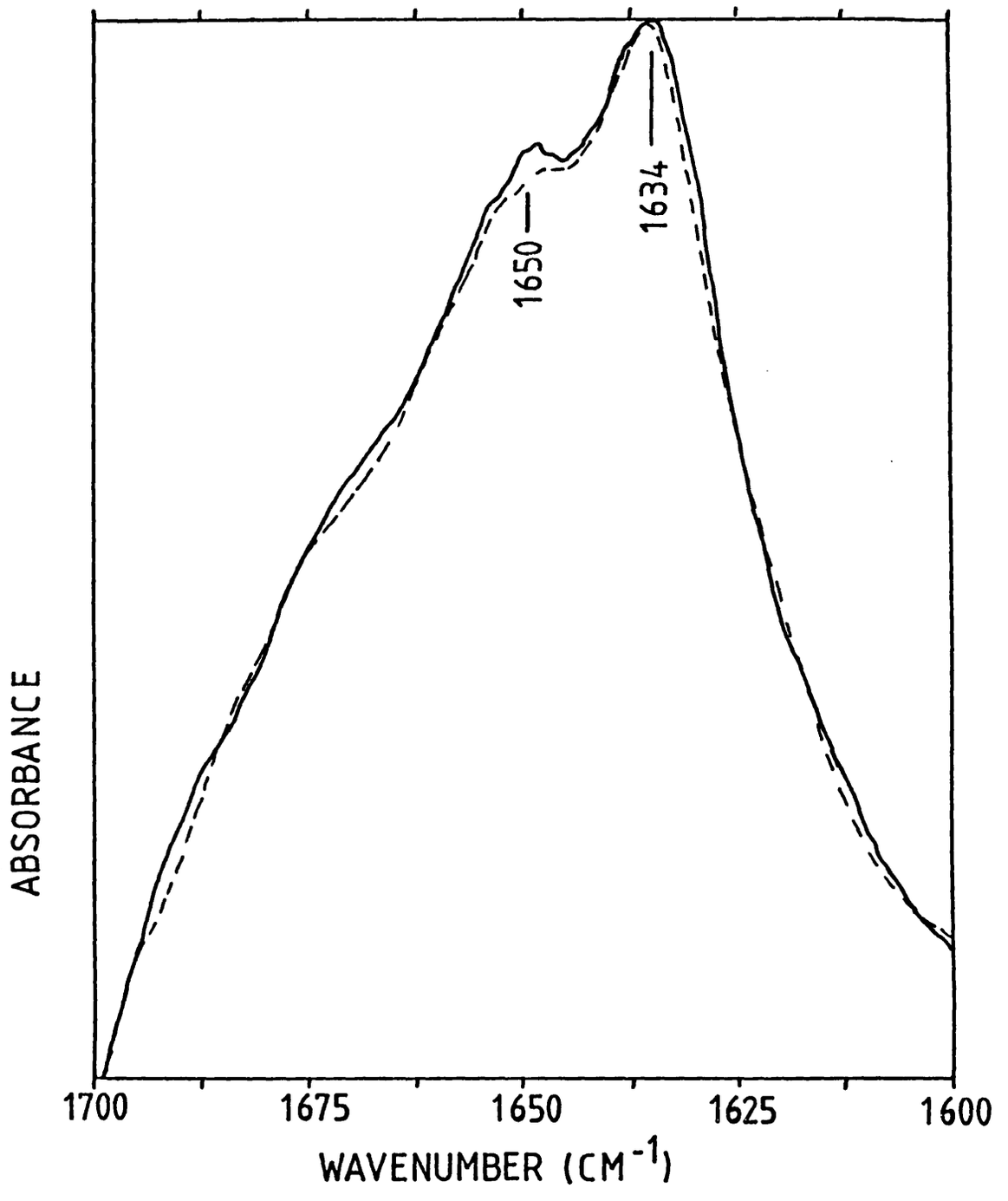
1650
1634
ABSORBANCE
1700
1675
1650
1625
1600
WAVENUMBER (CM-1)

The percentages of secondary structure were calculated using factor analysis of the amide I band of CRP in H_2O according to Lee et al., (1989). The values obtained are 51% ß-sheet, 39% turns, 10% α-helix and 10% unassigned structures. The region of the spectrum between 1700-1600 cm^{-1} corresponding to the amide I band of the spectrum of CRP in H_2O and the synthetic spectrum generated by factor analysis are shown in figure 5.4. Comparison of both spectra indicates that the band at 1650 cm^{-1} corresponding to α-helical structures has been underestimated to some extent and in the case of the region between 1660-1690 cm^{-1} the synthetic spectrum adjusts unsatisfactorily to the contour of the amide I band of CRP.

Figure 5.5A shows the absorption spectra of CRP in H_2O and in ^2H_2O solution recorded immediately after dissolution. The amide I band in ^2H_2O appears with a contour narrower than that shown in H_2O. Comparison of the rest of the amide I band in H_2O and ^2H_2O indicates a decrease in intensities of all components, except those at 1635-37 cm^{-1} as indicated in figure 5.5B. The amide II band of CRP at 1537 cm^{-1} in ^2H_2O shows a low intensity (figure 5.5B), indicative that almost complete $H/^2H$ exchange of the amide protons has occurred. The band at 1560-80 cm^{-1} (figure 5.5B) is attributed to stretching vibrations of ionized carboxylates of Asp and Glu sidechains (Venyanimov et al., 1991) and from

Figure 5.5

(A) Comparison of the spectrum of Human CRP in H_2O (solid line) and ^2H_2O (dashed line).

(B) Absorption spectrum of Human CRP in ^2H_2O (solid trace) and deconvolved spectra using K=2 and HWHH= 12 cm^{-1} (dashed trace).

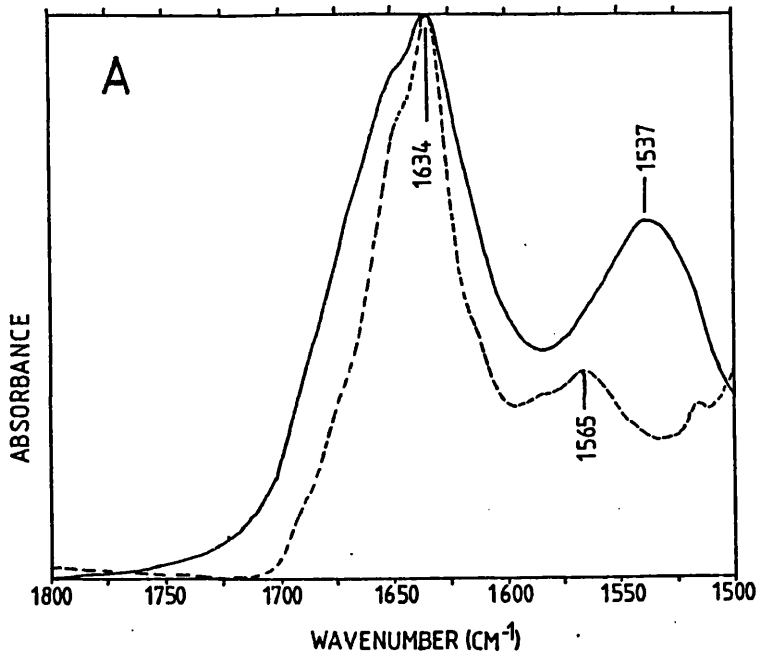
A
1634
1537
1565
ABSORBANCE
1800
1750
1700
1650
1600
1550
1500
WAVENUMBER (CM-1)

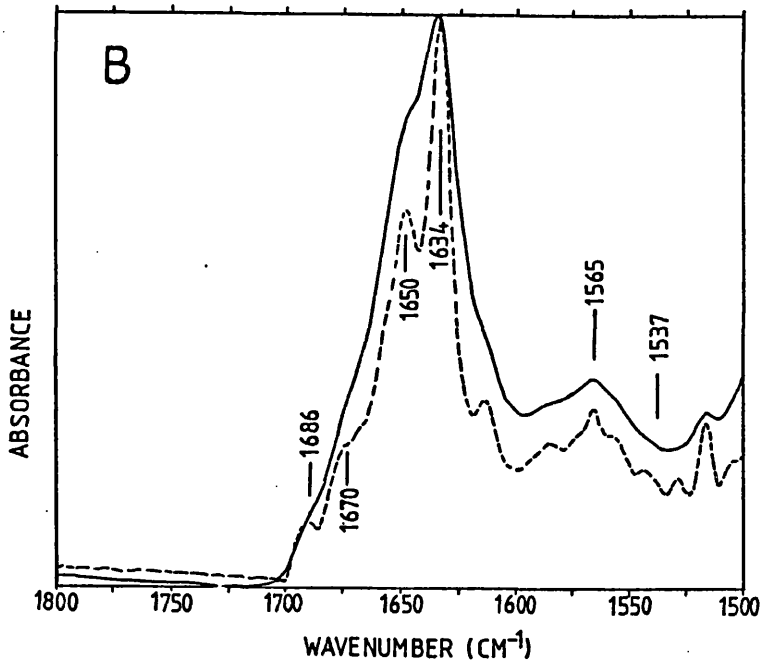
B
1686
1670
1650
1634
1565
1537
ABSORBANCE
1800
1750
1700
1650
1600
1550
1500
WAVENUMBER (CM-1)

Figure 5.6.

Absorption spectrum of Human CRP in Ca^{+2} 1mM $^{2}H_2O$ (solid line) and deconvolved spectrum (dashed line) using F=2 and W=14.

ABSORBANCE
WAVENUMBER (CM⁻¹)
1800
1750
1700
1650
1600
1550
1500
1686
1670
1650
1634
1566
1537

deuterium-shifted bands of Arg and Lys polar side chains (Azpiazu, unpublished results).

5.3.2. Binding of ligands: Ca^{2+} and lysolecithin.

The amide I band maximum of CRP in ^2H_2O solution in the presence of Ca^{2+} (figure 5.6) appears at 1634 cm^{-1}, at a similar frequency to that observed in the absence of Ca^{2+} (figure 5.5B). The region of the amide band between 1650-90 cm^{-1} shows the same intensity as that observed in the absence of Ca^{2+} (figure 5.5B). The extent of the reduction of the intensity of the amide II band, indicative of the degree of $H/^2H$ amide exchange, is lower than that observed in the absence of Ca^{2+}.

Binding of CRP to lysolecithin micelles in the presence of Ca^{2+} in ^2H_2O solution does not show changes in the amide I and II bands of the protein (spectrum not shown) when compared to the spectrum of CRP in ^2H_2O.

5.3.3. Binding to C-polysaccharide.

In the presence of Ca^{2+}, CRP binds and quantitatively precipitates C-polysaccharide at weight ratios lower than 1:10 (Young & Williams, 1978). The amide I band of CRP in ^2H_2O at a 10:1 (w/w ratio) CRP:C-polysaccharide shows a similar contour to that observed in the presence of Ca^{2+} (spectrum not shown). Studies of the rate of $^1H/^2H$ exchange in the presence of the C-polysaccharide are not possible due

to interference to the spectra of the amide II band of the protein occurring from components of the C-polysacharide such as murein and n-acetyl-galactosamine-phosphate.

5.3.4. Homologous proteins to human CRP.

The second derivative spectra of human CRP and SAP are shown in figure 5.7. The ß-sheet components of both proteins appear at the same frequencies (1634 cm^{-1}), those that correspond to α-helical bands in SAP appear at 1654 cm^{-1} (figure 5.7 solid trace). The region of the spectra between 1660-90 cm^{-1} shows significant differences in both proteins. CRP shows two components at 1672 and 1692 cm^{-1} (figure 5.7 dashed trace), whilst SAP shows a single band at 1684 cm^{-1}. These components may arise both from ß-turn III and high-frequency components of ß-sheet (Krimm & Bandekar, 1986; Susi & Byler, 1987). The amide II band maximum in SAP is seen at 1560-55 cm^{-1}, at a higher frequency than that observed at 1536 cm^{-1} in human CRP.

Limulus CRP is a lectin, homologous to human CRP, found in the hemolimph of the horseshoecrab *Limulus polyphemus*. In the presence of Ca^{2+} it has been shown to bind phosphoryl-choline and sialic acid-containing oligosacharides (Kaplan et al., 1977). The amide I band maximum of this protein in ^2H_2O in the presence of Ca^{2+} appears at 1637 cm^{-1}, indicative of a predominantly ß-sheet structure (figure 5.8 dashed trace).

Figure 5.7.

Second derivative of absorption spectrum of Human SAP (solid trace) and CRP in H_2O (dashed trace).

ABSORBANCE / WAVENUMBER 2
1692
1684
1672
1654
1650
1634
1560
1536
1800
1750
1700
1650
1600
1550
1500
WAVENUMBER (CM-1)

Figure 5.8.

Absorption spectrum of Limulus CRP in Ca^{+2} 1mM $^{2}H_{2}O$ (solid line) and second derivative (dashed line).

ABSORBANCE
1800
1750
1700
1650
1600
1550
1500
WAVENUMBER (CM-1)
1692
1674
1654
1635
1566
1554
ABSORBANCE / WAVENUMBER 2

The second derivative spectrum of Limulus CRP reveals a band at 1654 cm^{-1}, assigned to α-helical structures. The band at 1674 and 1692 cm^{-1} arise from high frequency components of ß-sheet and ß-turn structures.

The amide II band shows a low intensity at 1550-40 cm^{-1}, indicative of some $H/^2H$ exchange in the Limulus protein. The band at 1560-70 cm^{-1} corresponds to vibrations of Glu and Asp side-chains and partially arises from ^1H-^2H exchanged Arg and Lys side-chains (Azpiazu, unpublished results).

5.4. DISCUSSION.

5.4.1. Human CRP.

A number of biophysical and biochemical studies have been carried out with the aim of studying basic features of the CRP structure such as its dimensions and binding specificity to the PC group (Osmond et al., 1977; Liu et al., 1982). CD studies have reported secondary structure values of 35% in α-helix and 45% in ß-sheet structures (Young & Williams, 1978). Our quantitative results obtained with the factor analysis method indicate percentages of secondary structure of 10% for α-helix, 51% for ß-sheet, 39% for turn structures and 10% for unassigned structures. The factor analysis method (Lee et al., 1990) gives satisfactory predictions of percentages of secondary structure when the structures and spectrum of the analysed protein are similar

paging error- next page 206

Same as 205 !?

to those of the bank of reference proteins. For proteins, such as CRP, with non-typical secondary structures and therefore unusual spectra, the prediction is likely to be less accurate. Comparison of the amide I band of CRP with the synthetic amide I band generated by factor analysis indicates that the component observed at 1650 cm^{-1} has not been fitted satisfactorily. In this case the content in α-helix may well be higher than 10%.

The unusual high content of turn structures in CRP is likely to arise from the contribution of components of the amide I band between 1660-90 cm^{-1} (figure 5.2). Other ß-sheet rich proteins such as concanavalin, prealbumin, ribunoclease A (Lee et al., 1989; Haris et al., 1986) have lower contents of turn structures (28-19%, respectively) and their amide I bands do not show components at 1690-60 cm^{-1} as intense as those appearing in the amide I band of CRP. A recent study of the scrapie-associated protein PrP (Caughey et al., 1991) shows an infrared spectrum with a ß-sheet band at 1630-40 cm^{-1} and also a broad band at 1660-90 cm^{-1}, both similar to those appearing in the amide I band of CRP in H_2O. Quantification of secondary structure from the spectra of the PrP protein in H_2O gave values of 47% ß-sheet, 31% ß-turns and 17% α-helical structures, similar to those of human CRP. The prion PrP protein is the main component of fibril deposits in animal brain tissues of scrapie-

infected animals (Mertz et al., 1981). Analysis of these type of protein is possible only with infrared or Raman spectroscopy techniques, as these type of proteins are insoluble in aqueous media and therefore are untractable for analysis using CD spectroscopy and for crystallisation by X-ray diffraction analysis.

An intriguing observation suggested by Bandekar (1992) on the latter study of the PrP protein indicates that this distribution of secondary structure in the PrP protein may correspond to a cross-ß-sheet structure, which is usually observed in amyloid fibres (Kirschner et al., 1986). He notes that the PrP protein has little or no random structure, a high ß-sheet and ß-turn content and suggests that the band at 1651-55 cm^{-1} can actually arise from ß-turn III structures (Krimm & Bandekar, 1986). This would indicate a high ratio of turns to ß-sheet structures in the PrP protein and also in CRP, which is similar to the percentage of secondary structures expected in a cross-ß-sheet structure (Bandekar, 1992). It is highly speculative to suggest that CRP, and possibly SAP, may have an amyloid-type of structure. However both proteins are rich in ß-sheet and turn structures with an apparently low content in random structures. The first observations on X-ray diffraction data on CRP crystals (DeLucas et al., 1987) and also SAP crystals (Wood et al., 1988) did not indicate the presence of line

spacings in the diffraction pattern typical of a cross ß-structure, as is observed in amyloid proteins found in Akzheimer plaques and denatured proteins such as insulin fibrils (Burke et al., 1972; Kirschner et al., 1986). Otherwise the rare spectral features of CRP may correspond to a tertiary structure very rich in turns and ß-sheet with a low content in α-helix and random structures.

The rapid $H/^2H$ exchange of the amide protons of CRP in Ca^{2+}-free ^2H_2O solution is consistent with an open and solvent-accessible structure. The marked reduction in intensity of the components between 1660-90 cm^{-1} upon $H/^2H$ exchange can also result from an open structure in CRP and possibly from the presence of solvent-exposed turn structures such as those present in ribunoclease A (Olinger et al., 1986). It is intriguing that a similar drop in intensity of bands at 1650-90 cm^{-1} upon $H/^2H$ exchange is observed in the spectrum of the PrP protein (Caughey et al., 1991). The reduction in intensity of bands at 1660-90 cm^{-1} can also be explained, to some extent, by a shift upon $H/^2H$ exchange of bands that originate from Arg and Lys sidechain vibrations (Venyaminov et al., 1991) to a lower frequency (1600-1580 cm^{-1}) (Azpiazu, unpublished results).

5.4.2. Binding of ligands: Ca^{2+}.

The binding of the ligands to CRP does not induce significant changes in the spectrum of CRP in ^2H_2O. This is indicative of no substantial changes occurring in the secondary structure of CRP upon ligand-binding. The decrease in the rate of $H/^2H$ exchange upon Ca^{2+} binding is consistent with the structure of the protein becoming more compact and hence less solvent accessible. A similar decrease has been observed in studies of transferrin, an iron-binding protein, which shows a reduction in the rate of $H/^2H$ exchange upon iron-binding which is also accompanied by an increase in thermostability (Hadden & Bloomenthal, unpublished results (a)). The temperature of denaturation of CRP has been shown to increase by approximately 20°C upon Ca^{2+}-binding (Potempa et al., 1983). Binding of other important ligands such as PC and the C-polysacharide does not induce changes of secondary structure or cause a further reduction in the rate of $H/^2H$ exchange. This suggests that only Ca^{2+} induces changes in the conformation of human CRP as indicated by the rate of $H/^2H$ exchange.

5.4.3. Homologous proteins of human CRP.

Human SAP, a highly homologous protein to CRP, has been shown to contain similar values of secondary structure (35% turn structures, 60% ß-sheet, 8% α-helix) to those observed in human CRP. Comparison of the amide I band of the two

proteins in H_2O indicates small differences: the α-helical band in SAP appears at 1654 cm^{-1}, a higher frequency than that observed at 1650 cm^{-1} in CRP (figure 5.7). This suggests that the α-helical segments in SAP have a weaker hydrogen-bonding or are less hydrated than the α-helical segments in CRP (Jackson et al., 1989a). The region of the amide I band between 1690-1660 in CRP is different to that of SAP (figure 5.7). This suggests that these homologous proteins may be different in their ß-turn or ß-sheet structures.

protein

Limulus CRP is an homologous to the human protein that binds sialic-group and PC-containing molecules (Kaplan et al., 1977). The spectrum of Limulus CRP in ^2H_2O indicates the presence of secondary structures similar to those observed in human CRP. In the spectrum obtained in ^2H_2O solution, the ß-sheet components appears at a similar frequency to that of human CRP. The band assigned to α-helical structures is observed at a higher frequency than human CRP, indicating a weaker hydrogen-bonding or less hydration of the amide groups in the Limulus protein.

5.5. SUMMARY.

The secondary structure of human CRP has been investigated using FT-IR spectroscopy. The amide I band maximum of human CRP in H_2O occurs at 1634 cm^{-1} indicative of a ß-sheet rich structure. The amide I components at 1660-80 cm^{-1} show more intensity than in the spectra of other ß-sheet rich proteins. The band at 1650 cm^{-1} has been assigned to α-helical structures. Quantitative analysis of the amide I band of CRP in H_2O indicates secondary structure percentages of 51% ß-sheet, 39% ß-turns and 10% α-helix, similar to those observed in the homologous human SAP (Hadden, unpublished results (a)).

$H/^2H$ exchange studies of CRP in Ca^{2+}-free ^2H_2O, indicate that the amide I band of CRP shows a reduction in intensity of bands at 1660-90 cm^{-1}. It is suggested that this results from solvent-exposed turn structures in the tertiary structure of CRP. The rate of $H/^2H$ amide exchange, as indicated by the reduction of the intensity of the amide II band, was fast and complete. In the presence of Ca^{2+}, the rate of $H/^2H$ exchange was slower than in the absence of Ca^{2+}. These results are consistent with a solvent-accessible conformation in the human CRP made more compact upon Ca^{2+} binding. The spectrum of Limulus CRP in Ca^{2+}-^2H_2O indicates secondary structures similar to those observed in human CRP.

CHAPTER 6

FUTURE WORK

6. FUTURE WORK.

Most of the assignment guidelines to the frequencies of the amide I band components of proteins are based upon experimental correlation of the percentage of those types of secondary structures with those from X-ray diffraction data.

There are, however, a number of problems to be addressed in order to improve the certainty of the assignments. So far amide I band components at 1650-56 cm^{-1} in ^2H_2O were assigned solely to α-helical secondary structures as random structures appear at the H/^{2}H-shifted frequencies at approximately 1640-45 cm^{-1} (Jackson et al., 1989). Recent studies of soluble proteins indicate that amide I bands at 1650-56 cm^{-1} in ^2H_2O can also originate from random structures in some proteins (Wilder et al., 1992; Prestrelki et al., 1991b). This possibility may be explored in order to understand the relevance of these observations. Information on the experimental conditions, such as incomplete H/^{2}H amide exchange and the type of conformations, i.e. the geometry and hydrogen-bonding of the peptidic backbone that give rise to these bands, would be desirable.

The amide I band components at 1640 and 1660-5 cm^{-1} in H_2O have been attributed to the presence of 3_{10} helical structures. Byler & Susi (1986) have observed an amide I band component at 1640 cm^{-1} in α-helical proteins such as cytochrome C and hemoglobin. It has been suggested that this

is due to the existence of distorted helical turns at the ends or starts of α-helical segments, possibly being part of a 3_{10}-structure. It is intriguing that the amide I band of the Pf1 and fd proteins in the three environments in H_2O, do not show bands at 1640 cm^{-1}. The basis of these differences in the spectra of α-helical proteins can be explored and complemented with studies of structures of other proteins with long α-helical segments such as coiled-coil proteins i.e. myosin, tropomyosin. The understanding of the basis of the difference in frequencies of the amide I band between the two coat proteins can be explored using synthetic chimeric peptides containing parts or domains of the Pf1 and fd proteins.

There is also a need to characterise other conformations such as the π-helix (Sasaki et al. 1981) and the collagen-type of helix (Soman & Ramakrishnan, 1983). The latter has been predicted as part of the structure of some proteins.

The assignments of the amide I band components between 1675-95 cm^{-1} to ß-turns and/or ß-sheet components are uncertain. Factor analysis of the amide I band has shown for the first time a strong correlation between percentage of turn structures in proteins and the intensity of the band at 1684 cm^{-1} in H_2O (Lee et al., 1990). The infrared spectra of peptides known from their X-ray structure or NMR spectroscopy

to adopt turn structures will provide additional information on the assignment of different ß-turn types.

Recent works have indicated that the sidechains of aminoacid such as Arg, Gln, Asn and Lys absorb weakly within the amide I and II bands in H_2O (Venyanimov et al., 1990). Although their individual contributions depend on their content in each protein, they deserve further analysis. Subtraction of their individual contribution to obtain the peptidic amide bands is a valuable approach, but is subject to uncertainties on the frequencies and widths of their original bands in proteins. Recent observations of synthetic polypeptides such as polyarginine, polylysine (Azpiazu, unpublished results) suggest that the bands associated to Arg and Lys sidechains at 1670 and 1640 cm^{-1}, observed in H_2O, undergo a shift upon $H/^2H$ exchange to frequencies between 1600-1500 cm^{-1}. Those of Asn and Gln seemed to shift less to approximately 1640-1650 cm^{-1}. It would be desirable to analyse these preliminary observations in future studies in order to be useful for the evaluation of the contribution of aminoacid sidechains to the amide I and II band.

FT-IR spectroscopy can be applied to the study of protein:protein or protein:DNA interaction with the use of ^{13}C- and ^{15}N-labelled biomolecules obtained from cultures of bacteria grown on mineral carbon and nitrogen isotopic sources. A recent work carried out in our lab indicates that

this approach is promising (Haris et al., 1992). The ^{13}C-labelling of serines in the Pf1 coat protein presented in this thesis introduces a new way for molecular structure assignment. The frequency of the $^{13}C=O$ stretching modes appears 40 cm^{-1} down with respect to that of the $^{12}C=O$ mode, to a region of the infrared spectra (1620-1590 cm^{-1}) which is relatively free from interfering species. For small proteins, the frequency of the $^{13}C=O$ amide I band gives an indication of the secondary structure, e.g. α-helix or random, in which the aminoacids are present. Polarization studies of membrane proteins in lipid films using ATR techniques can be used to examine the likely orientation of their secondary structures. In this respect the use of the amide A band and its ^{15}N-shifted amide A has been suggested as indicators of secondary structure, specially if these studies are combined with information on the amide $H/^{2}H$ exchange.

The development of time-resolved FT-IR spectroscopy has shown its potential for the characterisation of the dynamics of bacteriorhodopsin upon photo-illumination (Rothschild et al., 1985). Time-resolved studies permits the observation of changes in a 1msec-10sec time-resolution in the infrared spectra that occur upon ligand-binding and associated conformational changes (Rath et al., 1991b). The ligand can be kept trapped in a caged-inactive compound in the presence

of the protein of interest, and when desired the release of the ligand in the media is triggered by a flash of UV light. The rate of the reaction or kinetics of the proccess can be down-regulated in some cases by working at low temperatures (Mäntele et al., 1985). The observed changes do not necessarily indicate changes in the secondary structures, however they may provide information on the type of sidechains of aminoacids intervening or affected by the conformational changes occurring in the protein. Assignments to specific aminoacids could be further analysed with the use of isotopically ^{13}C- or ^{15}N-substituted aminoacids incorporated in the protein.

In general all these experimental inroads in the dynamics and the structure of proteins will depend on the application of other techniques such as microbiology, enzyme kinetics, organic chemistry, molecular modelling, etc. and some basic FT-IR studies.

REFERENCES

REFERENCES.

Azpiazu, I. (unpublished results).

Baldwin, J.M., Henderson, R., Beckman, E. and Zemlin, F. (1988). J. Mol. Biol. 202, 585-591.

Bandekar, H. and Krimm, S. (1979). Proc. Natl. Acad. Sci. USA 76, 774-777.

Bandekar, H. and Krimm, S. (1986). Biophys. J. 49, 295-302.

Bandekar, J. (1992). Biochim. Biophys. Acta 1190, 123-143.

Bartlett, G.R. (1959). J. Biol. Chem. 234, 466-471.

Benner, S.A. and Gerloff, D. (1990). Adv. Enz. Reg.31, 121-181.

Birktoff, J.J. and Blow, D.M. (1972). J. Mol. Biol. 68, 187-240.

Blake, C.C., Geisow, M.J., Oatley S.J., Rerat, B. and Rerat, C. (1978). J. Mol. Biol. 121, 339-356.

Blume, A., Hübner, W. and Messner, G. (1988). Biochem. 27, 8239-8249.

Boggs, J.M. and Moscarello, M.A. (1978). Biochem. 17, 5734-5739.

Brauner, J.W., Mendelsohn, R. and Prendergast, F.G. (1987). Biochem. 26, 8151-8518.

Bruckner, H. and Cirat, H. (1983). Experientia 39, 528-530.

Budzynski, A.Z. (1971). Biochim. Biophys. Acta 229, 663-671.

Burke, M.J. and Rougvie, M.A. (1972). Biochem. 11, 2435-2439.

Byler, D.M. and Susi, H. (1986). Biopolymers 25, 469-487.

Caughey, B.W., Dong, A., Bahat, K.S., Ernst, D., Hayes, S.F. and Caughey, W.S. (1991). Biochemistry 30, 7672-7680.

Chamberlain, B.K., Nozaki, Y., Tanford, C. and Webster, R.E. (1978). Biochim. Biophys. Acta 510, 18-37.

Chapman, D. (1975). Quart. Rev. Biophys. 8, 185-235.

APPENDED REFEREMCES.

Buchet, R., Varga, S., Seidler, N.W., Molnar, E. and Martonosi, A. (1991). Bichimi. Biophys. Acta 1068, 201-216.

Ter-Minassian-Saroga, L., Okamura, E., memura, J. and Takenaka, T. (1988). Biochim. Biophys. Acta 946, 417-423.

Weaver, A.J., Kemple, M.D., Brauner, J.W., Mendelsonn, R. and Prendergast, F.G. (1992). Biochem. 31, 1301-1313.

Chapman, D. and Urbina, J. (1971). FEBS Let. 12, 169-172.

Chen, J.P., Shurley, H.M. and Vickroy, M.F. (1972). Biochem. Biophys. Res. Commun. 71, 754-761.

Cherry, C. (1979). Biochim. Biophys. Acta 559, 502-516.

Chirgatze, Y.U., Fedorov, O.V. and Trushina, N.P. (1975). Biopolymers 14, 679-694.

Chothia, C. and Lesk, A.M. (1986). EMBO J. 5, 823-826.

Chou, P.Y. and Fasman, G.D. (1974). Adv. Enzymol.47, 45-148.

Cierniewski, C.S., Kloczewiak, M. and Budzynski, A.Z. (1986). J. Biol. Chem. 261, 9116-9121.

Cierniewski, C.S. and Budzynski, A.Z. (1987). J. Biol. Chem. 262, 13896-13901.

Cohen, C., Weisel, J.W., Phillips, G.N., Jr., Stauffacher, C.V., Fillers, J.P. and Daub, E. (1983). Ann. N.Y. Acad. Sci. 408, 194-213.

Cortijo, M., Alonso, A., Gomez-Fernandez, J.C. and Chapman, D. (1982). J. Mol. Biol. 157, 597-618.

Crawford, J.L. & Lipscomb, W.N. (1973). Proc. Natl. Acad. U.S.A. 70, 538-542.

Day, L.A. and Wiseman, R. (1978).J. Mol. Biol. 102, 549-553.

Day, L.A., Wiseman, R.L. and Marzec, C.J. (1979). Nucleic Ac. Res. 7, 1393-1403.

Day, L.A., Marzec, S.A.R. and Casadevall A. (1988) Ann. Rev. Biophys. Chem. 17, 509-539.

Deisenhofer, J., Epp, O., Miki, K., Huber, R. and Michel, H. (1985). J. Mol. Biol. 316, 618-623.

DeLucas, L.J., Greenhough, T.J., Rule, S.A., Myles, D.A.A., Babu, Y.S., Volanakis, J.E. and Bugg, C.E. (1987). J. Mol. Biol. 196, 741-742.

Deutsch, D.G. and Mertz, E.T. (1970). Science 170, 1095-1096.

Devaut, P.F. and Seigneuret, M. (1985). Biochim. Biophys. Acta 822, 63-125.

Doolittle, R.F. (1973). Adv. Prot. Chem. 27, 1-109.

Doolittle, R.F., Goldbaum, D.M. and Doolittle L.R. (1978). J. Mol. Biol. 120, 311-325.

Doolittle, R.F. (1984). Ann. Rev. Biochem. 53, 195-229.

Dray-Attali, L. and Larrieu, M.J. (1977). Thromb. Res. 10, 575-586.

Earnest, T.N., Herzfeld, J. and Rothschild, K.J. (1990). Biophys. J. 58, 1539-1546.

Elliot, A. and Ambrosse, E.J. (1950). Nature 165, 921-923.

Endow, S.A. (1991). Trends Biochem. Sci 16, 221-225.

Epp, O., Colman, P., Felhlhammer, H., Schaffer, M. Huber, R. and Palm, W. (1974). Eur. J. Biochem. 45, 513-524.

Fowler, W.E., Fretto, L.J., Erickson, H.P. and McKee, P.A. (1980). J. Clin. Invest. 66, 50-56.

Engelman, D.M., Steitz, T.A. and Goldman, A. (1986). Ann. Rev. Biophys. Chem. 15, 321-353.

Fox, R. and Richards, F.M.(1982). Nature 300, 325-330

Fringeli, U.P. (1977). Z. Naturforsch. 32c, 20-45.

Fringeli, U.P. and Fringeli, M. (1979). Proc. Natl. Acad. Sci. USA 76, 3852-3856.

Fringeli, U.P. and Gunthard, Hs.,H.(1981). Mol. Biol. Biochem. Biophys. 31, 270-332.

Frizsche, H., Cross, T.A., Opella, S.J. and Kallenbach, N.R. (1981). Biophys. Chem. 14, 283-291.

Gallusser, A. and Kuhn, A. (1990). EMBO J. 9, 2723-2729.

Garnier, J., Osguthorpe, D.J. and Robson, B. (1978). J. Mol. Biol. 120, 97-120.

Gomez-Fernandez, J.C., Goni, F.M., Bach, D., Restall, C.J. and Chapman, D. (1980). Biochim. Biophys. Acta 598, 502-516.

Goormaghtigh, E. and Ruysschaert, J.-M. (1990). In 'Molecular Description of Biological Components' (Brasseur, R., Ed.) 1, 285-329, CRC Press, Boca Raton.

Griffiths, P.R. and De-Haseth, J.A. (1986). Fourier Transform Infrared Spectroscopy, Vol. 83, Chemical Analysis Monograph Series, ed. Elving, P.J. & Winefordner, J.D., Wihley, J. & Sons

Hadden, J. and Bloementhal, M. (unpublished results)a.

Hadden, J. (unpublished results)b.

Hames, B.D. and Rickwood, D. (eds.) (1981). Gel Electrophoresis of Proteins- A Practical Approach, IRL Press, Oxford.

Haris, P.I., Lee, D.C. and Chapman, D. (1986). Biochim. Biophys. Acta 874, 255-266.

Haris, P.I. (1989). PhD Thesis, University of London, U.K..

Haris, P.I., Robillard, G.T., Van Dijk, A.A. and Chapman, D. (1992). Biochem. 31, 6279-6284.

Haris, P.I. and Chapman, D. (1992). Trends Biochem. Sci. 17, 328-333.

Haverkate, F. and Timan, G. (1977). Thromb. Res. 10,803-812.

Henderson, R. and Unwin, P.N.T. (1975), Nature 257, 28-32.

Henry, G.D. and Sykes, B.D. (1992) Biochem. 31, 5284-5297.

Hesketh, T.R., Smith, G.A., Houslay, M.D., McGill, K.A., Birdsall, N.J.M., Metcalfe, J.C. and Warren, G.B. (1976). Biochem. 15, 4145-4151.

Hoffman, W., Pink, D.A., Restall, C. and Chapman, D. (1981). Eur. J. Biochem. 114, 585-589.

Jackson, M., Haris, P.I. and Chapman, D. (1989a). J. Mol. Struct. 214, 329-355.

Jackson, M., Haris, P.I. and Chapman, D. (1989b). Biochim. Biophys. Acta 998, 75-79.

Jackson, M. (1990). PhD thesis, University of London, U.K.

Jackson, M., Haris, P.I. and Chapman, D. (1991). Biochem. 30, 9681-9686.

Jap, B.K., Walian, P.J. and Gehning (1991). Nature 350, 167-170.

Jones, O.T. et al., (1986). In Finby, J., (Ed.). Solubilisation and Reconstitution of Membrane Proteins; a Practical Approach., IRL Press.

Kaplan, R., Li, S.S.-L. and Kehoe, J.M. (1977). Biochem. 16, 4297-4303.

Kauppinen, J.K., Moffat, D.J., Mantsch, H.H. and Cameron, D.G. (1981). Anal. Chem. 53, 1454-1457.

Kawato, S., Kinosita, K. and Ikegarai, A. (1977). Biochem. 16, 2917-2924.

Kassel, W. and Kay, J. (1973). Science 180, 1022-1027.

Katayama, K., Ericksson, L.H., Enfiled, D.L., Walsh, K.A., Neurath, H., Davie, E.W. and Titani, K. (1979). Proc. Natl. Acad. Sci. USA 76, 4990-4994.

Kemmler, W., Peterson, J.D. and Steiner, S.D. (1971). J. Biol. Chem. 246, 6786-6791.

Kendrew, J.C., Bodo, G., Duitzis, H.M., Parrish, R.G., Wyckoff, H.W. and Phillips, D.C. (1958). Nature 181, 662-668.

Kendrew, J.C., Dickerson, R.E., Stranberg, B.E., Hart, R.G., Davies, D.R. and Phillips, D.C. (1960). Nature 185 , 422-427.

Kendrew, J.C., Watson, T., Stranberg, B.E., Dickerson, R.E., Davies, D.R. and Phillips, D.C. (1963). Nature 190, 666-670.

Kennedy, D., Crisma, M., Toniolo, C. and Chapman, D. (1991). Biochem. 30, 6541-6548.

Kessler, C.M. and Bell, W.R.B. (1979). J. Lab. Clin. Med. 93, 758-767.

Kinoshita, C.M., Ying, S.-C., Siegel, J.N., Potempa, L.A., Jiang, H., Houghten, R.A. and Gewurz (1989). Biochem. 28, 9840-9848.

Kirschner, D.A., Abraham. C. and Selkoe, D.J. (1986). Proc. Natl. Acad. Sci. USA 83, 503-507.

Kleeman, W. and McConnell, H.M. (1976). Biochim. Biophys. Acta 419, 206-222.

Kloczewiak, M., Wegrzynowicz, Z., Mathias, F.R. and Heene, D.L. (1976). Thromb. Res. 9, 359-368.

Knowles, P.F., Watts, A. and Marsh, D. (1979). Biochem. 18, 4480-4487.

Koenigg, J.L. and Tabb, D.L. (1980). In'Infrared Spectra of Globular Proteins in Aqueous solution', Analytical Applications of FT-IR in Molecular and Biological Systems, 241-255, Durig, J.,R. (ed.), Reidel P.C..

Koj, A. (1974). In 'Structure ann Function of Plasma Proteins', A.C. Allison, Ed.1, 73-131, Plenum Press, N.Y.

Krimm, S. and Bandekar, J. (1986). Adv. Prot. Chem. 38, 181-364.

Lakowicz, J.R. (1983) In 'Principles of fluorescence spectroscopy', pp 112-152, Plenum Press, New York & London.

Laudano, A.P., Cottrell, B.A. and Doolittle, R.F. (1983). Ann. N.Y. Acad. Sci. 408, 315-329.

Lee, D.C., Herzyk, E. and Chapman D. (1987). Biochem. 26, 5775-5783.

Lee, D.C., Haris, P.I., Chapman, D. and Mitchell, R.C. (1990). Biochem. 29, 9185-9193.

Leo, G.C., Colnago, L.A., Valentine, K.G. and Opella, S.J. (1987). Biochem. 26, 854-862.

Lewis, P.N. and Momany, F.A. (1973). Biochim. Biophys. Acta 303, 211-229.

Liu, T.-Y., Robey, F.A. and Wang, C.-M. (1982). Ann. N.Y. Acad. Sci. 389, 151-161.

Löberman, H., Tokuoka, R., Deisenhofer, J. and Huber, R. (1984). J. Mol. Biol. 177, 531-556.

McElhaney, R.N. (1984). Biochim. Biophys. Acta 864, 361-421.

Makino, S., Woolford, J.L., Tanford, C. and Webster, R.E. (1975). J. Biol. Chem.250, 4327-4332.

Mäntele, A., Nabedryk, E., Tavitian, B.A., Kreutz, W. and Breton, J. (1985). FEBS Let. 187, 227-232.

Marshall, G.R., Hodgkin, E.E., Lang, D.A., Smith, G.D., Zabrocki, J. and Leplawy, M.T. (1990). Proc. Natl. Acad. Sci. USA 87, 487-491.

Marvin, D.A. & Wachtel E.J. (1975) Nature 253, 19-23.

Marx, J., Hudry-Clergeon, G., Capet-Antoninin, F. and Bernard, L. (1979). Biochim. Biophys. Acta 578, 107-115.

Melved', L.V., Privalov, P.L. and Ugarova, T.P. (1982). FEBS Let. 146, 339-342.

Melved', L.V., Litvinovich, S.V. and Privalov, P.L. (1986). FEBS Let. 202, 298-302.

Mertz, P.A., Sommerville, R.A., Wisniewski, H.M. and Iqbal C. (1981). Acta Neuropat. 54, 63-74.

Miller, J.H. (1972). Experiments in Molecular Genetics, Cold Spring Harbor Laboratory, Cold Spring Harbor, NY.

Mirabella, F.R. (1985). Appl. Spectr. Rev. 21, 45-178.

Mold, C.C., Rogers, C.P., Richards, R.L. and Alving, C.R. (1981). J. Immunol. 122, 1185-1189.

Nabedryck, E., Gingold, M.P. and Breton, J. (1982). Biophys. J. 38, 243-249.

Nakashima, Y., Wiseman, R.L., Konisberg, W. and Marwin, D.A. (1975). Nature 253, 68-71.

Nambudripap, R., Stark, W., Opella, S.J. & Makowski, L. (1991). Science 252, 1305-1307.

Namba, K., Caspar, D.L.D. and Stubbs, G.J. (1985). Science 227, 773-776.

Narkates, A.J. and Volanakis, J.E. (1982). Ann. N.Y. Acad. Sci. 389, 172-182.

Nikishikawa, K. (1983). Biochim. Biophys. Acta 748, 285-299.

Ny, T., Elgh, F. and Lund, B. (1984). Proc. Natl. Acad. Sci. USA 81, 5355-5359.

Olexa, S.A., Budzynski, A.Z., Doolittle, R.F., Cottrell, B.A. and Greene, T.C. (1981). Biochem. 20, 6139-6145.

Olinger, J.M., Hill, D.M., Jakobsen, R.J. and Brody, R.S. (1986). Biochim. Biophys. Acta 869, 89-98.

Oliveira, E.B., Gotschlich, E.C. and Liu, T.-Y. (1979). J. Biol. Chem. 254, 489-502.

Oliveira, E.B., Gotschlich, E.C. and Liu, T.-Y. (1980). J. Immunol. 124, 1396-1402.

Osmond, A.P., Friedenson, P.B., Gewurtz, H., Painter, R.H., Hofmann, T. and Shelton, E. (1977). Proc. Natl. Acad. Sci. U.S.A. 74, 739-743.

Pace, C.N. (1990). Trends Biochem. Sci. 15, 14-17.

Parry, D.A.D. (1975). J. Mol. Biol.98, 519-535.

Pauling, L., Corey, R.B., Branson, H.R. (1951a). Proc. Natl. Acad. Sci. USA 37, 205-211.

Pauling, L. and Corey, R.B. (1951b). Proc. Natl. Acad. Sci. USA 37, 235-240.

Pauling, L. and Corey, R.B. (1951c). Proc. Natl. Acad. Sci. USA 37, 729-740.

Pink, D.A., Chapman, D., Laidlaw, D.J. and Wiedmer, T. (1984). Biochem. 23, 4051-4058.

Plow, E.F., Edginton, T.S. and Cierniewski, C.S. (1983). Ann. N.Y. Acad. Sci. 408, 45-59.

Potempa, L.A., Maldonado, B.A., Laurent, P, Zemel, E.S. and Gewurtz, H. (1983). Mol. Immunol. 20, 1165-1175.

Prestrelski, S.J., Arakawa, T., Kenney, W.C. and Byler, D.M. (1991a). Arch. Biochem. Biophys. 285, 111-115.

Prestrelski, S.J, Byler, D.M. and Liebman, M.N. (1991b). Biochem. 30, 133-143.

Privalov, P.H., Medved', L.V. (1982). J. Mol. Biol. 159, 665-683.

Quinland, R.A. and Stewart, M. (1987). J.Cel.Biol.105, 403-415.

Ramachandran, G.N. and Sasisekharan, V. (1968). Adv. Prot. Chem. 23, 283-437.

Rao, S.P.S., Poojary, M.D., Elliot, B.W., Melanson, L.A., Oriel, B. and Cohen, C. (1991). J. Mol. Biol. 222, 89-98.

Rath, P., Bousché, O., Merrill, A.R., Cramer, W.A. and Rothschild, K.J. (1991a). Biophys. J. 59, 516-522.

Rath, A., Mäntele, W. and Kreutz, W. (1991b). Biochim. Biophys. Acta 1057, 115-123.

Reeke, G.N. et al., (1975). J. Biol.Chem. 250, 1525-1547.

Richards, R.L., Gewurtz, H., Oswand, A.P. and Alving, C.R. (1977). Proc. Natl. Acad. Sci. U.S.A. 74, 5672-5676.

Richardson, J.S. (1981). Adv. Prot. Chem. 34, 167-339.

Roux, K.H., Kilpatrick, J.M., Volanakis, J.E. and Kearney, J.F. (1983). J. Immun. 131, 2411-2415.

Ryba, N.J.B. and Marsh, D. (1992). Biochem. 31, 7511-7518.

Sasaki, S., Yasumoto, Y. and Uemastsu, I. (1981). Macromol. 14, 1797-1801.

Schägger, H. and Jagow, G.V. (1987). Anal. Biochem. 166, 368-379.

Schiksnis, R.A., Bogusky, M.J., Tsang, P. & Opella, S.J. (1987) Biochem. 26, 1373-1381.

Semin, B.K., Saraste, M. and Wikstrom, M. (1984). Biochim. Biophys. Acta 769, 15-22.

Shinitzky, M., Dianoux, A.C. and Weber, G. (1971). Biochem. 10, 2106-2113.

Shimizu, A., Nagel, G.M. and Doolittle, R.F. (1992). Proc. Natl. Acad. Sci. U.S.A. 89, 2888-2892.

Scholey, J.M., Heuser, J., Yang, J.T. and Goldstein, L.S.B. (1989). Nature 338, 355-357.

Shon, K.-J., Kim, Y., Colnago, L.A. & Opella, S.J. (1991) Science 252, 1303-1305.

Singer, S.J. and Nicholson, G.L. (1972). Science 175, 720-731.

Smilowitz, H., Carson, J. and Robbins, P.W. (1972). J. Supramol. Struct. 1, 8-18.

Soman, K.V. and Ramakrishnan, C. (1983). Mol. J. Biol. 170, 1045-1048.

Surewitz, W.K. and Manstch, H.H. (1988). Biochim. Biophys. Acta 952, 115-130.

Susi, H., Timasheff, S.N. and Stevens, L. (1967). J. Biol. Chem. 242, 5460-5466.

Susi, H. (1969). 'Infrared spectra of biological macromolecules and related systems', in Structure and stability of biological molecules (Timasheff, S.N. and Fasman, G.D., eds), Marcel Dekker, NY.

Susi, H. and Byler, D.M. (1983). Biochem. Biophys. Res. Commun. 115, 391-397.

Susi, H. and Byler, D.M. (1986). Methods Enzym. 130, 290-311.

Susi, H. and Byler, D.M. (1987). Arch. Biochem. Biophys. 258, 465-469.

Tanford, C. (1980). The Hydrophobic Effect: Formation of Micelles and Biological Membranes, (2nd ed.), Wiley & Sons, N.Y..

Tillett, W.S. and Francis, T. (1930). J. Exp. Med. 52, 561-571.

Torio, H. and Tasumi, M. (1992). J. Chem. Phys. 96, 3379-3387.

Toyoshima, C., Sasabe, H. and Stokes, D.L. (1990). Nature 362, 469-471.

Van Hoden, E.J.J., Van Dijk, P.W., De Kruijff, B., Verkley, A.J. and Van Deenen, H.M. (1978). Biochim. Biophys. Acta 514, 9-29.

Váradi, A. and Scheraga, H.A. (1986). Biochem. 25, 519-528.

Venkatachalam, C.M. (1968). Biopolym. 6, 1424-1436.

Venyaminov, S.Yu. and Kalmin, N.N. (1991). Biopolym. 30, 1243-1257.

Volanakis, J.E. and Kaplan, H.H. (1971). Proc. Natl. Acad. Sci. U.S.A. 136, 612-614.

Webster, R.E. and Cashman, J.S. (1973). Virology 55, 20-38.

Wickner, W. (1975). Proc. Natl. Acad. Sci. U.S.A. 72, 4749-4753.

Wilder, C.L., Friedrich, A.D., Potts, R.O., Daunny, G.O. and Francoeur, M.L. (1992). Biochem. 31, 27-31.

Wood, S.P., Oliva, G., O`Hara, B.P., White, H.E., Blundell, T.L., Perkins, S.J., Sardharwalla, I. and Pepys, M.B. (1988). J.Mol. Biol. 202, 169-173.

Yang, P.W., Stewart, L.C. and Mantsch, H.M. (1987). Biochem. Biophys. Res. Commun. 145, 298-302.

Young, N.M. and Williams, R.E. (1978). J. Immun. 121, 1893-1898.

PUBLICATIONS

LIST OF PUBLICATIONS.

I. Azpiazu, D. Chapman (1992). Biochim. Biophys. Acta 1119, 268
Spectroscopic studies of Fibrinogen and its plasmin-derived fragments.

I. Azpiazu, P.I. Haris and D.Chapman (1992). Biochem. Soc. Trans. 645th Meeting RFH London, 82.
Conformation of the Pf1 coat protein in the phage and in a lipid membrane.

I. Azpiazu, J.C. Gomez-Fernandez and D. Chapman (1993). Biochem. (accepted for publication, in press).
Biophysical studies of the Pf1 coat protein in the filamentous phage, in detergent micelles and in a membrane enviroment.

Biochimica et Biophysica Acta, 1119 (1992) 268–274

BBAPRO 34126

Spectroscopic studies of fibrinogen and its plasmin-derived fragments

I. Azpiazu and D. Chapman

Department of Protein and Molecular Biology, Division of Basic Medical Sciences, Royal Free Hospital School of Medicine, University of London, London (U.K.)

(Received 27 May 1991)
(Revised manuscript received 7 October 1991)

Key words: Fibrinogen; Spectroscopy; Fragment

The secondary structure of human fibrinogen and its plasmin-fragments have been studied by FTIR spectroscopy. The quantitative results for fibrinogen are in good agreement with previous studies using circular dichroism spectroscopy. After treatment of fibrinogen with plasmin in buffer containing Ca^{2+}, two major fragments are produced: fragment E (Mw 45 000) and fragment D (Mw 100 000). Fragment E is shown to contain 50% α-helical values, attributed to its coiled-coil portions, and minor β-strands and turn structures. Its deuteration gives evidence of the presence of solvent-exposed α-helical structures. On the other hand, fragment D contains a distribution of secondary structure values of 35% α-helix, 29% β-sheet segments and 17% turn structures. Fragment D itself has two domains: a portion of the original coiled-coil and also a thermally labile globular domain. The coiled-coil portion (Mw 27 000) was isolated and showed a high α-helical content (around 70%). The globular domain is estimated to be rich in β-sheet structures. The spectra of fibrin clots formed in Ca^{2+}-containing buffer have a lower amide I / amide II ratio than fibrinogen spectra, which is interpreted as being due to aggregation.

Introduction

Human fibrinogen has been extensively studied using a variety of biochemical and physical techniques. On the basis of these studies a model has been proposed [1,2]. This model (Fig. 1) consists of a triple α-helical coiled-coil which connects two distal globular domains to a central domain. From each distal domain, the carboxy-termini of the α-chain extends forming a polar appendage which is accessible to proteolysis. The central domain of fibrinogen contains active sites, which are exposed by thrombin cleavage. The distal domain bears complementary sites for those in the central ones. Thrombin-attack on fibrinogen produces fibrin monomers, which self-polymerise forming a clot.

When fibrinogen is digested [3,4] with plasmin in the presence of Ca^{2+}, two major fragments are recovered: the E fragment (Mw 45 000) corresponding to part of the central domain and the coiled-coil and the D fragment (Mw 100 000) which includes the whole distal domain and a portion of the coiled-coil. Fragment E has lost its active sites after plasmin digestion [5]. The D fragment still contains the complementary sites and inhibits the polymerisation of fibrin [6,7]. Fragment D treated with 5 M guanidine HCl, loses fibrin-binding affinity and does not inhibit fibrin-clot formation [7].

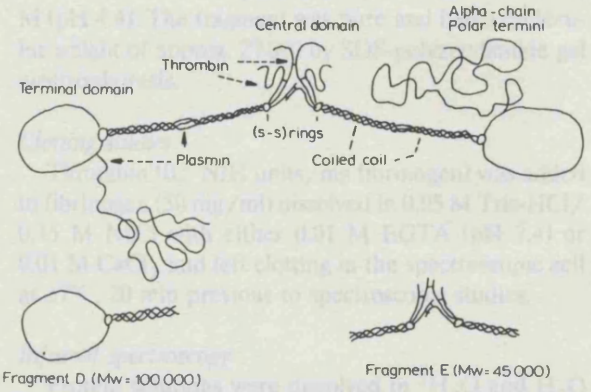

Fig. 1. Schematic model of fibrinogen and fragments resulting from plasmin digestion, showing main domains and points of proteolytic attack. Data obtained from Ref. 1 and 2.

Correspondence: I. Azpiazu, Department of Protein and Molecular Biology, Division of Basic Medical Sciences, Royal Free Hospital School of Medicine, University of London, Rowland Hill Street, London NW3 2PF, U.K.

Integrity of the native structure is essential for the expression of complementary sites in fragment D [7] and possibly in fibrinogen.

The elucidation of the secondary structure of either fibrinogen or its fragments is relevant for the construction of a three-dimensional atomic model [8]. Knowledge of the tertiary and secondary structure of the domains is limited [1,2,9,10]. Early studies [11–13] on fibrinogen (Raman and circular dichroism spectroscopy, CD) reported the presence of 35% α-helical content. Raman spectroscopy techniques indicated the presence of smaller amounts of β-sheet (10%) in fibrinogen than deduced from CD spectroscopy (20%). The present work examines the secondary structure of fragments E and D obtained after digestion of fibrinogen with various proteinases (plasmin and pepsin). This information is used to study and to deduce the secondary structure of the globular domains of fibrinogen.

Fourier transform infrared spectroscopy (FTIR) can be used to report on protein secondary structure [14]. This technique is more sensitive to β-sheet and turn structures than CD, and permits solution studies on denaturation and clotting processes, without light scattering problems. In the infrared spectra the amide I and II bands of the backbone peptidic groups are specially sensitive to protein secondary structure (α-helix, β-sheet and turn structures). The amide I band (1690–10 cm^{-1}) arises mainly from peptidic C=O stretching vibrations and the amide II band (1580–20 cm^{-1}) from the bending of the N–H bonds and other minor vibrations. Deconvolution and derivative routines are used to resolve the underlying components within the original amide I and II bands of the infrared spectra of the proteins.

Materials and Methods

Materials

All reagents were of analytical grade and obtained from commercial sources. Streptokinase, pepsin and fibrinogen (Type I, 95% of protein clottable) and thrombin were provided by Sigma. Plasminogen was purified from outdated plasma, according to D.G. Deutsch et al. [15]. Its purity was checked by SDS-polyacrylamide gel electrophoresis, giving an approximate molecular weight of 85 000.

Preparative procedures: fragment D (Mw 100 000) and fragment E (Mw 45 000)

Fibrinogen (10 mg/ml) was dissolved in Tris-HCl 0.05 M/ NaCl 0.15 M (pH 7.4). Before the digestion, $CaCl_2$ (final = 0.025 M) was added and then digestion was initiated by coadding plasminogen (final = 10 μg/ml) and streptokinase (final = 5 units/μg plasminogen). After 6 h at 37°C, digestion was stopped with phenylmethylsulfonyl fluoride (final = 0.2 mM). Approx. 100 mg digest volume was diluted in distilled water and Tris acetate (ionic strength 0.1, pH 8.01) and applied to an ion-exchange Q-Sepharose column (1.5 × 25 cm) equilibrated at 4°C in Tris acetate (ionic strength 0.1, pH 8.01) and eluted isocratically as described [16].

Pools were concentrated by ultrafiltration and recromatographed on Sephacryl S-300 (1.5 × 55 cm) or in the case of fragment E, on Sephadex G-100 (1.5 × 55 cm), both equilibrated at 4°C in Tris-HCl 0.05 M/NaCl 0.15 M (pH 7.4). Pools were dialysed at 4°C against distilled water and freeze-dried. The purity was assessed by SDS-polyacrylamide gel electrophoresis under non-reduced and reduced conditions, so as to determine the molecular weight of fragments and polypeptide chains. Both fragments D and E (fragment E_3 in S.A. Olexa et al. [5]) were shown to be pure, and their molecular weights were approx. 100 000 and 45 000, respectively. In reduced conditions, fragment D (Mw 100 000) turned into three chains of Mw 12, 45 and 48 000.

Coiled-coil containing fragment

Fragment D (Mw 100 000) (10 mg/ml) was dissolved in 0.05 M glycine (pH 2.8) as described [17]. Digestion was started with pepsin (final = 50 μg/ml), and after 80 min at 25°C, was stopped by passing the digest through a Pepstatin-Affinity column (1 × 2 cm) equilibrated with 0.05 M glycine (pH 2.8). The coiled-coil containing fragment was purified at 4°C on Sephadex G-75 (1.5 × 55 cm), equilibrated with acetate buffer 0.2 M (pH 4.4). The fragment was pure and had a molecular weight of approx. 27 000 by SDS-polyacrylamide gel electrophoresis.

Clotting studies

Thrombin (0.5 NIH units/mg fibrinogen) was added to fibrinogen (50 mg/ml) dissolved in 0.05 M Tris-HCl/ 0.15 M NaCl with either 0.01 M EGTA (pH 7.4) or 0.01 M $CaCl_2$ and left clotting in the spectroscopic cell at 37°C, 20 min previous to spectroscopic studies.

Infrared spectroscopy

Protein solutions were dissolved in ^2H_2O and H_2O buffers containing 0.05 M Tris-HCl/NaCl 0.15 M (pH 7.4/p*D*) 7.4 or 0.2 M phosphate (pH 3.5). About 50 μl of sample was placed between two CaF_2 windows separated by a 12 μm tin or 50 μm plastic spacer and mounted on a thermostated cell holder, within an air-purged chamber. For each sample 400 interferograms in H_2O or 100 in ^2H_2O solution, were recorded at 4 cm^{-1} resolution, signal-averaged and apodized using a raised cosine function on a Perkin-Elmer 1750 Fourier transform infrared spectrometer and processed with a Perkin-Elmer data station. Buffer and sample spectra were recorded separately and subtracted, to

obtain the difference spectra of the protein. Traces of water vapour were subtracted, until a flat line was obtained in the frequency region of 1800–1700 cm^{-1}.

Deconvolution and second derivative routines were used to provide information about the underlying bands in the recorded spectra. With the first routine, for most cases an estimated natural half-bandwidth (W) of 15 cm^{-1} was used and a resolution enhancement factor (K) of 2–2.25. With the second routine, a range of 13 data points was used to calculate the rate of change of slope along the spectra. We quantify the secondary structure by factor analysis of the spectra [18]. This method has a standard error of prediction of 3.9% for α-helix, 8.3% for β-sheet and 6.6% for turns. This quantification method uses factor analysis of reference spectra of a range of proteins with different amino acid sequence and secondary structure based on X-ray structure data. The contribution of aminoacid side-chains to the spectra is accounted in the error of prediction for each secondary structure.

Results

FTIR spectroscopy furnishes information attributed on the average distribution of secondary structures in proteins. Information about domains and regions of proteins remain undistinguishable in the spectra.

Fibrinogen and fibrin

CD and Raman [11–13] studies of fibrinogen and fibrin gave a value of 33% content of α-helical structure and the presence of minor segments of β-sheet. The spectrum of fibrinogen in H_2O (Fig. 2a) shows a broad amide I band at 1651 cm^{-1} typical of proteins with high α-helical content. Its deconvolved spectra (Fig. 2a) shows spectral bands located at frequencies of 1686, 1667, 1653, 1642, 1631 and 1617 cm^{-1}. The band at 1653 cm^{-1} originates from α-helical and/or random structures [14]. The band at 1631 cm^{-1} arises from β-sheet structures [14,19], while the elements at 1642 cm^{-1} could be attributed to either β-sheet [20] or β-turn (type I or III) [21]. High frequency components in the amide I band at 1667 and 1686 cm^{-1} can be assigned to turns and elements of β-sheet [14]. Amino acid side-chains like those from Arg, Asn, Gln and Lys absorb along the whole amide I band, and may affect specially the intensity of the latter two bands and that at 1630 cm^{-1} [22] and their whole contribution to the amide I and II bands is estimated to be around 20% of the total absorbance. We quantified [18] the content of secondary structure of the protein and obtained a distribution of 37% α-helix, 30% β-sheet, 14% β-turns and 16% unassigned structures.

We obtained a similar distribution of secondary structures from spectra of fibrin clots made in the presence of EGTA 10 mM. In the presence of Ca^{2+} at 15 mM, the amide I band of the spectrum of this clot (Fig. 2b) becomes smaller and the β-sheet associated bands increase slightly (7%) with some reduction in the intensity of α-helical/random structural bands (1650–55 cm^{-1}). A similar result has been reported by Marx et al. [11] in their Raman spectroscopic studies of fibrin clots.

The above data provides an idea of the average distribution of secondary structures in fibrinogen and fibrin clots. When digested with plasmin, fibrinogen renders two fragments which contain domains of the original molecule. As these fragments result from limited plasmic digestion, one can not discard the possibility that changes in the conformation of fragment E may

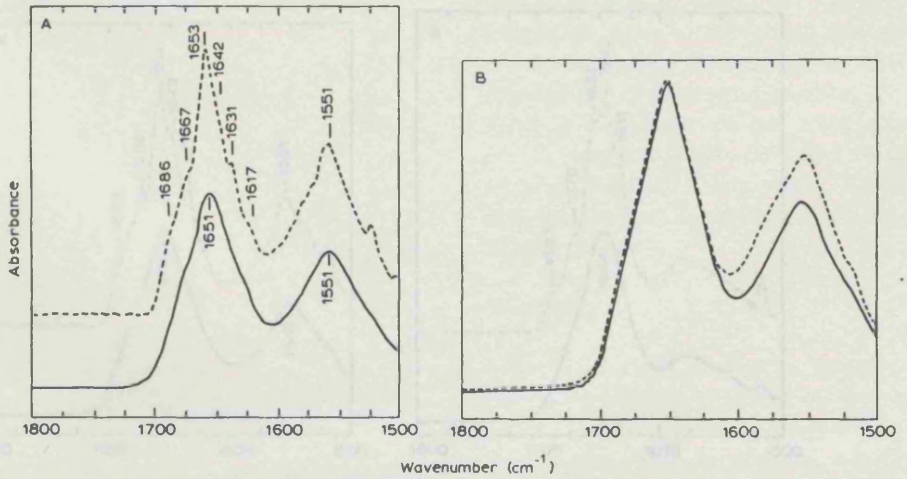

Fig. 2. (A) Absorption spectrum (bottom trace) from 1800 cm^{-1} to 1500 cm^{-1} of 5% (w/v) of human fibrinogen in H_2O buffer (pH 7.4), Tris-HCl 0.05 M NaCl 0.15 M after buffer spectrum subtraction. Deconvolution of spectrum (top trace), using a resolution enhancement factor of 2.125 and bandwidth of 15 cm^{-1}. (B) Absorption spectra of fibrin clot in buffer solution, including EGTA (solid line); and absorption spectrum of fibrin clot in buffer solution, including Ca^{2+} (dotted line) (see Materials and Methods).

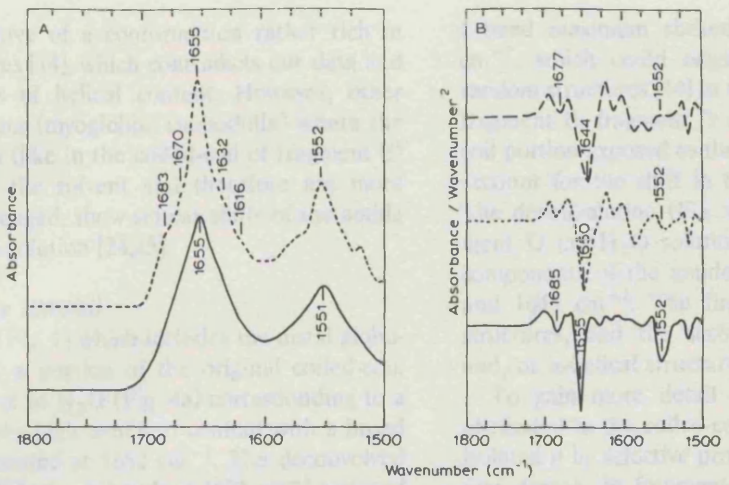

Fig. 3. (A) Absorption spectrum (bottom trace) of 5% (w/v) of fragment E in H_2O buffer (pH 7.4). Deconvolution of spectrum (top trace), using a resolution enhancement factor of 2 and a bandwidth of 15 cm^{-1}. (B) Second derivative spectra of fragment E, where the data range was 13 points. (Bottom trace) Spectrum obtained of fragment E in H_2O buffer. (Centre trace) Spectrum obtained after 1 h in ^2H_2O buffer (p*D* 7.4), showing partial deuteration. (Top trace) Spectrum obtained after 12 h later in ^2H_2O buffer (p*D* 7.4), showing complete deuteration.

occur. As to fragment D, it originates from plasmin cleavage of the free appendage of the α-chain off the distal domain and the plasmin sensitive sites along the coiled-coil region. It inhibits fibrin-polymerisation [6], binds with high affinity ($K_d \approx 12$ nM) to fibrin [7] and contains one Ca^{2+} binding site ($K_d \approx 9$ μM) [23]. This is evidence of preservation of functional activity and as such, it implies structural integrity. Using these two fragments, we are able to study separately (Fig. 1) different regions of the fibrinogen molecule.

Fragment E (Mw 45 000)

This fragment (Fig. 1) contains most of the central domain of the molecule and two portions of the coiled-coil. Its difference spectrum (Fig. 3a) in H_2O shows an amide I band maximum at 1655 cm^{-1}, which is observed in α-helical proteins. Its deconvolved spectrum (Fig. 3a) reveal small components at 1632, 1670 and 1693 cm^{-1} assigned to small components of β-sheet and β-turns (type II). According to circular dichroism studies [12] this fragment contains 35% of α-helical content, whilst our method reports 50% of α-helical structures, 19% of β-sheet, 14% of turn structures and 15% unassigned structures.

In H_2O solution, random and α-helical structures overlap each other at 1653–56 cm^{-1}. In ^2H_2O solution, we observe (Fig. 3b) a continuous shift of the amide I band maximum from 1655 to 1644 cm^{-1}. This

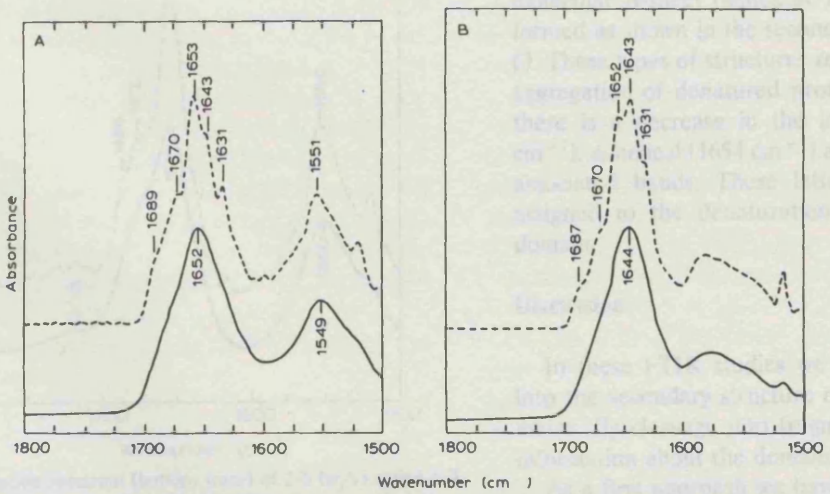

Fig. 4. (A) Absorption spectrum (bottom trace) of 5% (w/v) fragment D in H_2O buffer (pH 7.4). Deconvolution of spectrum (top trace), using a resolution enhancement factor of 2.25 and a bandwidth of 15 cm^{-1}. (B) Absorption spectrum (bottom trace) of deuterated fragment D (3% w/v) in ^2H_2O buffer. Deconvolution of spectrum (top trace), with a resolution enhancement factor of 2.125 and a bandwidth of 15 cm^{-1}.

could be indicative of a conformation rather rich in random structures [14], which contradicts our data and the CD reports of helical content. However, other studies of proteins (myoglobin, calmodulin) where the helical segments (like in the coiled-coil of fragment E) are exposed to the solvent and therefore are more completely exchanged, show similar shifts of the amide I band in ^2H_2O solution [24,25].

Fragment D (Mw 100 000)

Fragment D (Fig. 1) which includes the distal globular domain and a portion of the original coiled-coil, shows a spectrum in H_2O (Fig. 4a) corresponding to a protein containing high α-helical content with a broad amide I band located at 1652 cm^{-1}. The deconvolved spectrum (Fig. 4a) reveals bands at 1631 cm^{-1} assigned to β-sheet structures and 1643 cm^{-1} from β-sheet [14,20] or β-turn (type I or III) [21]. High frequency elements seen at 1670 and 1689 cm^{-1}, are attributed to β-turn, elements of β-sheet structures and side-chains of amino acids. Quantification [18] of the spectrum of fragment D shows a distribution of secondary structures of 34.5% α-helix, 29.5% β-sheet, 17% turns and 17.5% unassigned structures. Previous CD spectroscopic studies [12] give a value of 40% α-helical content in this fragment. Fragment D, obtained from digested non cross-linked fibrin clots, showed a spectrum similar to the one in Fig. 4a.

In ^2H_2O solution (Fig. 4b), the amide II band at 1549 cm^{-1} is almost absent after 5 h, indicative of a solvent-accessible structure. In this spectrum the amide I band maximum shifted from 1651 cm^{-1} to 1644 cm^{-1}, which could originate from the presence of random structures [14] in this fragment. However, as in fragment E, fragment D contains an α-helical coiled-coil portion exposed to the solvent, which may partially account for the shift in the amide I band maximum. The deconvolution (Fig. 4b) of the spectrum of fragment D in ^2H_2O solution shows now that the main components of the amide I band are located at 1652 and 1643 cm^{-1}. The first is attributed to α-helical structures, and the second originates from random and/or α-helical structures as pointed out above.

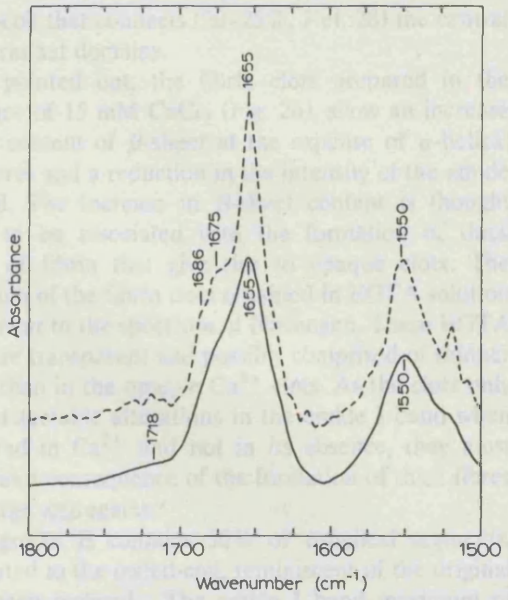

Fig. 5. Absorption spectrum (bottom trace) of 2% (w/v) coiled-coil portion, in H_2O buffer (pH 3.5), 0.2 M sodium phosphate. Deconvolution of spectrum (top trace), using a resolution enhancement factor of 2 and bandwidth of 15 cm^{-1}.

To gain more detail of the secondary structures attributed to the coiled-coil portion of fragment D, we isolated it by selective proteolysis. At pH < 3, the globular domain in fragment D unfolds [17] whereas the coiled-coil portion (Mw 27 000) is stable and can be recovered after pepsin digestion at pH 2.8 of fragment D. Confirming previous CD studies [17], the coiled-coil portion (Fig. 5) of fragment D contains a high α-helical content (band frequency at 1654 cm^{-1}), approx. 70% according to our method and some β-turn (band at 1670 cm^{-1}) structures.

Thermal denaturation of the globular domain of fragment D

The globular domain of fragment D is labile to temperature and can be denatured at 55°C [26], whereas the coiled-coil portion is stable. To see what bands are affected by the thermal denaturation, we followed the spectral changes of the amide I band of solutions of fragment D at 55°C (Fig. 6). The experiments were conducted in ^2H_2O solution. This allows spectrum to be obtained in 3 min with a good signal to noise ratio. All the spectra were recorded after complete $H/^2H$ exchange, as shown by disappearance of the amide II band. As the thermal denaturation proceeds, intermolecular β-sheet (bands at 1616 and 1685 cm^{-1}) is formed as shown in the second derivative spectra (Fig. 6). These types of structures result from unfolding and aggregation of denatured proteins. At the same time there is a decrease in the intensities of turn (1670 cm^{-1}), α-helical (1654 cm^{-1}) and β-sheet (1631 cm^{-1}) associated bands. These latter bands are therefore assigned to the denaturation of the distal globular domain.

Discussion

In these FTIR studies we attempt to gain insight into the secondary structure of fibrinogen and its domains. By cleavage into fragments, we have obtained information about the domains of fibrinogen.

As a first approach we have studied its structure in water solution and in the clotting process, for comparison with previous studies. The FTIR spectrum shows,

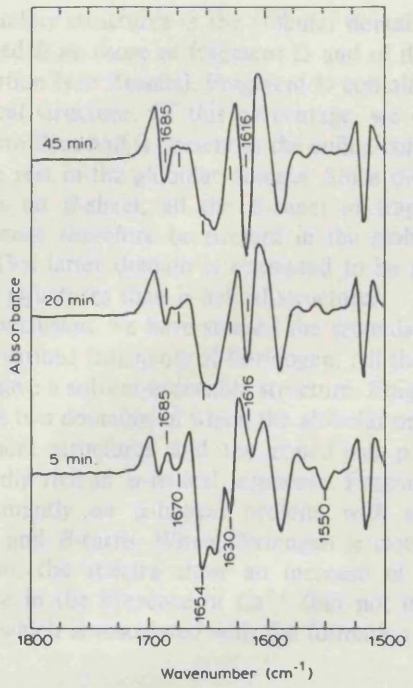

Fig. 6. Second derivative spectra of fragment D in ^2H_2O solution, obtained at 55°C at different times of exposure (from the bottom to the top spectrum).

according to the factor analysis method [18], that fibrinogen is an α-helical (37%) protein, but with a high content of β-sheet (30%). These data compare well with previous data [11–13], though Raman Spectroscopy reports a lower content of β-sheet. The high α-helical content can be partially attributed to the coiled-coil that connects (20–25%, Ref. 28) the central and terminal domains.

As pointed out, the fibrin clots prepared in the presence of 15 mM $CaCl_2$ (Fig. 2b), show an increase in the content of β-sheet at the expense of α-helical structures and a reduction in the intensity of the amide I band. The increase in β-sheet content is thought [2,11] to be associated with the formation of thick fibres of fibrin that give rise to opaque clots. The spectrum of the fibrin clots obtained in EGTA solution are similar to the spectrum of fibrinogen. These EGTA clots are transparent and possibly comprised of thinner fibres than in the opaque Ca^{2+} clots. As the clots only show detectable alterations in the amide I band when prepared in Ca^{2+} and not in its absence, they must occur as a consequence of the formation of thick fibres and large aggregates.

Fragment E contains 50% of α-helical segments, attributed to the coiled-coil, reminiscent of the original fibrinogen molecule. The amide I band maximum of both fragment E (Fig. 3a) and the isolated coiled-coil portion (Fig. 5) absorb at 1654–5 cm^{-1}, what suggests that they contain similar α-helical structures. Other secondary structures have been suggested to occur in this fragment by A.Z. Budzynski [12]. We propose it contains additional β-strands (less than 20%) and turn structures of various types. This fragment contains eleven disulphur bridges, which entangles together two pairs of three polypeptides, forming a dimer. It may allow only structures sterically demanding, probably composed of irregular β-strands and turns in similar proportions. The shift in ^2H_2O solution (Fig. 3b) of the amide I band is mostly attributed to the α-helical coiled-coil portions of this fragment. The cause of the shift is not well understood [24], but has been observed in other proteins such as calmodulin and is associated with the presence of solvent-exposed helical regions [24,25].

Fragment D (Fig. 4a) shows a similar spectrum to fibrinogen (Fig. 2a). This is not surprising since two fragments D are equivalent to almost two-thirds of the original fibrinogen molecule, and thus dominate the spectrum. Most of the β-sheet structure of the fibrinogen molecule seems to be present in this fragment. The assignment of the band at 1643 cm^{-1} in H_2O is not clear, although the quantifying method identifies it as a β-sheet component. The spectra in H_2O of ribunoclease A [20] and other proteins like aprotinin show β-sheet bands at around 1640 cm^{-1}. The high frequency of these bands has been attributed to a pronounced twisting [29] of the β-sheet or by the presence of short and distorted strands [20]. Nonetheless we must note that β-turn type I or III structures [21] may absorb at this frequency.

As shown in the deuterium exchange experiments (Fig. 4b), the shift of the amide I band maximum in the spectrum of fragment D could be interpreted as indicative of the presence of random structures. This shift could be partially caused by solvent-exposed α-helical segments of its coiled-coil portion. On the other hand, the band at 1652 cm^{-1} indicates the presence of other α-helical segments, probably less exposed to the solvent and located in globular regions of the molecule.

Fragment D contains two domains of different thermal stability (Fig. 1) according to calorimetric studies [26]. The globular domain unfolds at 55°C, whereas the coiled-coil portion remains intact at temperatures up to 75°C. The thermal denaturation of fragment D at 55°C was studied by FTIR spectroscopy (Fig. 6). At this temperature drastic changes occur in the infrared spectra that indicate a reduction in the intensity of helical, turn and β-sheet associated bands. Concurrently two new bands at 1616 and 1685 cm^{-1} appear in the spectra, which are assigned to intermolecular β-sheet (indicative of protein unfolding). These changes are due to the thermal denaturation of the globular domain of fragment D. The quantification of secondary structures of the globular domain is not feasible from its thermal denaturation spectra. However the content

of secondary structures in the globular domain can be evaluated from those of fragment D and of its coiled-coil portion (see Results). Fragment D contains 34.5% of helical structure. Of this percentage, we calculate that more than half is present in the coiled-coil portion and the rest in the globular domain. Since the coiled-coil has no β-sheet, all the β-sheet of fragment D (29%) must therefore be present in the globular domain. This latter domain is estimated to be richer in β-sheet structures than α-helical structures.

In conclusion, we have studied the secondary structure of various fragments of fibrinogen. All these fragments have a solvent-accessible structure. Fragment D, contains two domains, of which the globular one is rich in β-sheet structures and the coiled-coil portion is expectedly rich in α-helical segments. Fragment E is predominantly an α-helical protein, with some β-strands and β-turns. When fibrinogen is clotted with thrombin, the spectra show an increase of β-sheet structure in the presence of Ca^{2+} (but not in its absence), which is associated with the formation of thick fibres.

References

1 Doolittle, R.F. (1984) Annu. Rev. Biochem. 53, 195–229.
2 Doolittle, R.F. (1973) Adv. Prot. Chem. 27, 1–109.
3 Havergatte, F. and Timan, G. (1977) Thromb. Res. 10, 803–822.
4 Fowler, W.E., Fretto, L.J., Erickson, H.P. and McKee, P.A. (1980) J. Clin. Invest. 66, 50–56.
5 Olexa, S.A., Budzynski, A.Z., Doolittle, R.F., Cottrell, B.A. and Greene, T.C. (1981) Biochemistry 20, 6139–6145.
6 Dray-Attali, L. and Larrieu, M.J. (1977) Thromb. Res. 10, 575–586.
7 Cierniewski, C.S., Kloczewiak, M. and Budzynski, A.Z. (1986) J. Biol. Chem. 261, 9116–9121.
8 Cohen, C., Weisel, J.W., Phillips, G.N., Jr., Stauffacher, C.V., Fillers, J.P. and Daub, E. (1983) Ann. N.Y. Acad. Sci. 408, 194–213.
9 Privalov, P.H. and Medved', L.V. (1982) J. Mol. Biol. 159, 665–683.
10 Medved', L.V., Litvinovich, S.V. and Privalov, P.H. (1986) FEBS Lett. 202(2), 298–302.
11 Marx, J., Hudry-Clergeon, G., Capet-Antoninin, F. and Bernard, L. (1979) Biochim. Biophys. Acta 578, 107–115.
12 Budzynski, A.Z. (1971) Biochim. Biophys. Acta 229, 663–671.
13 Kloczewiak, M., Wegrzynowicz, Z., Mathias, F.R. and Heene, D.L. (1976) Thromb. Res. 9, 359–368.
14 Jackson, M., Haris, P.I. and Chapman, D. (1989) J. Mol. Struct. 214, 329–355.
15 Deutsch, D.G. and Mertz, E.T. (1970) Science 170, 1095–1096.
16 Chen, J.P., Shurley, H.M. and Vickroy, M.F. (1972) Biochem. Biophys. Res. Commun. 71, 754–761.
17 Melved', L.V., Privalov, P.L. and Ugarova, T.P. (1982) FEBS Lett. 146 (2), 339–342.
18 Lee, D.C., Haris, P.I., Chapman, D. and Mitchell, R.C. (1990) Biochemistry 29, 9185–9193.
19 Susi, H. (1969) Infrared spectra of biological macromolecules and related systems, in Structure and Stability of Biological Molecules (Timasheff, S.N. and Fasman, G.D., eds.), Marcel Dekker, New York.
20 Olinger, J.M., Hill, D.M., Jakobsen, R.J. and Brody, R.S. (1986) Biochim. Biophys. Acta 869, 89–98.
21 Krimm, S. and Bandekar, J. (1986) Adv. Prot. Chem. 38, 181–364.
22 Venyaminov, S.Y. and Kalnin, N.N. (1991) Biopolymers 30, 1243–1257.
23 Nieuwenhuizen, W., Vermond, A., Nooijen, W.J. and Haverkate, F. (1979) FEBS Lett. 98(2), 257–259.
24 Jackson, M. (1990) PhD thesis, University of London, U.K.
25 Susi, H., Timasheff, S.N. and Stevens, L. (1967) J. Biol. Chem. 242, 5460–5466.
26 Privalov, P.L. and Melved', L.V. (1982) J. Mol. Biol. 159, 665–683.
27 Jackson, M., Haris, P.I. and Chapman, D. (1989) Biochim. Biophys. Acta 998, 75–79.
28 Doolittle, R.F., Goldbaum, D.M. and Doolittle L.R. (1978) J. Mol. Biol. 120, 311–325.
29 Haris, P.I. (1989) PhD Thesis, University of London, U.K.

Conformation of the Pf1 coat protein in the phage and in a lipid membrane.

IÑAKI AZPIAZU, PARVEZ I. HARIS and DENNIS CHAPMAN

Department of Protein and Molecular Biology, Royal Free Hospital School of Medicine, Rowland Hill Street, London NW3 2PF, U.K.

Following host-cell infection, the new filamentous phages (Pf1, fd, M13,...) arise by assembly of coat proteins through a membrane-mediated process [1, 2]. Initially inserted in the membrane, these small proteins (molecular weight of about 5 Kda) become one of the thousands of subunits that comprise around 90-95% of the mass of the phage.

Only 45-50 aminoacids long, they share a central hydrophobic segment and short hydrophilic regions on each terminus [2]. Neutron diffraction [1, 3] of the phages shows these coat proteins form a superstructure of helical rods packed parallel to the viral axis. The study of the coat protein structure in the membrane and in the phage can provide clues on how the phage assembly occurs.

Spectroscopic data shows the coat proteins conserve a high helical content in detergent micelles and in membranes [2, 4]. According to NMR reports the M13 and Pf1 coat protein [4-6] in detergent micelles form a long helical segment interrupted by an irregular loop, similar to that in the phage. A molecular model for the Pf1 coat protein in the membrane has been proposed [6] which basically consists of a long helix spanning the lipid bilayer and a short amphipathic helix that lies on the surface of the membrane. The relevance of this model and its postulated interactions with the lipid bilayer remain to be tested.

Fourier-Transform Infrared spectroscopy (FT-IR) reports on the secondary structure of proteins and is based on assessment of the amide bands that arise from vibrations of the peptidic backbone. FT-IR is extremely useful in studies of structure of biomolecules present in samples untractable for other molecular techniques such as NMR and X-ray diffraction. Here we have used FT-IR spectroscopy to study the secondary structure of the Pf1 coat protein, intact in the phage and after solubilisation in detergent micelles. We have reconstituted the coat protein in a phospholipid aqueous suspension and analysed as dried films using internal reflectance techniques (ATR).

Pf1 phage was purified as described by Schiksnis et al [4]. Concentration of phage was measured by UV spectroscopy using an extinction coefficient of 2.07 mg.cm^{-1} at 270 nm [7].

Transmission spectra of sample and buffer were recorded separately and treated as described [8] in a Perkin-Elmer 1750 spectrometer. The concentration of protein was 1-2.5% for studies in H_2O or ^2H_2O. Phage was concentrated with PEG 5% or solubilised in dodecyl-sulphate and dodecyl phospho-choline as described [4, 6]. The coat protein was reconstituted into phospholipid vesicles by sonication in a MTE bath at 30-33°C or by detergent dialysis method from deoxycholate solubilised solution of L-α-dimyristoil-phosphocholine (DMPC) and Pf1 phage.

For ATR studies suspensions of lipid vesicles were spread on a germanium crystal and dried until thin films formed. Lamellar orientation was checked by iridescent appearance of the films, and by the dichroism of the lipid bands at 2874 and 1202 cm^{-1}. ATR spectra were recorded in a Mattson FT-IR 4060 spectrometer [9].

Infrared spectra of the Pf1 filamentous phage in H_2O shows a narrow amide band at 1650 cm^{-1}, indicative of a high content of α-helical structure and a small band at 1675 cm^{-1}, assigned to turn structures. Manually oriented films of phage studied with polarised beams indicate that the helical structures (at 1652 cm^{-1}), turns (at 1675 cm^{-1}) and the tyrosine phenolic rings (at 1515 cm^{-1}) are aligned with the main axis of the phage filament. This data agrees with the current model for the Pf1 phage but also reveals, as suggested in previous studies [2,3], the existence of turn structures with a specific orientation along the axis of the phage.

In SDS and DPC detergent micelles the amide I band of the Pf1 coat protein is seen at 1657 cm^{-1} and was of narrow shape, similar to that observed in the phage. The spectrum of the coat protein reconstituted in lipid vesicles shows a narrow amide I band at 1657-8 cm^{-1} indicating a helical content close to that observed in the phage and in detergent micelles.

ATR polarised spectra of dried films obtained from suspensions of coat protein reconstituted in lipid vesicles shows that, unlike the amide II band, the amide I band at 1658^{-1} reveals a strong perpendicular dichroism with respect to the plane of the film. The dichroic ratios are 2.3-2.5 for the amide I band and 1.4-1.6 for the amide II band. These results suggest that the overall orientation of the helical segments is rather perpendicular to the plane of the bilayer.

Calorimetric studies of pellets of lipid suspensions with reconstituted protein are consistent with the presence of a single helix spanning the lipid bilayer whose perimeter occupies a circumference of four to five lipid molecules. Similar estimates are obtained from polarisation studies using a fluorescent probe (diphenylhexatriene) incorporated into phospholipid vesicles with various fractions of coat protein.

In conclusion our results show that the Pf1 coat protein maintains its high helical content on solubilisation from phage to detergent and also when reconstituted in phospholipid vesicles.

1. Marvin, D.A. & Wachtel E.J. (1975) Nature 253, 19-23.
2. Day, L.A., Marzec, S.A.R. & Casadevall A. (1988) Ann. Rev. Biophys. Chem. 17, 509-539.
3. Nambudripap, R., Stark, W., Opella, S.J. & Makowski, L. (1991) Science 252, 1305-1307.
4. Schiksnis, R.A., Bogusky, M.J., Tsang, P. & Opella, S.J. (1987) Biochem. 26, 1373-1381.
5. Henry, G.D., Sykes, B.D. (1992) Biochem. 31, 5284-5297.
6. Shon, K.-J., Kim, Y., Colnago, L.A. & Opella, S.J. (1991) Science 252, 1303-1305.
7. Day, L.E. & Wiseman, R. (1976). J. Mol. Biol. 102, 549.
8. Azpiazu, I. & Chapman D. (1992). Biochim. Biophys. Acta 1119, 268-274.
9. Azpiazu, I., Gomez-Fernandez, J.C., Haris, P.I. & Chapman, D (1992) In preparation